2013

CRITICAL EVENTS IN HUMAN METAPNEUMOVIRUS INFECTION: FROM ENTRY TO EGRESS

Brent A. Hackett
University of Kentucky, brentahackett@yahoo.com

STUDENT AGREEMENT:

I represent that my thesis or dissertation and abstract are my original work. Proper attribution has been given to all outside sources. I understand that I am solely responsible for obtaining any needed copyright permissions. I have obtained and attached hereto needed written permission statements(s) from the owner(s) of each third-party copyrighted matter to be included in my work, allowing electronic distribution (if such use is not permitted by the fair use doctrine).

I hereby grant to The University of Kentucky and its agents the non-exclusive license to archive and make accessible my work in whole or in part in all forms of media, now or hereafter known. I agree that the document mentioned above may be made available immediately for worldwide access unless a preapproved embargo applies.

I retain all other ownership rights to the copyright of my work. I also retain the right to use in future works (such as articles or books) all or part of my work. I understand that I am free to register the copyright to my work.

REVIEW, APPROVAL AND ACCEPTANCE

The document mentioned above has been reviewed and accepted by the student's advisor, on behalf of the advisory committee, and by the Director of Graduate Studies (DGS), on behalf of the program; we verify that this is the final, approved version of the student's dissertation including all changes required by the advisory committee. The undersigned agree to abide by the statements above.

<div align="right">

Brent A. Hackett, Student

Dr. Rebecca E. Dutch, Major Professor

Dr. Michael Mendenhall, Director of Graduate Studies

</div>

CRITICAL EVENTS IN HUMAN METAPNEUMOVIRUS INFECTION: FROM ENTRY TO
EGRESS

_____

DISSERTATION

_____

A dissertation submitted in partial fulfillment of the requirements for the degree of Doctor of
Philosophy in the College of Medicine at the University of Kentucky

By

Brent Allen Hackett

Lexington, Kentucky

Director: Dr. Rebecca E. Dutch, Professor of Molecular and Cellular Biochemistry

Lexington, Kentucky

2013

ABSTRACT OF DISSERTATION

CRITICAL EVENTS IN HUMAN METAPNEUMOVIRUS INFECTION: FROM ENTRY TO
EGRESS

Human metapneumovirus (HMPV) is a respiratory pathogen in Paramyxovirus family
that demonstrates extremely high morbidity in the population, with most individuals
having been infected by the age of five. Despite the prevalence of this negative-sense
RNA virus in the population for decades, it was only identified in 2001. As such, there is
currently no specific treatment for HMPV and the potentially severe consequences of
infection for elderly and immunocompromised individuals and particularly infants make
development of antivirals targeting HMPV of high significance. HMPV constitutes a
quarter of all respiratory hospitalizations among infants, placing it second only to RSV,
in addition to becoming a greater concern in concentrated populations of seniors. For
these susceptible populations, the consequences of infection have a much greater
probability of leading to pneumonia, bronchiolitis and even death.

These studies investigate events throughout the infectious cycle of HMPV. They
describe specific amino acids that modulate the triggering of viral fusion activity in
response to low pH. They also include a report on the dynamic and variable control
exercised over gene transcription by viral promoters. Finally, the interplay between viral
nonstructural proteins and their distinct roles in both replication and assembly are
examined. Ultimately, this work seeks to elucidate the goings-on within an HMPV-
infected cell at multiple points throughout the process.

Keywords: Human metapneumovirus (HMPV), RNA-dependent RNA polymerase
(RdRp), phosphoprotein, nucleocapsid, minireplicon

CRITICAL EVENTS IN HUMAN METAPNEUMOVIRUS INFECTION: FROM ENTRY TO EGRESS

by

Brent Hackett

_____Dr. Rebecca E. Dutch_____
Director of Thesis
____Dr. Michael Mendenhall_____
Director of Graduate Studies
_____7/16/2013_____
Date

ACKNOWLEDGEMENTS

I first and foremost have to acknowledge the fact that I could never have accomplished this goal of writing a dissertation without the help of so many people. Some I will name here but many I cannot for want of space. But I need to be clear that everyone has been in my life has aided me in getting to this moment and for that I thank you more than you will ever know.

My family has been my roc for as long as I can remember. Every encouraging word of early morning conversation has meant the world to me. This is not simply my accomplishment but yours as well because without you there would be no me as I am. Specifically, all my parents, Faye and Gary as well as Jesse and Linda have been there at times when I didn't know how I'd get through it. I also have to acknowledge my siblings, Jolynn, Jesse, Cassandra, Demetrius and Allison for not letting me get ahead of myself and providing invaluable support and encouragement throughout the years.

I'd be remiss to wait any longer to acknowledge my mentor Dr. Becky Dutch. Time and again, she has provided guidance, counsel and advice that helped me at every step of the way. Sometimes, it was what wasn't said but fully understood that was most helpful. I also have to thank her for having faith in me as a scientist. She was the one who allowed me to be led by my interests and to ask the questions that no one else was. Above all, she has shown me that you can be a top-rate scientist and still be a good person.

TABLE OF CONTENTS

LIST OF TABLES

LIST OF FIGURES

Chapter I: Introduction

Subsection I: General Overview

Paramyxoviruses are a diverse family of viruses that infect a range of host species and include many noteworthy human pathogens among their number. Some of the more well-characterized members of the family include measles and mumps viruses; additionally, emerging viruses are prevalent among paramyxoviruses, including the zoonotic Hendra and Nipah viruses, which feature alarmingly high levels of mortality in their contained outbreaks [1].   All paramyxoviruses display several common characteristics—their virions (infectious particles) are enveloped by a host cell-derived phospholipid membrane bilayer.   They each encode relatively few gene products, no more than 10 for any known member of the family, in a non-segmented negative-sense RNA genome, and all exhibit pleimorphism with regard to the size and shape of their infectious particles [2].   Paramyxoviruses are members of the phylogenetic order *Mononegavirales* due to their genomes, and phylogenetic analysis demonstrates the similarity of this viral family to some of the most dangerous pathogens known, including the filoviruses, such as Ebola and Marburg viruses and rhabdoviruses, including rabies (Figure 1.1) [3-8].

The focus of this research, however, features one particular paramyxovirus.   This pathogen, human metapneumovirus (HMPV), is symptomatically similar to other respiratory agents, such as influenza and human respiratory syncytial virus (hRSV) with a

tissue tropism throughout the human airway. Unlike these other pathogens, however, HMPV has only recently been characterized, being first isolated in 2001 in the Netherlands. Clinical samples from children presenting respiratory symptoms from an unidentified etiological agent were obtained and the virus isolated. Upon studying the characteristics of the virus, including the contents of its genome, homology to avian metapneumovirus led to the categorization of this agent as the second isolated metapneumovirus—HMPV. The researchers then were able to test children, first throughout the Netherlands and subsequently worldwide, and found that nearly all individuals over the age of five presented antibodies against this agent. Testing stored clinical samples also allowed for the determination that HMPV had been present in the population for at least fifty years prior to its characterization. [9].

HMPV has since been shown to be the second leading causative agent for respiratory-related hospitalizations for children under the age of five, trailing only the closely-related hRSV [10]. Further epidemiological studies have also revealed that HMPV accounts for 6-11% of respiratory tract infections in children under the age of five and that the percentage of HMPV-positive cases was significantly greater (up to 25%) for children under the age of two [11]. Additionally, due to the existence of several phylogenetic groupings or clades, to which unique immunological responses may be triggered, HMPV is a great threat later in life to large populations of individuals, such as elderly and immunocompromised persons as well as those with cardiopulmonary disease [12]. All of these groups, in addition to infants and young children, may suffer more severe

complications as result of HMPV infection also including bronchiolitis, pneumonia and death [13-14].

As dire as these statistics may seem, they may, in fact, underestimate HMPV cases, as serum etiological assays are often not performed to definitively identify an agent. This potential underrepresentation is due to similar symptomology to other respiratory pathogens for which—as in the case of HMPV—there is no specific course of treatment. Several proposed therapies have been tested, such as prophylactic antibody treatment, which is the only FDA-approved treatment for hRSV, but the efficacy of this therapy is unclear in the case of HMPV infection [15-17].

Another proposed treatment is the general antiviral compound ribavirin, an oral nucleoside analog that induces errors in the rapidly synthesized RNA genomes of the infecting agent, and there have been reports of success with this treatment [18]. This treatment would be extremely efficacious in treating these agents as their replicative cycle is dependent on RNA to the exclusion of DNA. However, the drug is also a potential teratogen, and recent evidence casts doubt on its efficacy in severe HMPV infection [19]. There are also other proposed treatments for which it is too premature to determine the clinical relevance [20]. The current state of clinically available treatments for HMPV underscores the desperate need for greater understanding of novel aspects of this recently characterized pathogen's infectious cycle as an initial step towards the develop of specific treatments for the afflicted and at-risk populations.

As this virus has only recently been identified, there is still much that is simply not yet understood about its function in host cells. In fact, much of what is accepted by the field on HMPV comes from correlations drawn to similar viruses, despite the observation that phylogenetic nuances tend to make such generalizations somewhat specious. It has been specifically determined that the HMPV virion contains a ribonucleoprotein (RNP) core composed of the negative-sense genomic RNA encapsidated by the nucleocapsid protein (N), which is packaged with the RNA-dependent RNA polymerase (RdRp) and the matrix protein (M), which is thought to be involved in maintaining virion structure [21]. Surrounding the outside of this core is a host-derived phospholipid membrane bilayer known as an envelope with fusion (F), attachment (G) and small hydrophobic (SH) glycoproteins decorating the surface (Figure 1.2) [22].

These early observations have served as the basis for countless subsequent studies of HMPV, and the knowledge base on this pathogen has steadily grown. The field now has a firm grasp on numerous characteristics of the infectious cycle. A number of studies have focused on the entry mechanism of the virus [23-28]. There have also been a small number of investigations into the dynamics of the HMPV-encoded proteins responsible for genome replication as well as a few studies on assembly of progeny viruses [29-30]. The overall goal of my thesis work has been to harmonize the findings of studies in all these areas of HMPV pathogenesis in order to shed light on some of the most critical events at several stages of infection from the triggering of membrane fusion and entry to viral RNA synthesis and assembly.

Subsection II: HMPV Fusion and Entry

The general life cycle of the virus, as with other paramyxoviruses, begins with the mediation of attachment and membrane fusion with a target cell and entry into the cytosol.   This is a necessary and initializing step in the process of infection, occurring well before any replication [31]. These first steps in the process—attachment, fusion and entry—provide tantalizing antiviral targets with the added incentive of being able to impede infection before it truly begins.

HMPV attachment and fusion can be performed by a single surface glycoprotein, the fusion (F) protein, at least in the case of clade A2 isolate CAN97-83 [23, 28]. This is a novel occurrence amongst paramyxoviruses, which would generally require a separate protein to perform each of these functions [32]. HMPV further exhibits deviation from the general paramyxoviral entry pathway in that, rather than entering at the cellular plasma membrane, the virus is likely first internalized by either endocytosis or macropinocytosis and gains access to the cell through fusing its lipid envelope with one of these membranous vesicles [25].   While this mode of entry is thought novel for paramyxoviruses, recent evidence suggests that hRSV also enters through such a process [33]. Given the diverse functions of the F protein, a greater understanding of its composition at the amino acid level (and interactions therein) as well as the observed effects from altering this sequence on activity will lend itself to explaining how this fusion protein performs these somewhat disparate roles.

While no complete structure has been solved for this protein, a combination of the structures of the fusion proteins from other paramyxoviruses via X-ray crystallography and a recently reported partial HMPV F structure demonstrate some overall homology among these Class I viral fusion proteins [25, 27, 34-35]. Upon performance of homology modeling, it became readily apparent that while there are significant differences between parainfluenza virus 5 (PIV5) F—the basis for the prefusion homology model—and HMPV F with regard to sequence identity, there is likely to be a degree of conservation with regard to folding, particularly the position of specific independently folded domains. These conserved regions allow for classification of fusion proteins into one of three classes with both HMPV F and PIV5 F being grouped into Class I.

Class I fusion proteins exist in a prefusion conformation of homotrimers that is metastable following a priming proteolytic event [36]. In yet another difference for HMPV from other paramyxoviruses, HMPV F is processed extracellularly, potentially by the cellular protease TMPRSS2 *in vivo*, rather than by an intracellular enzyme—an event that is recapitulated *in vitro* with the addition of low concentrations of trypsin [37]. This metastability means that all that is necessary to begin the process of fusion is a triggering event, which allows for the protein to begin to undergo conformational change (Figure 1.3) [38]. Interestingly, it would appear that all energy required not only for this change but also for the membrane fusion event overall is contained within the macromolecule itself. However, this is chiefly based on the lack of a known ATP- or GTP-dependent cofactor, and a contribution to the overall energetics within the system from changes to

lipid composition cannot be ruled out. Following, the triggering event, which varies depending upon the particular protein, the hydrophobic fusion peptide, heretofore buried within the prefusion structure, is released and targeted toward the membrane of a potential host cell. The hydrophobicity of this amino acid stretch allows it to embed within the acyl chains inside the lipid bilayer, effectively tethering the virus to the cell's membrane (Figure 1.3B) [39]. At this point in fusion, two sets of three helices—the set adjacent to the fusion peptide is called heptad repeat A (HRA), while the one abutting the transmembrane domain on the viral envelope is called heptad repeat B (HRB)—are each exposed to the solvent in a new manner (Figure 1.3C) [40]. The fusion protein, now fully extended and tethered to two membranes, folds back onto itself much like a spring, and as this occurs, the two sets of heptad repeats interlock with one another to form an extremely stable and energetically favorable six-helix bundle (Figure 1.3D) [41]. In so doing, the lipids of the membranes are brought into proximity and mixing occurs. This process, mediated by homotrimers of the F protein, , allows for the opening of a fusion pore through which the contents of the virion can enter the cell (Figure 1.3E).

While the end result is the same for all Class I fusion proteins, the means of initiating the process can vary. For the HMPV strain A2 isolate CAN97-83, the triggering of the fusion protein is pH dependent with fusion occurring at a permissive pH of 5 but not at neutral pH [23]. This, however, is not the case for other strains of the virus within all clades [24]. Such a fusion trigger is novel among paramyxoviruses but not to all viruses; in fact, a low-pH trigger is quite common overall.

The influenza virus also features a Class I fusion protein, influenza HA, and behaves in a similar manner and triggers at a pH of 5.4 [42]. Like HMPV F, HA is a homotrimeric integral membrane glycoprotein. However, the protein has more cylindrical shape, constituted into a central α helix coil. It is thought that repulsive electrostatic charges that arise between residues following their protonation at low pH and are responsible for the destabilization of the prefusion form. Such destabilization allows the protein to trigger and refold into its postfusion conformation [43-44]. While electrostatic interactions can impact overall protein stability, the degree to which this occurs is heavily dependent on the location of the interacting residues as well as the surrounding environment. For example, modeling studies showed a strong attraction between the positively charged HA1 subunits and the negatively charged HA2 subunits of influenza HA at neutral pH; however, at low pH, both subunits become protonated, increasing the repulsive force between them. The macromolecular result is greater protein destabilization, which facilitates the transition to the postfusion structure [27].

Similarly, a portion of this work focuses on amino acids within the heptad repeat A domain as well as in a conserved region of the F_2 peptide fragment of HMPV F—a portion of the protein that is cleaved from the rest of the polypeptide following protease treatment but attached by disulfide linkages—that had been shown to modulate triggering previously in PIV5 F [45]. It also seeks to expand upon the discovery of a putative pH-sensing histidine residue at position 435 within the HRB-linker domain of HMPV F, which previous analysis of the homology model showed to be surrounded by several positively-charged residues, notably K295, R396 and K438. The position of these

residues suggests that the electrostatic repulsion forces that arise upon protonation of H435 at low pH could be another driving force for fusion triggering of HMPV F [25]. This assertion is supported by mutagenesis studies showing that alanine substitutions to these basic residues resulted in a dramatic decrease in fusion. To that end, this same HRB-linker domain has also been demonstrated to have an important role in fusion for PIV5 F, so work to determine whether either region—HRA or HRB-adjacent residues—display primacy over the other with regard to importance in triggering HMPV fusion was also conducted.

These studies began with a ClustalW alignment of select paramyxoviral F proteins within the aforementioned domains (Figure 1.5). An enrichment in charged residues at the HRA-F_2 interface was observed for HMPV F relative to all other paramyxoviral fusion proteins. Considering the role of electrostatics in influenza HA-mediated fusion and that HMPV F is the only member of the family to require fusion at a pH below neutral, further study into the role of intramolecular electrostatic interactions in HMPV F and their effects on triggering fusion at different pH levels were the focus. Among the novel charged residues, substitution of E51, D54 and E56 resulted in drastic alterations to fusion activity, demonstrating their important role in the triggering and stability of the fusion protein. The results of these studies elaborate on the underlying mechanism of HMPV F-mediated membrane fusion triggering and posit that such interactions in multiple regions throughout the molecule impel conformational changes.

.

Subsection III: HMPV Replication & Assembly

In contrast to what is known about paramyxoviral fusion and entry, both generally and specifically regarding HMPV F function, there have been virtually no studies conducted on the ensuing steps in the infectious cycle, namely RNA synthesis and replication. There are currently very few articles in the literature that specifically addresses the RNP components of HMPV specifically. The authors of that publication characterize the ability of the HMPV nucleocapsid protein (N) and phosphoprotein (P) to interact when synthesized *in vitro* as measured by a variety of biochemical methods [30]. Additionally, they report these proteins to be the minimal component for the formation of viral inclusion bodies. Further, evidence from other viral systems suggests these bodies may be the major site of viral RNA synthesis [46-47]. Another paper discusses the ability of the polymerases of HMPV and avian metapneumovirus (AMPV) to complement one another [29]. The study found that attenuation of HMPV was observed *in vivo* when its polymerase gene was exchanged with that of AMPV while less pronounced effects had been observed *in vitro*.

While these studies represent an excellent beginning to replication studies for this virus, it certainly is only that—a beginning. Currently, many aspects of HMPV replication and processes downstream of that, including viral assembly, are based on research conducted on other negative strand viruses. While this extrapolation is understandable given the conserved mode of action amongst these viruses and the proteins used to carry them out, this work describes some aspects which have not been reported explicitly for other negative strand viruses.

Upon gaining entry to the host cell, the virus utilizes its own RNA-dependent RNA polymerase (RdRp) to synthesize mRNA from its genomic RNA, which is encapsidated with a helicoidal nucleocapsid protein [48]. The RdRp is composed of the large protein (L) and its obligate cofactor P. The gene encoding the L protein occupies nearly half of the HMPV genome, and the protein is thought to contain all enzymatic functionality for the RNA synthesis, including an active site, methyltransferase and guanylyltransferase. These area regions of enzymatic activity have been demonstrated to be well-conserved among *Mononegavirales* into discrete domains that may even fold independently of one another [49-50].

There is some structural evidence to support L oligomerization, as electron micrograph results with VSV L suggest that dimerization occurs, though it is as yet unclear if this is relevant in the context of infection [50-52]. Work with several viruses within *Mononegavirales* suggest a mechanism by which P, as an oligomer, may deter aggregation of the large protein in the cytosol, allowing for proper folding and catalytic activity of the polypeptide in the RdRp complex [53]. In addition to this possible chaperone-like role, the phosphoprotein is the sole component within the viral complement of proteins that directly contacts both the nucleocapsid protein as well as the large protein, bringing the conserved Domain II of L in proximity with an encapsidated RNA template [54].

The mono- and polycistronic RNA transcripts produced by the RdRp include a 7-Me-guanosine cap and poly-A tail, making them indistinguishable from cellular mRNA (Figure 1.5) [51, 55-59]. Among other observations in negative strand viruses, is an apparent correlation between the abundance of a viral protein during infection and its distance from the 3' promoter, resulting in a gradient where the most proximal gene, N, is most abundant and the most distal gene, which encodes the large protein is the least. This gradient has been implicated by some in the regulation of different activities of the RdRp, namely viral gene transcription and synthesis of antigenomic RNA. It is accepted that viral transcription likely precedes genomic replication [2, 60].

One challenge for HMPV and similar viruses is that all RNA synthesis occurs in the cytosol where naked RNA would readily elicit a strong immune response through RNA detection proteins such as RIG-I or MDA5 [61]. Encapsidation provides some protection of viral RNA, but that may not be the only viral counter measure. Much of the synthesis process is posited to occur within viral inclusions, which are punctate structures within infected cells with concentrated amounts of viral RNA and RNA-associated proteins. In fact, there is some evidence for RNA to synthesis to occur in these structures at least initially in the case of rhabdoviruses, such as rabies and vesicular stomatitis virus (VSV) [46-47]. However, no such study exists for any paramyxovirus, though it has been shown that the minimal composition of such bodies does appear to be the N and P proteins for HMPV [30].

The presence of paramyxoviral RNP proteins and complexes thereof—namely L, P and N—within inclusion bodies during infection is well established [62-64]. Inclusion bodies have been observed readily in hRSV, and techniques such as immunofluorescence microscopy have even offered a glimpse of the potential organization of these bodies in the case of hRSV infection [65]. Within infected cells these punctate structures show the large protein is present exclusively at the periphery while both the phosphoprotein and— to a greater degree—nucleocapsid proteins permeate the bodies. By contrast, a more diffuse pattern is observed when antibodies specific to the hRSV matrix protein are used to probe the cell. However these experiments, while informative, do not take into account changes over time as they were all performed at a single point post infection.

Such an arrangement may not only further shield viral RNA from the innate immune system in the cytosol but also allow for a vast interacting face of the large protein to be exposed to the cytosol. Such an arrangement would be an efficient strategy for binding necessary host cell factors while maintaining any polymerase activity or viral protein contacts. It should be noted, however, that no study has shown the temporal-spatial relationship of these proteins with regard to where they localize throughout HMPV infection. This aim is a focus of the research presented herein. This work includes a timecourse study of HMPV-infected cells which suggests the hypothesis that inclusions are potential sites of RNA replication, as metabolically-labeled RNA species were detected in bodies at all times post-infection similar to those containing HMPV N and/or P.

For efficient infection, the virus must be able to balance polymerase activity between that of transcription of open reading frames and replication of the entire genome from antigenomic templates [66-67]. Therefore my thesis work also examined the initiation of these events through manipulation of the promoter properties. The two viral promoters, the 3' leader and 5' trailer complement (as oriented in the genomic RNA), are canonically responsible chiefly for mediating RNA transcription and genome replication, respectively [68]. As viral RNA polymerization always occurs at the 3' end of the linear nucleic acid template, the polymerase will bind the leader on the negative sense genomic RNA and either stop at gene junctions to create mRNA or read through these to synthesize a full-length antigenome, which will serve as a genomic template via binding of the polymerase at its 3' promoter, the trailer (Figure 1.5) [2]. Additionally, the 36 nucleotide trailer-terminal sequence (TTS) of hRSV has been shown to be indespensible for proper encapsidation of progeny RNA [69]. Despite quite a bit of understanding of hRSV and its promoter dynamics, there is no such analysis present for HMPV; as such, comparative studies between the two systems were performed as a part of this research to gain understanding on the differences between the two pathogens in this regard.

This work offers data to suggest that there are signficant differences in the promoter efficiency between HMPV and hRSV despite large sequence conservation and similar predicted RNA structure. Further, it appears that the TTS, which found is absent in HMPV may be responsible for some of this observed difference in viral promoter strength. This work represents a first step in the process of elucidating the contribution of

promoter-polymerase dynamics as a factor in the large-scale ability of a virus to efficiently establish a productive infection in host cells.

While it is crucial to understand where and when the viral RNP goes about RNA synthesis over the course of infection, the story is incomplete without addressing how these same proteins facilitate the exit of nascent virions from the infected cell. Again, quite a bit can be carefully inferred about the workings and interplay of the HMPV nonstructural proteins from previous studies in closely related systems. For example, these viral proteins often exhibit high levels of intrinsic disorder, likely to enable maximal plasticity with regard to interacting partners (both viral and cellular) [70].

Such flexibility is displayed throughout *Mononegavirales* and lends itself to different activities being performed by the same factors throughout infection; this is made more complex when one also considers the importance of the temporal component of viral infection. Different interactions can (and must) be made at specific points during infection to further the overall process [71]. This interplay of numerous interactions along with temporal and spatial pleiotropy throughout infections enable a relatively small number of viral factors to be the initiators for all steps necessary to produce a substantial infection in host cells, including entry, RNA synthesis, virion assembly and egress from cells.

The potential role of inclusion bodies in the centralization of RNA synthesis has already been discussed; however there is also a broader question concerning these bodies and

their long-term fate within an infected cell. If these sites are RNA replication centers, it is unclear whether and by what mechanism they incorporate into the HMPV assembly machinery or if there is no difference between the two and it is simply a case of maturation and differential protein recruitment and organization. While characterization of protein-protein interactions that govern HMPV infection is key to gaining insight into the underlying mechanisms of HMPV infection, this goal cannot be fully attained without first understanding the spatial and temporal link between viral factors and activity at the whole-cell level.

Thusly, this work also features studies seeking to shed light on the overlying HMPV infectious cycle at the cellular level by focusing on the interplay between HMPV N and P throughout the entire process. We report that overexpression of HMPV N morphologically mimics early stages of HMPV infection, such as 6 hours post infection (hpi), with the protein seemingly aggregating. Conversely, overexpression of HMPV P leads to peripheral localization and induction of filamentous extensions at the plasma membrane—a cellular visage more similar to a more progressive stage of infection. Interestingly, co-expression of HMPV N with a phosphoprotein construct that does not localize to inclusions leads to tight co-localization at the cellular periphery, suggesting that HMPV P may be modulating some of the characteristic late-stage morphology of HMPV infection. Taken together, these results suggest a model in which HMPV P may favor activities directed toward egress while HMPV N may enhance assembly and/or RNA synthesis. Productive infection requires interactions between these proteins in which one may exert dominance over the other at different points during infection.

Overall, these studies examine various points throughout HMPV infection that represent irreversible checkpoints. Whether it be the triggering of membrane fusion under permissive conditions, the ramping up of viral RNA synthesis and the underlying processes that mediate this event or the conglomeration of the HMPV nonstructural proteins at later stages of infection, the overarching theme is an analysis of the orchestrated steps by which an HMPV particle first encounters a host cell through the time at which progeny virus egress.
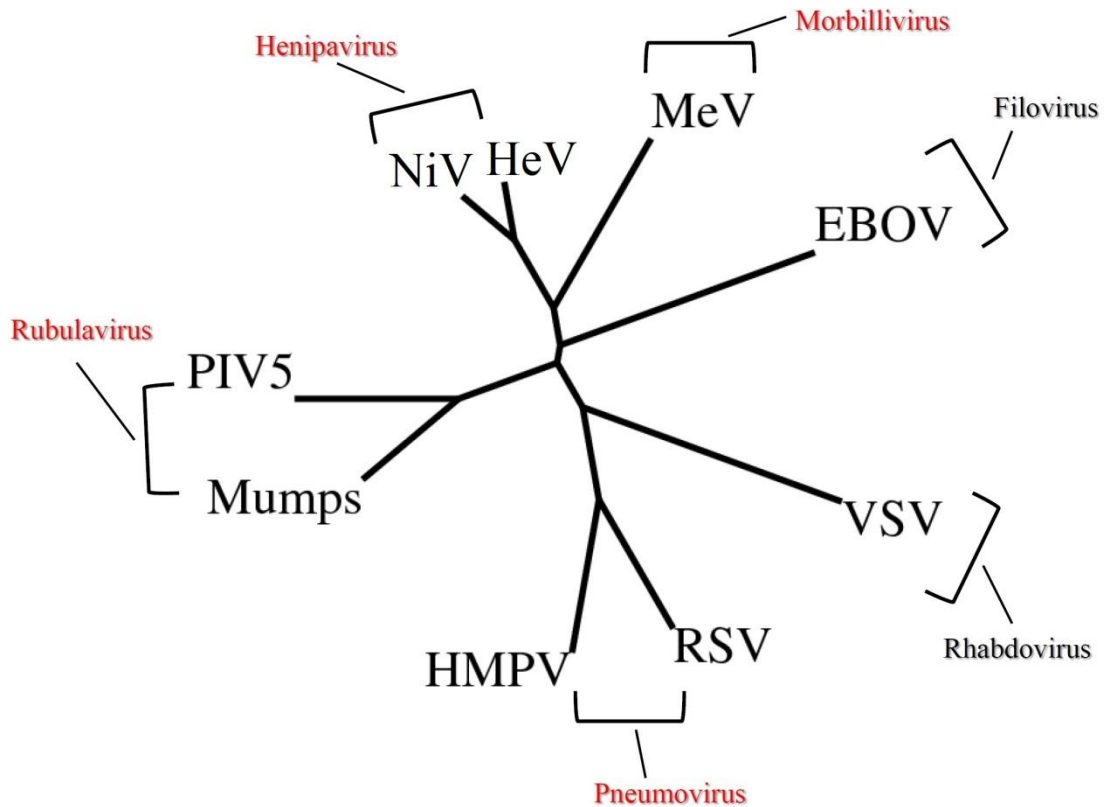
Figure 1.1. Phylogenetic tree lineage analysis of negative-sense RNA viruses.

The phylogenetic tree diagram illustrates the diversity of select members of the order *Mononegavirales* based upon primary protein sequence similarity of the phosphoprotein. Longer branches indicate greater phylogenetic distance between viruses. Subfamilies within *Paramyxoviridae* highlighted in red while distinct viral families are denoted in black. HMPV falls into its own subfamily with hRSV within the paramyxoviral family.
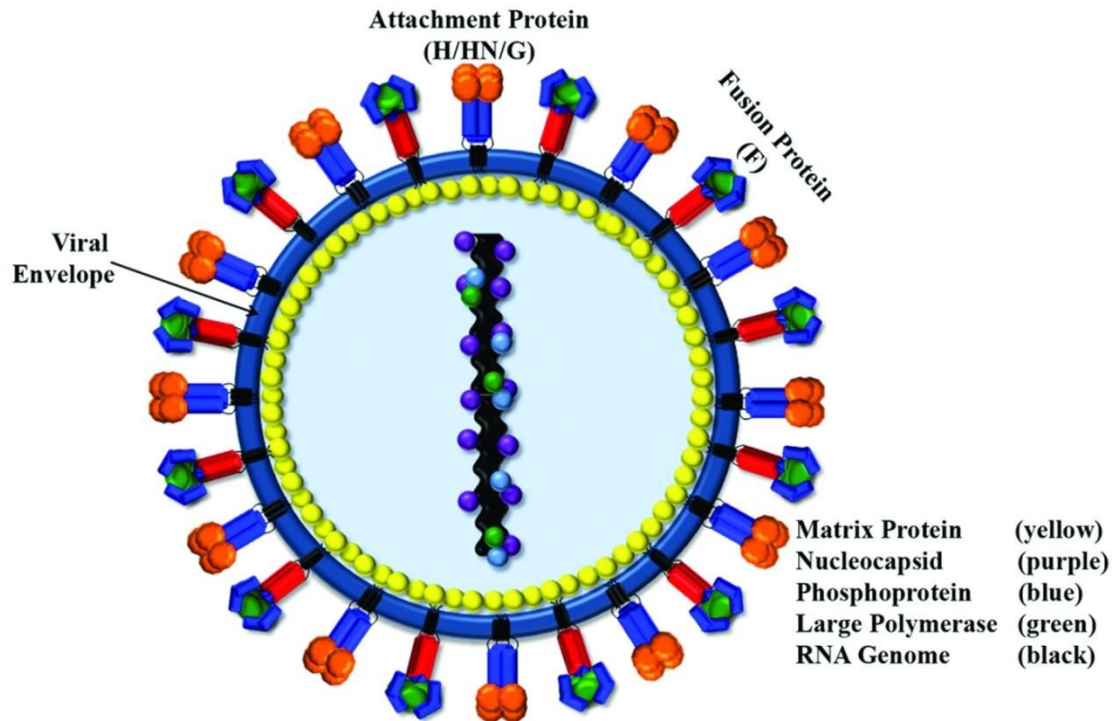
Figure 1.2. Architecture of a generalized Paramyxovirus infectious particle.

Paramyxoviruses produce pleiomorphic virions that contain a ribonucleoprotein core, also known as the nucleocapsid. It contains all necessary components necessary for viral RNA synthesis, including the negative-sense RNA gene as well as the N, P and L proteins. The viral envelope is the outer leaflet of the particle's host-derived lipid bilayer and contains the spike glycoproteins F and G about its surface while the matrix protein is closely associated with the inner leaflet of the bilayer, maintaining the virion's shape. Image reused with permission from journal (modified from Smith EC, et al. *FEBS J.* 276(24):7217-27, 2009).
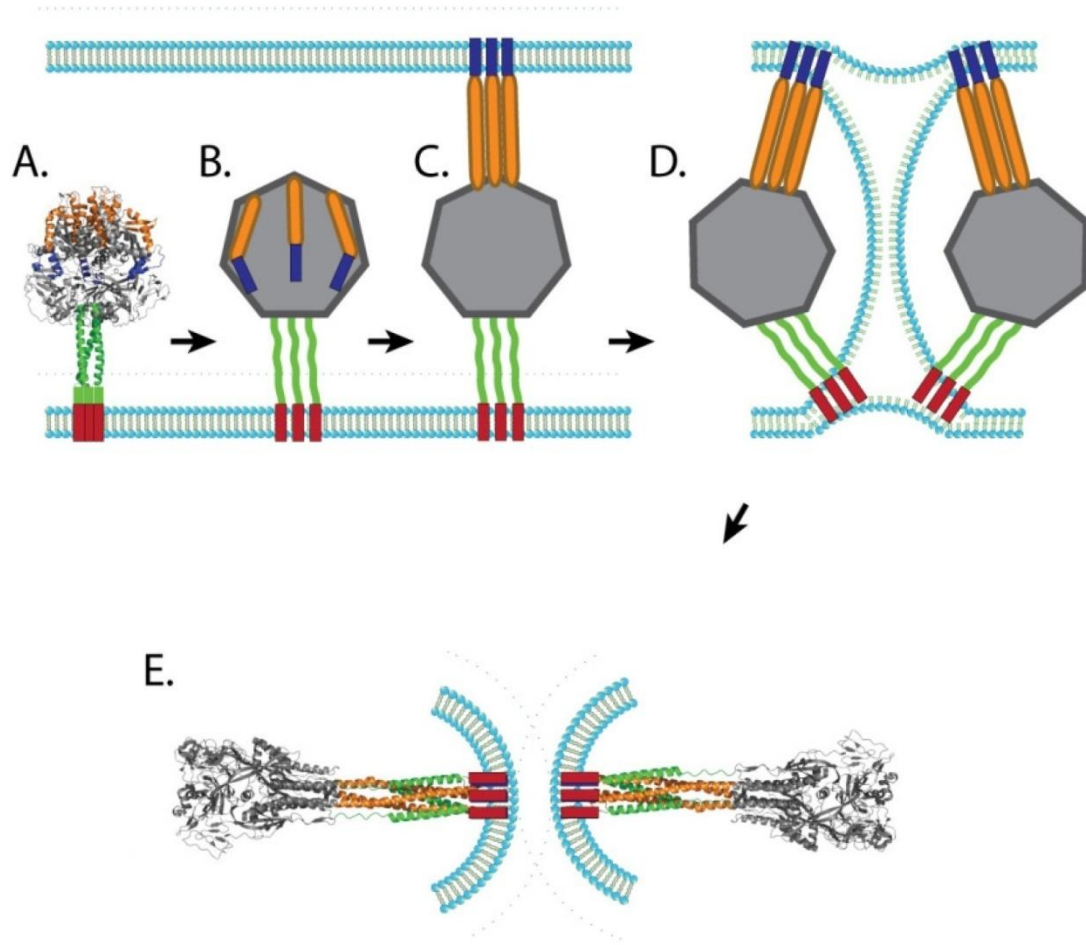
Figure 1.3. Schematic of the Class I viral fusion mechanism.

This cartoon depicts the Class I viral fusion protein mode of action. (A) The metastable prefusion form is triggering, (B) releasing the fusion peptide, (C) which then inserts into the target membrane. (D) The protein undergoes a large-scale conformational rearrangement such that the two sets of exposed heptad repeats coalesce to form a (E) six-helix bundle, resulting in the irreversible postfusion conformation. The consequence of the proteins actions is lipid mixing between the outer leaflets of the two bilayers and fusion pore formation. Image reused with permission from journal (modified from Chang A, et al. *Viruses* 4(4):613-36).
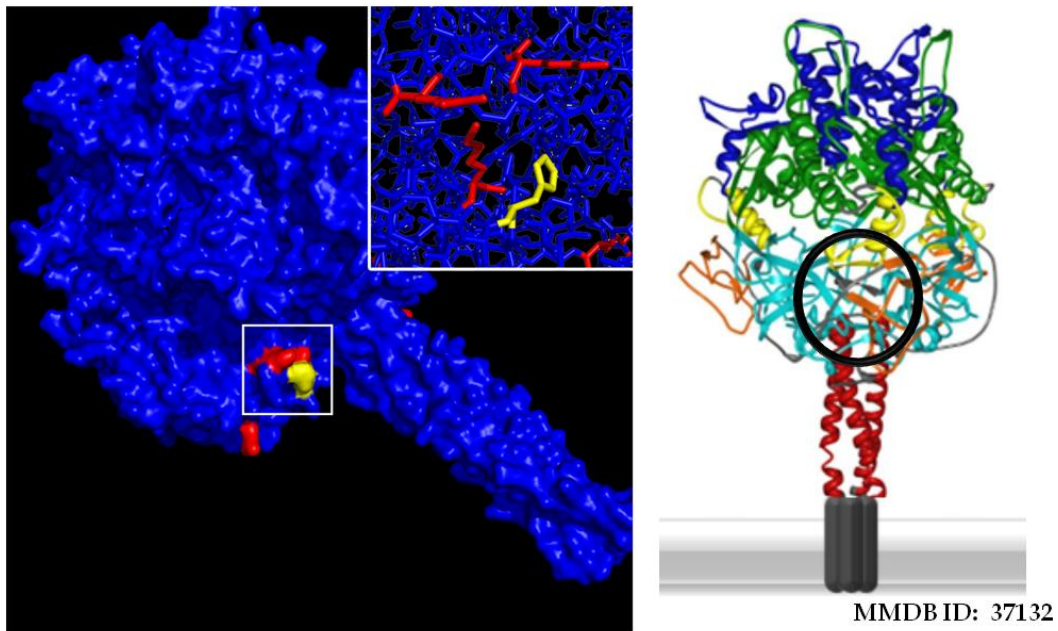
MMDB ID: 37132

Figure 1.4. HMPV F models well onto the PIV5 F crystal structure.

HMPV CAN97-83 fusion protein was threaded through the PIV5 F crystal structure (MMDBID: 37132). The modeling exhibited high similarity to the original structure with no secondary structural anomalies, such as prolines or glycines modeled within alpha helices. Further, the disulfide linkage that is common among all paramyxoviral F proteins is properly oriented with the cysteine residues in register to form such a bond. The inset of the homology model (left) illustrates the predicted orientation of H435 (yellow) about several adjacent positively-charged moieties (red). The region is also circle within the PIV5 crystal structure (right).
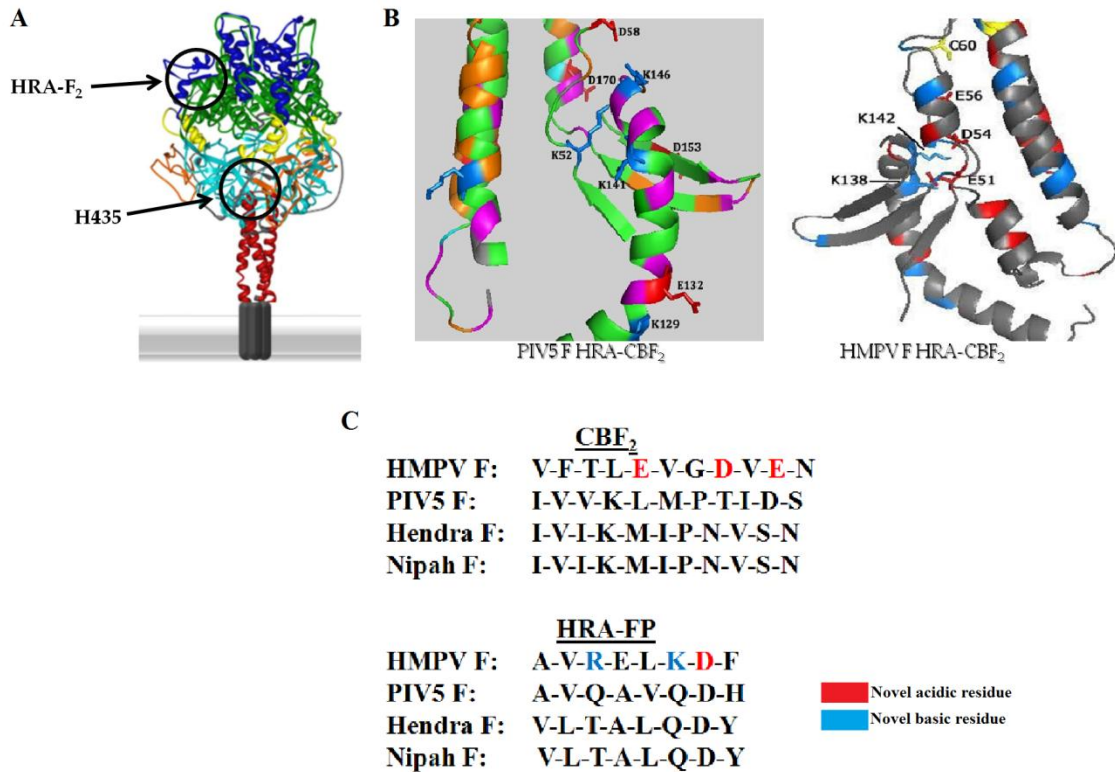
Figure 1.5. HMPV F is enriched with charged amino acids in the F2-HRA region.

(A) Illustration of approximate location of areas of interest within HMPV F using the PIV5 F crystal structure. (B) Comparison of HMPV F CAN97-83 and PIV 5 F homology within HRA-F2 region. Select charged residues are labeled in each rendering. (C) HMPV F (amino acids 47-57 [top] and 161-168 shown) was aligned to other viral fusion proteins using the ClustalW alignment tool. The conserved block F2 (CBF2) region possesses a much greater amount of charged amino acids relative to the other viral fusion proteins. There were also novel charged amino acids observed in the heptad repeat A (HRA) region of HMPV, the adjacent area to CBF2 in prefusion models of the protein. The circled residues were selected for further study and site-directed mutagenesis.
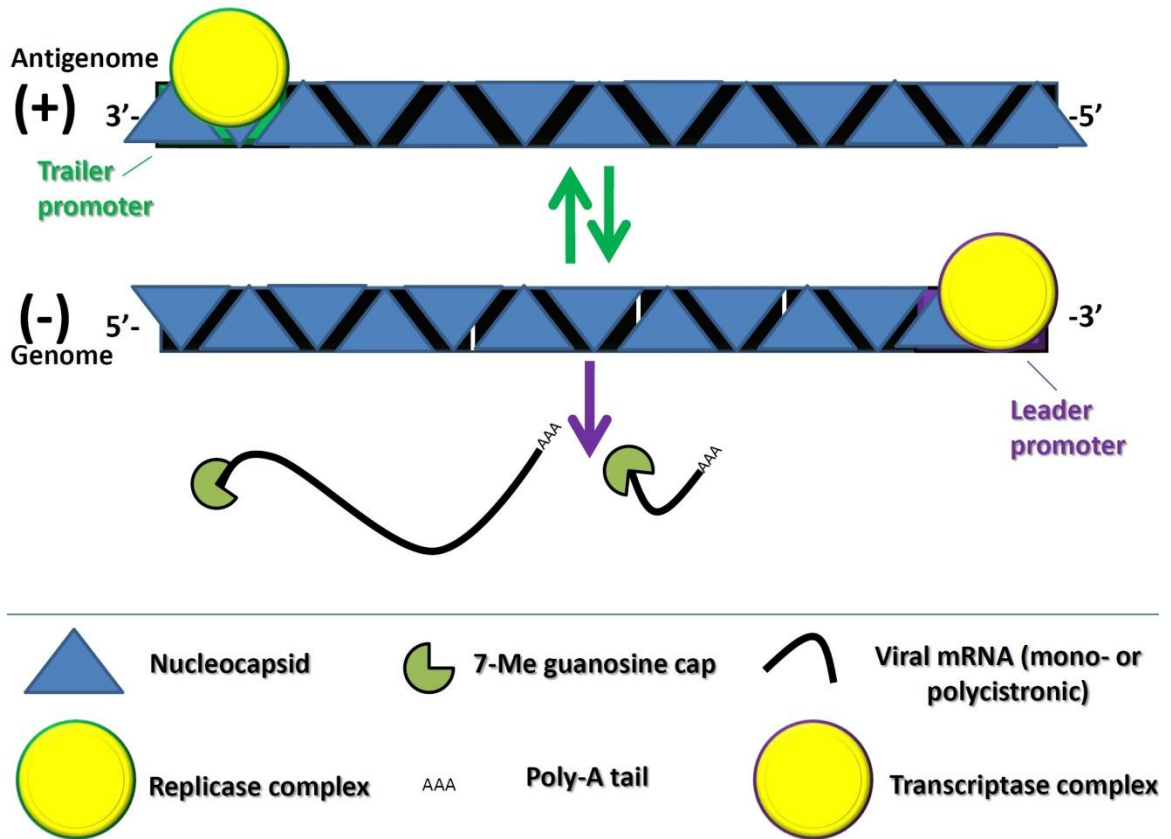
Figure 1.6. Paramyxoviral RNA synthesis requires two promoters.

Nucleocapsids are shown as arrays of triangles, each binding six nucleotides of viral RNA, with white lines denoting gene junctions. During transcription, the polymerase reads from the 3' end after initiating synthesis at the leader promoter region. It synthesizes capped, poly-adenylated mRNA transcripts made by stopping and restarting at each junction. These are read through during replication, yielding antigenomic RNA, which serves as a template for more RNA genomes by synthesis initiated at the trailer promoter region.

Chapter II: Methods and Materials

Subsection I: HMPV Fusion Project

Cell Lines. Vero and BSR cells (provided by Karl-Klaus Conzelmann, Max Pettenkofer

Institut) were grown in Dulbecco's modified Eagle's medium (DMEM; Gibco Invitrogen,

Carlsbad, CA), supplemented with 10% fetal bovine serum (FBS) and 1% penicillin and

streptomycin (P/S). The media of BSR cells was supplemented with 0.5mg/mL G418

sulfate (Gibco Invitrogen, Carlsbad, CA) every third passage to select for T7 polymerase

expression.

Plasmids and Antibodies. The HMPV F gene within the pGEM-3Zf(+) vector was

provided by Ursula J. Buchholz (NIAID, Bethesda, Maryland) with permission from Guy

Boivin (Centre Hospitalier Universitaire de Québec, Quebec City, Quebec, Canada). The

HMPV F H435R, H435K, H435D, H435E, E51A, D54A, E56A, R163A, R166A, E51K,

E51K/H435R, D54A/E56A, D54A/E56A/H435R, D54A/H435R, E56A/H435R,

D54N/E56Q, and D54N/E56Q/H435R protein mutants were created using QuikChange

site-directed mutagenesis according to manufacturer's protocol (Stratagene). The HMPV

F wild type (WT) and mutant genes were released from pGEM-3Zf(+) and ligated into

the pCAGGS mammalian expression vector and sequenced in their entirety after ligation.

Antipeptide antibodies against HMPV F (Genemed Synthesis, San Francisco, CA) were

generated using amino acids 524-538 of HMPV F.

Viruses. Recombinant, GFP-expressing HMPV (rgHMPV) strain CAN97-83, a genotype group A2 virus with a codon stabilized SH gene (2) was kindly provided by Peter L. Collins and Ursula J. Buchholz (NIAID, Bethesda, Maryland). HMPV, at a starting MOI of 0.01, was propagated in Vero cells incubated at 32°C with Opti-MEM supplemented with 200mM L-glutamine and replenished with 0.3µg/mL TPCK-trypsin every day. On the seventh day, cells and media were collected and frozen at -80°C. The virus-containing solution was thawed to 37°C and subjected to centrifugation at 2500 rpm for 10 min at 4°C on a Sorval RT7 tabletop centrifuge. The supernatant was then subjected to a centrifugation over a 20% sucrose cushion for 2 hours and fifteen minutes at 27,000 rpm 4°C using a SW28 swinging bucket rotor on a Beckman Optima L90-K Ultracentrifuge. The resulting pellet was resuspended in 500µL of Opti-MEM, left at 4°C overnight, divided into aliquots the next morning and stored at -80°C. Viral titers were performed by on a 96-well plate and counting the number of GFP-expressing cells the following day.

Syncytia Assay in Transfected Cells. Subconfluent monolayers of Vero cells plated in 6-well plates were transiently transfected with a total of 0.5µg of DNA consisting of pCAGGS-HMPV F WT, pCAGGS-HMPV F protein mutants, or the empty pCAGGS vector (MCS control) using Lipofectamine and Plus reagents (Invitrogen) according to the manufacturer's instructions. The next morning, confluent cell monolayers were incubated at 37°C in 1mL Opti-MEM with 0.3µg/mL TPCK-trypsin for 1.5 hours. Cells were then subjected to four 4-minute pH pulses every 2 hours with 1 mL of PBS of the indicated pH buffered with 10mM HEPES and 10mM MES at 37°C. After an overnight

incubation at 32°C in order to allow final cellular rearrangements to take place, digital photographs of syncytia were taken with a Spot Insight Firewire digital camera mounted on a Carl-Zeiss Axiovert 100 inverted microscope using a 10x objective (Thornwood, NY).

Reporter Gene Fusion Assay. Vero cells in sixty-millimeter dishes were transfected with 0.55μg pCAGGS-HMPV F wild type (WT) or mutant F protein and 0.55μg T7 control plasmid (Promega, Madison, WI) containing luciferase cDNA under control of the T7 promoter using Lipofectamine and Plus reagents according to the manufacturer's instructions. The following day, Vero cells in one sixty-millimeter dish were lifted from the plate surface and subjected to centrifugation at 1300 rpm, 4°C in a Sorval RT7 tabletop centrifuge for 5mins. Cells were resuspended in 2 mL of DMEM plus 10% FBS and 1% P/S and overlaid onto two 35-millimeter dishes of confluent BSR cells (1mL of Vero cells per 35-millimeter dish). Cells were incubated at 32°C for 1.5 hours and then treated with 1mL of PBS of the indicated pH buffered with 10mM HEPES and 10mM MES for 4 minutes at 37°C. Buffered PBS was replaced by 1mL of Opti-MEM with 0.3μg/mL TPCK-trypsin and the pH pulse was repeated one hour after. Cells were then incubated in 2mL DMEM with 10% FBS and 1% P/S at 37°C for 4 hours to allow for luciferase production. Luciferase activity was assessed using a luciferase assay system (Promega) according to manufacturer's protocol. Light emission was measured using an Lmax luminometer (Molecular Devices, Sunnyvale, CA) for 5 seconds with a 1.6 second delay between each measurement.

Protein Expression, Metabolic Labeling, Surface Biotinylation, and Immunoprecipitation. Cells in sixty-millimeter dishes were transfected with 1.10μg pCAGGS-HMPV F wild type (WT) or mutant F proteins (empty pCAGGS as control MCS) using Lipofectamine and Plus reagents according to manufacturer's' protocol. At 18-24 h post-transfection, cells were starved in methionine- and cysteine-deficient DMEM for 1 hour and then metabolically labeled with Tran[^{35}S] label (100μCi/mL; Perkin-Elmer) with 0.3μg/mL TPCK-trypsin for 4 hours. Following radiolabeling, cells were washed three times with ice-cold pH 8 PBS and surface proteins were biotinylated with 1mg/mL EZ-Link Sulfo-NHS-Biotin (Pierce, Rockford, IL) diluted in pH 8 PBS for 30 minutes, rocking at 4°C and then for 20 min at room temperature. Cells were lysed in 1mL RIPA buffer containing 1 KalliKrein inhibitory unit of aprotinin (Calbiochem, San Diego, CA), 1mM phenylmethylsulfonyl fluoride (Sigma, Saint Louis, MO) and 25mM iodoacetamide (Sigma) after removal of the biotin solution. The lysates were subjected to centrifugation at 136,500 × g for 15 min at 4°C, and supernatants were collected. Antipeptide sera and protein A-conjugated sepharose beads (Amersham, Piscataway, NJ) were used to immunoprecipitate the F proteins as previously described (27). Immunoprecipitated protein was boiled away from the beads using a total of 100μL of 10% SDS (40μL for first boil and 60μL for second boil). Fifteen percent of total protein collected was used for total expression analysis and the remaining 85% was diluted in 500μL biotinylation dilution buffer (20mM Tris [pH 8], 150mM NaCl, 5mM EDTA, 1% Triton X-100, 0.2% bovine serum albumin) and incubated with immobilized streptavidin (Thermo Scientific, Rockford, IL) for 1 hour at 4°C. Samples were washed, resolved by

SDS-15% polyacrylamide gel electrophoresis (SDS-PAGE), and visualized using the Typhoon imaging system.

Homology modeling. A model of the prefusion conformation of the HMPV F protein was generated via a threading methodology from the molecular coordinates (mmdbId: 37132) determined from the crystal structure of the prefusion form of PIV5 F [35]. Modeling was performed with DeepView/Swiss-PdbViewer v4.0.1 (www.expasy.org/spdbv) as previously described [72]. This method yielded a protein that maintained all predicted secondary structure (e.g. no glycine or proline in alpha helices) and disulfide linkages (Figure 1.4).

Subsection II: HMPV Minireplicon Project

Plasmid vectors. The HMPV P and M2-1genes were synthesized by RT-PCR from HMPV strain CAN97-83 and cloned into the pCAGGS expression vector using EcoRI and either XhoI or ClaI, respectively. Codon-optimized HMPV N and L genes (provided by Dr. Ursula J. Buchholz, NIAID, Bethesda MD) were also expressed in pCAGGS. The RSV luciferase minigenome plasmid was a generous gift from Dr. Richard Plemper (Emory University, Atlanta, GA) in addition to the RSV N, P, L and M2-1 vectors. PIV5 N, P and L plasmids were provided by Dr. Anthony Schmitt (Pennsylvania State University, University Park, PA). PCR extension was implemented in order to obtain the HMPV P-FLAG construct from the wildtype construct within a pGEM2X vector. This method was also employed to add the RSV trailer-terminal sequences to the HMPV minireplicon plasmids.

Viruses. Recombinant, GFP-expressing forms of different viruses were provided by the following: hRSV by Mark Peeples (Ohio State University), parainfluenza virus 5 (PIV5) by Robert Lamb (Howard Hughes Medical Institute, Northwestern University) and vesicular stomatitis virus (VSV) by Michael A. Whitt (University of Tennessee Health Science Center, Memphis, Tennessee).

Minireplicon assay. BSR cells were grown overnight in 24-well plates and then co-transfected with a specific minireplicon plasmid along with other various combinations of DNA constructs (total of 2.5µg) with Lipofectamine LTX and Plus reagents according to manufacturer's protocol. After overnight incubation, cells were washed twice with PBS

and dispensed 1mL/well DMEM with FBS and antibiotic was added. Cells were then incubated at 37°C for 1h prior to infection at an MOI of 5 with specific virus stock or SPG buffer (mock infection). Again cells were incubated overnight with virus stock at 37°C. 24 or 36 hours post infection, cells were washed twice with PBS and lysed in 0.1mL Promega 1X reporter gene lysis buffer. Plates were then briefly stored at -20°C before being thawed. Lysates were transferred to centrifuge tubes on ice and spun at 13,000rpm for 1 min at 4°C. 25µL of the supernatant was then transferred to an opaque luminometer plate. Luciferase activity was assessed using a luciferase assay system (Promega) according to manufacturer's protocol. Light emission was measured using an Lmax luminometer (Molecular Devices, Sunnyvale, CA) for 30 seconds with a 1 second delay between each measurement.

Subsection III: HMPV Assembly Project

Cell Lines. A549 cells (provided by Hsin-Hsiung Tai, University of Kentucky) were grown in RPMI medium supplemented with 10% FBS and 1% P/S.

Antibodies. HMPV P rabbit antiserum was kindly provided by Dr. John V. Williams (Vanderbilt University, Nashville TN). Monoclonal antibodies against HMPV P (NBP-21631, Novus Biologicals, Littleton, CO) and HMPV N (ab94802, Abcam, Cambridge, MA) were purchased commercially.

Protein Expression, Metabolic Labeling, and Immunoprecipitation. A549 cells in thirty-five millimeter dishes were transfected with 2.75µg HMPV N, P or L constructs in pCAGGS (empty vector as control [MCS]) using Lipofectamine LTX and Plus reagents according to manufacturer's protocol. At 18-24 h post-transfection, cells were infected or mock infected for 24h. Cells were then starved of methionine and cysteine in DMEM lacking these amino acids for 30min and metabolically labeled with Trans[35S] label (100µCi/mL; Perkin-Elmer) for 4 hrs. Following radiolabeling, cells were washed three times with ice-cold pH 7.2 PBS before being lysed in 0.5mL lysis buffer (20mM Tris-HCl pH 7.5, 150mM NaCl, 1mM Na2EDTA, 1mM EGTA, 1% Triton-X 100, 2.5mM sodium pyrophosphate, 1mM beta- glycerophosphate, 1mM sodium orthovanadate, 1µg/ml leupeptin). The lysates were subjected to centrifugation at $136,500 \times g$ for 15 min at 4°C, and supernatants were collected. Antipeptide sera or monoclonal antibodies and protein A-conjugated sepharose beads (Amersham, Piscataway, NJ) were used to immunoprecipitate the proteins of interest as previously described above. Samples were

washed, resolved by SDS-15% polyacrylamide gel electrophoresis (SDS-PAGE), and visualized using the Typhoon imaging system.

Western Blotting. Following transfection or infection as previously described, A549 cells in thirty five millimeter dishes were lysed in 0.5mL RIPA buffer containing and 1X concentration of Complete Mini protease inhibitor cocktail (Roche, Indianapolis, IN). Lysates were then homogenized and centrifuged at 13,000rpm for 25min at 4°C. The supernatants were then collected and either treated with antibodies and protein-A sepharose beads as described above or fractions of whole lysates were resolved by 15% SDS-PAGE. Proteins were then transferred to PVDF membranes (Millipore, Billerica, MA) with a BioRad Trans-Blot SD semi-dry transfer cell and transfer buffer (48mM tris, 38.9mM glycine in 20% methanol). Antibody dilutions were conducted in 5% milk tTBS with primary incubation overnight and secondary for 1h, both at 4°C. Proteins were visualized using the Odyssey infrared imaging system (LI-COR, Lincoln, NE).

Immunofluorescent detection of proteins. Following treatments, A549 cells on glass coverslips within thirty five millimeter dishes were washed three times with pH 7.2 PBS+0.02% NaN3 (PBSN) before being fixed with 4% formaldehyde for 15 minutes at RT. Cells were washed twice more in PBSN then permeabalized with 1% Triton X-100 at 4°C for 15 minutes. Coverslips were then blocked in PBSN containing 1% FBS for at least 1h before administration of primary antibodies in the same buffer overnight at 4°C. Secondary antibodies were applied in the dark at 4°C for 1h before mounting coverslips

to glass slides with Vectashield mounting medium (Vector Laboratories, Burlingame, CA).

Confocal microscopy. Immunofluorescence images were acquired from the Nikon A1confocal microscope and processed using NIS Elements software (Nikon Instruments, Melville, NY).

Measurement of viral particle release from infected cells. A549 cells were infected with HMPV viral stock (MOI=5) in sixty millimeter dishes as previously described for variable lengths of time with the medium being changed at 4h post infection. At the end of the infection period, the whole supernatant was collected and stored at -80°C overnight. The medium was thawed to 37°C, centrifuged at 2500rpm for 10min at 4°C on a Sorval RT7 tabletop centrifuge with the supernatant then subjected to centrifugation over a 20% sucrose cushion for 2.5h at 27,700rpm 4°C using a SW41 swinging bucket rotor on a Beckman Optima L90-K Ultracentrifuge. The resulting pellet was resuspended in 30μL OptiMEM and boiled for 10min prior to being resolved with 15% SDS-PAGE. Western blotting was conducted as previously described.

BrUTP incorporation into cellular RNA and detection. The protocol for this experiment was adapted from one previously described for VSV [20]. Briefly, BSR cells on glass coverslips within thirty five millimeter dishes were infected with WT HMPV stock (MOI=5) for variable lengths of time. Five hours prior to the end of the infection period, cells were washed with PBS and dispensed glucose-free DMEM supplemented with 1mM glucose and 20mM GlcNac for a period of 2h. A portion of the same media

was then pre-incubated at RT with 10mM 5-bromouridine 5′-triphosphate sodium salt (Sigma) and Lipofectamine 2000 for 30min prior to being added to the cells for 3h. Cells were then fixed with 2% paraformaldehyde for 15min at RT, treated with ice cold methanol for 3min and then permeabalized in PBS containing 1% bovine serum albumin (PBSA) and 0.1% Triton X-100 for 10min at RT. Cells were blocked overnight in PBSA then treated with anti-BrdU mouse monoclonal antibody conjugated to AlexaFluor488 (Invitrogen) diluted 1:50 overnight in PBSA+0.05% Triton X-100 (PBSAT). GAM-FITC (Jackson ImmunoResearch Laboratories, West Grove, PA) was added at 1:300 in PBSAT for 1h before mounting coverslips to glass slides.
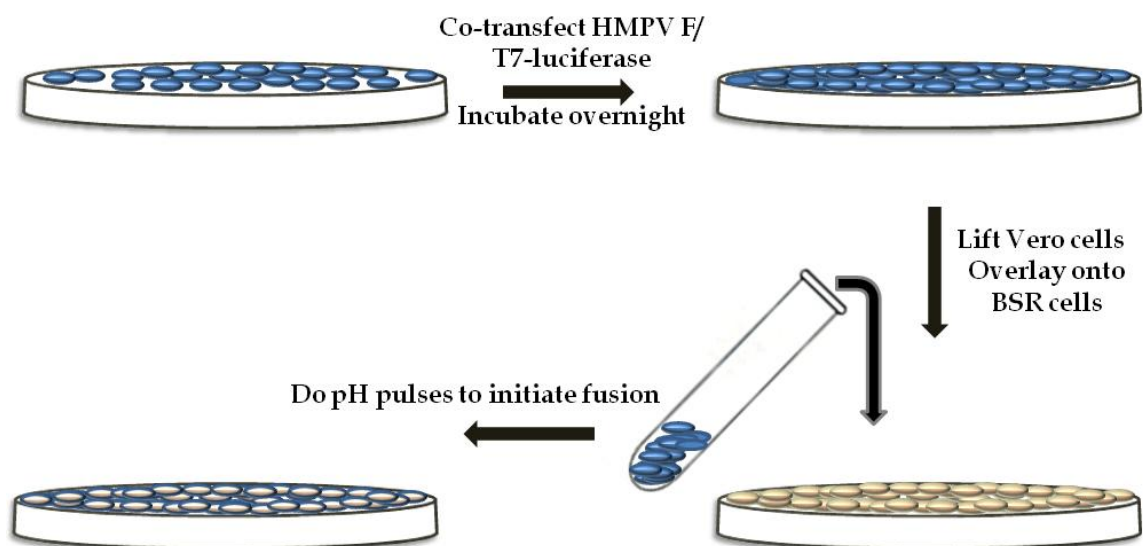
Figure 2.1. HMPV reporter gene fusion assay protocol.

The reporter gene fusion assay is similar to the syncytia assay in that a plasmid encoding HMPV F is transfected into Vero cells to gauge fusogenicity. However, in addition to HMPV F, a T7 luciferase construct is co-transfected. Luciferase is an enzyme whose expression can be quantified by the measurement of the product of the chemiluminescent reaction it catalyzes. In this case, the enzyme can only be expressed in the presence of the T7 polymerase, which is lacking in Vero cells. 24 hours post-transfection, the Veros are lifted and overlayed onto BSR cells, which constitutively express T7 polymerase. After allowing for attachment of the cells, 2 minute pH pulses are perfomed. Ultimately, active fusion proteins will be able fuse the membranes of the Vero and BSR cells, allowing for expression of luciferase. At that point, a luminometer can quantify luciferase expression as a readout on fusion activity.
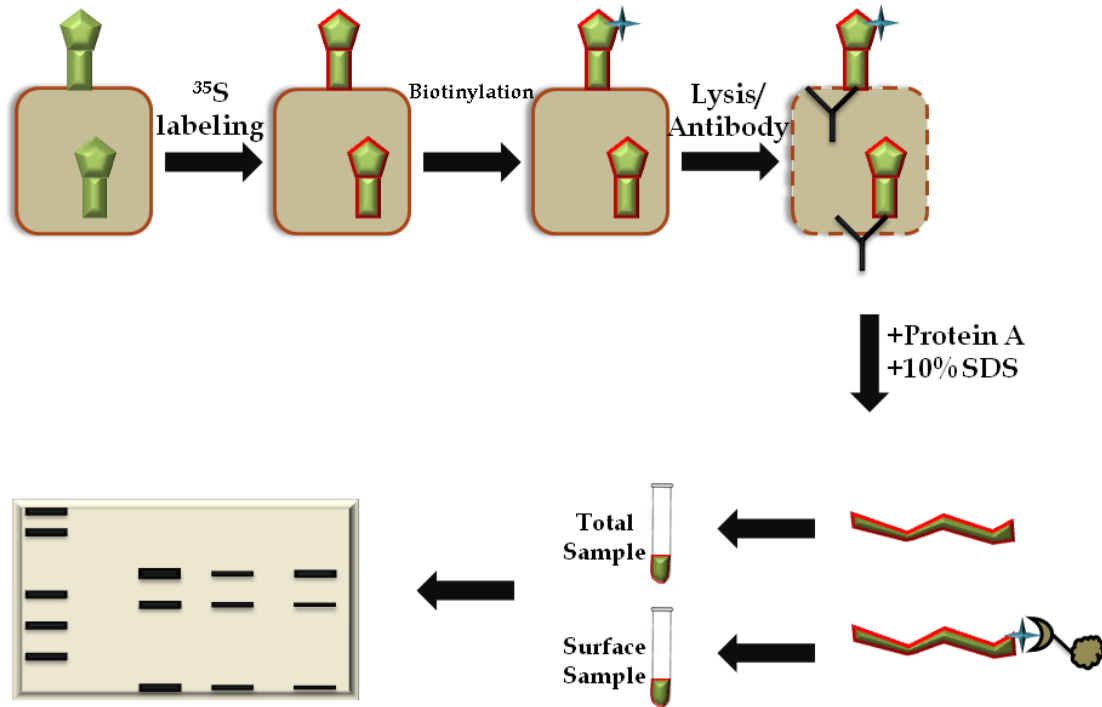
Figure 2.2. HMPV F surface biotinylation assay protocol.

Surface biotinylation is performed to quantify total F protein expression level as well as the population that persists on the cell surface. It entails transfecting cells with HMPV F followed by metabolic radiolabeling with ^{35}S to allow for visualization. Next the cells are biotinylated, which will mark the surface expressed protein only. Afterward, the cells are lysed and antibody to HMPV F applied. All bound protein is pulled down with Protein A followed by treatment with 10% SDS. At this point, a portion of each sample is kept retained to represent the total protein. The rest is then treated with streptavidin beads, which can then be pulled down. This portion of the sample is kept to represent the surface population of the protein. Each set of samples can then be resolved via SDS-PAGE.
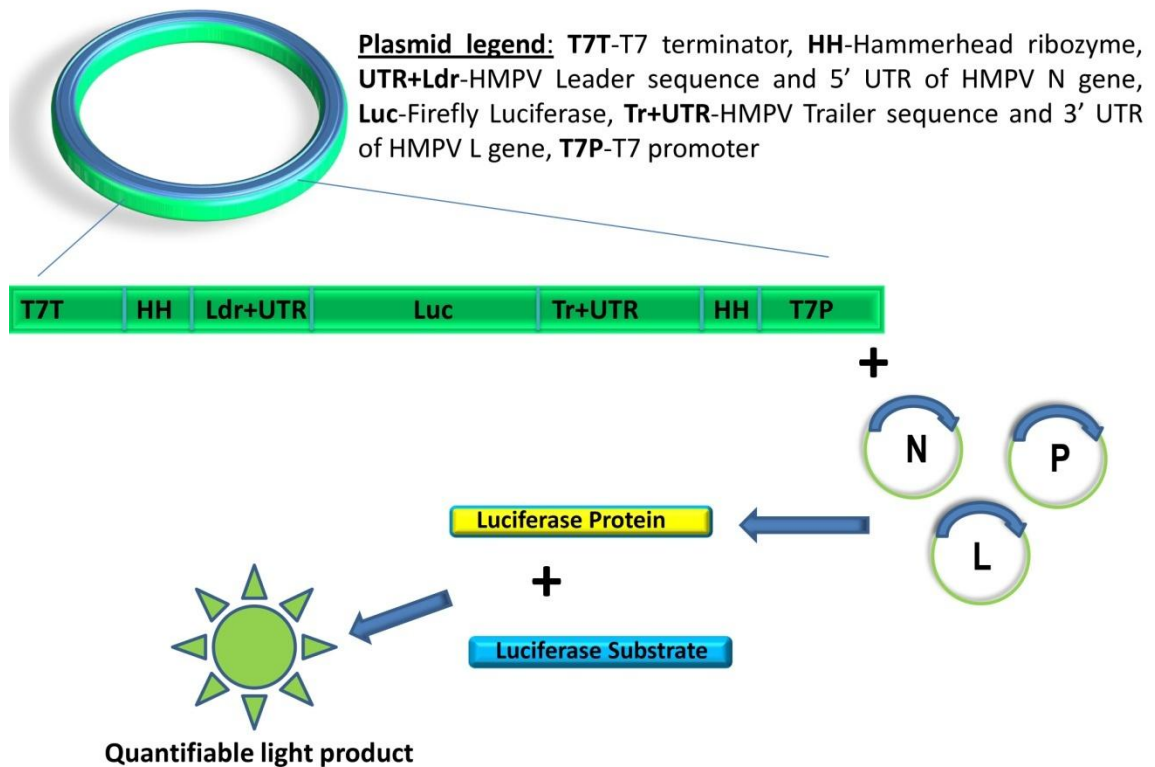
Figure 2.3. Schematic of HMPV minireplicon assay.

Plasmid constructs all feature leader and trailer sequences specific to HMPV or RSV flanking the luciferase open reading frame. Plasmids are either co-transfected into BSR cells with plasmids encoding viral replication proteins (N, P and L) or transfected alone. If transfected alone, cells are infected with live virus at 24hours post transfection to allow T7 polymerase to create minireplicon RNA prior to infection. At 24 hours post infection (or transfection if no infection), cells are lysed and luciferase levels measured using its ability to catalyze a chemiluminescent reaction.

Chapter III: Experimental Results

Subsection I: HMPV Fusion Project

An electrostatic-rich region in F_2 modulates HMPV F low pH-dependent fusion

Previous work in the lab had established that the activity of the fusion protein of the

HMPV strain CAN97-83 (Clade A2) is pH-dependent [23, 25]. One region that has been

demonstrated to be critical for pH sensing is centered around H435. This residue is in

proximity to basic amino acid side chains (K295, R396, and K438) in the homology

modeling based on the crystal structure of PIV5 F. The working model for H435 as a pH

sensor is that upon exposure to low pH, the residue is protonated and that this event

results in an electrostatic repulsion. Subsequently, the protein is able to trigger fusion.

This model is supported by mutagenesis studies that showed that substitution with an

acidic side chain (H435D, H435E) yielded a protein incapable of fusion while H435R

exhibited a hyperfusogenic phenotype [27].

Further analysis of the HMPV F homology model indicated that a region of the protein

that had been shown to be crucial to triggering in PIV5 F, CBF2-HRA, was enriched in

charged amino acids in HMPV F [73-74]. The CBF2 amino acids of interest included

E51, D54 and E56 (Figure 1.5). These were in proximity within the model to HRA

residues R163 and K166 (Figure 1.5). These findings led to the hypothesis that charge-

charge interactions in this region could potentially contribute to the low pH triggering of

HMPV F. Measurements from our homology model estimated the distance between β-

carbons of these residues to be between 4 and 11Å, a distance permissible for the

formation of salt bridges between side chains at neutral pH, potentially stabilizing the overall structure of HMPV F (Table 3.1) [27]. It is known that charged groups of the side chains need to be less than 4Å apart for salt bridge formation [75-76]. While the modeling places some of these distances slightly outside this parameter, it is possible that such a highly charged microenvironment could facilitate alteration to side chain pKa. This would allow protonation upon exposure to a pH 5 environment and make up the distance between potentially bridged moieties. Such a change to the protonation state of E51, D54 and/or E56 may also result in destabilization and triggering of fusion.   To determine what role, if any, these residues, play in low pH-dependent fusion activity, the HMPV F mutants E51A, D54A and E56A (F_2 mutants) as well as R163A and K166A (HRA mutants) were created and tested for proper expression and fusogenic activity at various pH.

With the exception of the E51A mutant, for which surface F_1 expression was 66% of WT, all F_2 and HRA mutants were expressed close to or above WT levels on the surface of transfected Vero cells (Figure 3.1A and 3.1B). After determining the expression level for each mutant, fusogenicity was determined for each mutant protein via syncytia and reporter gene fusion assays. In the former, the protein is transfected into Vero cells, which are subsequently treated with various buffers in the pH range of 5-7. The ability of the protein to facilitate fusion is qualitatively measured by the number of multi-nucleated cells observed at four such pH pulses. For the reporter gene assay, the Vero cells are co-transfected with F and a luciferase gene with a T7 promoter. These are overlaid with

BSR cells containing a T7 polymerase. Fusion between the cell types is then measured by the amount of luciferase produced and quantified by biochemiluminescence.

All mutants were able to promote efficient syncytia formation at pH 5 except HMPV F E51A (Figure 3.2B). Cells expressing the HMPV F D54A, E56A, R163A and K166A mutants produced more numerous and larger size syncytia compared to WT at pH 5. Conversely no syncytia formation was observed in cells transfected with HMPV F E51A despite a significant presence of protein on the cell surface (Figures 3.1 and 3.2). Surprisingly, all mutants save HMPV F E51A also demonstrated syncytia at pH 6, albeit smaller (Figure 3.2A). Syncytia formation was significantly lower at pH 6 relative to pH 5 and was undetectable at pH 7.

In agreement with the syncytia assay, all the mutant HMPV F proteins with the exception of E51A were able to efficiently promote fusion at pH 5 in the reporter gene assay (Figure 3.2B). In fact, the D54A, E56A and K166A mutants promoted fusion by at least 25% above WT. The HMPV F R163A mutant exhibited similar fusion activity to WT while fusion activity for HMPV F E51A was at near background levels. The HMPV F D54A, E56A and K166A mutants all promoted fusion above WT levels at pH 5.5 as well though, as seen with WT, the fusogenic activity was reduced by more than 50% relative to pH 5. Fusion levels for HMPV F R163A were similar to WT, but no fusion above background was observed for HMPV F E51A at pH 5.5. Interestingly, treatment with pH 6 buffers drove no fusion activity above background for any of the mutants.

This result likely highlights the difference between the syncytia and the reporter gene assays in terms of how each measures the kinetics of fusion as well as by different amounts of activate F present at the surface. While luciferase production was assessed after two pulses spaced one hour apart, syncytia formation was induced by a total of four pH pulses given every two hours. Further, for the luciferase reporter to be synthesized, a pore large enough to transfer plasmid DNA or the T7 polymerase must be formed between the time of the pH pulse and cell lysis (4 hours). In contrast, syncytia formation is measured after an overnight incubation, which allows sufficient time for slower proteins to undergo the conformational changes needed to enlarge the fusion pore [77].

E51 is required for the proper local folding and cleavage activation of HMPV F

The results for the F2 and HRA mutants suggest that this region plays two important yet different roles in the stability and triggering of HMPVF. E51 appears to be involved in the overall fusion activity of HMPV F and could potentially serve as another pH sensor. Therefore, to test whether E51 acts similarly to H435, expression and fusion of the HMPV F E51K mutant were assessed.

Substitution of E51 with a lysine (E51K) decreased the surface expression levels of the F_1 form of HMPV F by nearly 50% (Figure 3.4A and B). While we did not test this directly, the observed reduction in surface expression observed for both the E51A and E51K mutants suggests that the negative charge at this position is important for stability of the protein at the cell surface. The importance of this residue is underscored by the fact that the portion of the HMPV F E51K mutant that remained on the surface also failed to

41

promote cell-to-cell membrane fusion at any pH, as assessed by our reporter gene and syncytia assays.

To test whether there is crosstalk between E51 and H435, the mutation E51K/H435R was also made and analyzed. Like HMPV F E51K, surface expression of E51K/H435R was reduced. Furthermore, cell-to-cell fusion activity was not detected at any pH despite the introduction of the hyperfusogenic mutation H435R (Figure 3.5). These results suggest that the E51K mutation is dominant over H435R and confirms that residue E51 plays a key role in the overall function of F.

Although the HMPV F E51A, E51K AND E51K/H435R mutants showed a lower surface expression, a significant amount of the mutant F reached the cell surface, suggesting that the effect of these mutations on the overall structure is not severe enough to result in complete ER retention due to gross misfolding. Since E51 is near the cleavage site of HMPV F, electrostatic interactions involving this moiety may be important for the proper folding and positioning of the proteolytic processing site. To test this, surface expression of HMPV F E51A and E51K was examined in the absence of trypsin. Though HMPV F strains or mutants have been identified in which some processing to the mature F_1+F_2 is observed in the absence of exogenous trypsin [78-79], WT HMPV CAN97-83 F protein cleavage *in vitro* has been shown in our laboratory and others to require trypsin treatment [80-82]. Fitting with this, WT HMPV F protein was observed in the mature, cleaved F_1 form only after addition of trypsin whereas more than 30% of the E51A and E51K mutants were observed to cleaved in the absence of trypsin (Figure 3.3). This result

suggests that the removal of the negative charge at position 51 caused local misfolding that exposed a cleavage site normally not accessible to an endogenous protease. Consequently, this aberrant cleavage event did not result in a fusogenically active F protein whenever this amino acid was substituted. These results therefore suggest that E51 is important for positioning of the fusion peptide for proper proteolytic processing.

D54 and E56 in F_2 are important for HMPV F prefusion and postfusion stability

The hyperfusogenic phenotype observed for HMPV F D54A and E56A suggests that these residues are involved in modulating the stability of the protein, potentially through salt bridge interactions with R163 and K166 in the prefusion state. At low pH, neutralization of D54 and/or E56 may disrupt these salt bridges, allowing F to trigger. HMPV F double mutants D54A/E56A and D54N/E56Q were created and analyzed to determine the effects of disrupting these potential interactions. The latter mutation, D54N/E56Q, is a more conservative, isosteric substitution that removes the charged residues while maintaining polarity at these residues. Analysis of the R163 and K166 mutations was not pursued further due to the location of these residues in HRA, as their potential role in six-helix bundle formation means fusion changes may not be directly attributed to triggering. Additionally, HMPV F D54A/H435R, E56A/H435R, D54A/E56A/H435R and D54N/E56Q/H435R mutants were made to test whether changes in one region influence the other.

While the HMPV F D54A or E56A mutants expressed at or above WT levels (Figure 3.1A), surface expression of the F_1 form of the double alanine mutant (D54A/E56A)

43

decreased by more than 40% (Figure 3.4). Consistent with a decrease in surface expression levels, a reduction in fusion activity was also observed for the HMPV F D54A/E56A mutant. The more conservative polar substitutions (D54N/E56Q), in contrast, restored the surface expression to WT levels (Figure 3.4), suggesting that either polar residues or steric similarity is needed to stabilize the prefusion form of the protein.

According to our reporter gene fusion assay, fusion activity was significantly enhanced for HMPV F D54N/E56Q at pH 5 (Figure 3.5A) to levels equivalent to E56A. However, the effect of these mutations on the stability and fusogenic activity of the protein is different. D54N/E56Q is more hyperfusogenic at pH 5.5 compared to E56A and, while the addition of the H435R mutation to D54N/E56Q (D54N/E56Q/H435R) had a modest effect on fusion at pH 5.5, E56A/H435R exhibited a dramatic increase in fusion activity at the same pH. More importantly, analysis of the syncytia assay revealed that cells expressing the HMPV F D54N/E56Q and D54N/E56Q/H435R mutants produced numerous syncytia but significantly smaller in size compared to WT, E56A and E56A/H435R when triggered at pH 5 (Figure 3.5B). The greater amount of smaller syncytia agree with the hyperfusogenic phenotype observed in the reporter gene fusion assay as this would result more cells fusing and increased luciferase production. Thus, our data indicate that the replacement of the negative charges at positions 54 and 56 alter the stability of the fusion protein as evidenced by changes in surface expression and fusogenic activity.

The addition of the hyperfusogenic mutation H435R (D54A/H435R, E56A/H435R, D54A/E56A/H435R and D54N/E56Q/H435R) did not significantly alter the fusion levels of the mutant proteins at pH 5 (Figure 3.5). However, the presence of the H435R mutation led to a modest increase in fusion activity at pH 5.5 with the notable exceptions of D54A/H435R and E65A/H435R, where the increase in fusion was significantly more pronounced. Together with a minor decrease in F_1 surface expression (Figure 3.4), our data suggest that H435R also affects the stability of the protein, allowing it to trigger at a higher pH. This destabilizing addition of a basic residue to an already positively charged region can indeed be responsible for the hyperfusogenic phenotype of H435R, as disruptions of charge-charge interactions has been shown to alter the triggering threshold of influenza HA [83-84]. The pH dependency of HMPV F-mediated membrane fusion, however, was not abolished by mutations at positions 54 and/or 56. Therefore, while H435 mediates the stability of the HRB-linker region to behave as a pH sensor, the stability effect conferred by residues D54 and E56 is not involved in sensing low pH.

Summary

The work on this project has illustrated the complexities in the process of triggering the HMPV fusion protein. While we originally hypothesized that electrostatic interactions at both H435 and in the CBF2 region change in response to a lower pH environment, thus triggering the conformational changes needed for fusion, the fact that mutations in these regions could not overcome the requirement for low pH suggests that at least one other area of the protein may be playing a role. Further, the combination of hyperfusogenic mutations, such as H435R with D54A and E56A seemed to only destabilize the prefusion

form while isosteric substitutions for the latter two demonstrated that more than electrostatic interactions are likely responsible for maintenance of metastability. Finally, the mutagenesis at E51 showed that this region that has a role in triggering may also be in control of other processes, such proteolytic processing, adding yet another layer of complexity.

Subsection II: HMPV Minireplicon Project

While my initial work focused on the regulation of the HMPV F protein and viral entry, far less is known about the processes governing transcription for HMPV. As such, the next studies focused on what occurs after entry, namely RNA synthesis, through the use of a minireplicon system. This plasmid-based assay allows for study of viral promoter activity as measured through the transcription of a reporter gene, which was luciferase in this case. My hypothesis was that HMPV and hRSV promoter sequences would be able to equally drive gene expression given HMPV- or hRSV-specific RNA synthesis proteins. The basis for this position is the fairly high identity (45.5% ,100% through the first 11nt) for the leaders and trailers (83%, 100% through the first 12nt).

Drastic differences observed in the predicted RNA structure of various NNS viral promoters.

Prior to initiating experimental examination of the HMPV promoter region, the predicted RNA fold of each of the native viral promoters was assessed using SplicePort software. Because of the several reported studies on the activities of hRSV promoters and that pathogen's similarity to HMPV in other aspects, both the leader and trailer folding predictions of these two members of the *Pneumovirinae* subfamily were compared.

There was an overall similarity of fold between the trailer promoters, despite the hRSV trailer being significantly longer, with both featuring a large loop with two stem loops— one minor and one major (Figure 3.6A). The principal differences were the angle

47

between the two stem loops (roughly perpendicular for hRSV and approx. 135° for HMPV) and the terminal addition to the RSV promoter. This addition appeared to be a self-folding portion of the trailer directly abutting the portion with predicted structural homology to HMPV. Given these structural predictions, it seemed plausible that the polymerase of one virus could recognize and drive transcription from the promoter of the other.

Consequently, the predicted folds of the HMPV and hRSV leader promoters were largely similar (Figure 3.6B). In both cases, the predicted structure was almost entirely linear with a terminal stem loop. In fact, the only observed difference between the predictions was a variation in the size of the stem and loop with the hRSV structure being larger.

Additionally, similar NNS viral promoters were run through the software for the purpose of noting conservation of features in a larger context. The viruses selected were PIV5, another paramyxovirus from a different subfamily and the rhabdovirus VSV. The predicted RNA folds for the trailer promoters were similarly disparate when compared to those of HMPV and RSV (Figure 3.7A). Interestingly, the predicted structure of the PIV5 trailer mirrored that of the leaders of *Pneumovirinae* with a prominent terminal stem loop, though the linear portion of the promoter was dramatically shorter. The VSV trailer, however, was predicted to take on a completely novel fold relative to the selected paramyxoviruses, featuring a short stem and large loop with the remaining RNA adopting a circular pattern. Overall, the predicted folds from both viruses displayed a sufficient

degree of similarity such that it still remained plausible that either promoter could be used with HMPV or hRSV to initiate RNA synthesis.

When analyzing the leader RNA folding predictions for PIV5 and VSV, the only similarity between these and the pneumoviruses was the presence of some linear character, and even the extent of that characteristic varied greatly (Figure 3.7B). The PIV5 leader was predicted to have a much larger stem loop with an additional stem within the loop while the VSV leader was predicted to have a small loop in the middle of its linear RNA fold.

Minireplicon constructs with various promoters synthesized are functional.

HMPV-based minireplicon systems were based upon the hRSV luciferase construct plasmid provided by Dr. Richard Plemper at Emory University. This vector, which contained both RSV promoter sequences with specific endonuclease sites at either end of each, also served as an internal control. HMPV CAN97-83 trailer and leader cDNA sequences were obtained via RT-PCR and synthesized with restriction endonuclease recognition sequences at their termini. After subcloning into the hRSV base vector, there were a total of four constructs—two homotypic and two heterotypic. The former group contained trailer and leader sequences derived from the same virus, either HMPV (MPV) or the hRSV (RSV) internal control (Figure 3.8A). The heterotypic constructs were modified from the base vector at only one promoter such that they contained an HMPV trailer (H-trailer) or leader (R-trailer).

Preliminary optimization tests were conducted in which several variables were adjusted. These included incubation time, which was tested at 12, 24, 36 and 48hpt as well as sample size, using different size well plates. Additionally, luminometer settings were varied in the endpoint assay before settling upon a 30sec integration period for all assays. Overall, the results suggested that all constructs were functional.

Treatment of minireplicon constructs with different viral stocks exhibit differential activities.

Each of the synthesized constructs displayed luciferase activity significantly above background when transfected into BSR cells followed by infection with rgHMPV, rgRSV or PIV5-GFP viral stock. Conversely, transfection of the plasmids followed by infection with the rhabdovirus VSV was unable to drive transcription at appreciable levels. This result is in contrast with findings when co-transfection with RSV-specific plasmids for the N, P, L and M2-1 proteins elicited a much more variable signal in all constructs tested (Figure 3.8B). These results suggest that all paramyxoviruses can drive transcription though not VSV while other factors are likely modulating levels of expression.

PIV5 L but not RSV L exhibits complementation with HMPV N and P in the minireplicon assay. Despite the synthesis of two HMPV L gene constructs (one codon-optimized), no enzymatic activity was detected in this assay despite an association with HMPV P. As such, complementation with the other HMPV RNP proteins and other

paramyxoviral large protein plasmids was attempted. hRSV and PIV5 were selected given the previous results showing the ability of these viruses to drive the HMPV leader/trailer minireplicon. While hRSV L could not complement with any combination of HMPV N, P, P-FLAG and M2-1 to drive transfection above background levels, PIV5 L was able to give a signal that was approximately 2-7 fold above background levels (Figure 3.9). This result suggests that the large polymerase of PIV5 may be more similar to HMPV L with regard to binding the promoter regions relative to the RSV L protein.

Addition of the RSV 36-nucleotide terminal trailer sequence (TTS) to the HMPV promoter creates a more RSV-like RNA fold. Given the similar predicted folds for the RNA trailers for both HMPV and RSV, I hypothesized that addition of the 36 residue trailer terminal sequence (TTS) of the RSV promoter, the deletion of which had been previously shown to be deleterious to RNA synthesis in that system [85], may improve the promoter strength of the HMPV trailer (Figure 3.10A). Doing so could have had an effect on luciferase expression, as more efficient replication could increase the amount of minigenomes present for gene expression. It was first imperative to determine that the RNA fold was predicted to resemble that of the RSV trailer, so the constructs' sequences were imported into the SplicePort RNA prediction software.

The prediction software analysis suggested that the HMPV-TTS combination more greatly resembled the RNA fold of hRSV than that predicted for HMPV alone (Figure 3.10B and C). However, this was only the case when the 30 nucleotide linker sequence between the TTS and the region with homology to HMPV was also incorporated. These

predictions, along with previous minireplicon data, suggested that addition of the entire TTS and linker, which represent the first 66nt of the RSV trailer, may make the HMPV constructs more robust in their reporter gene expression.

RSV terminal trailer sequence confers greater transcriptive activity to HMPV minireplicon constructs.

Synthesis of the new vectors began with construction of custom primers that added first the linker cDNA sequence and the TTS in two mutagenesis-like PCR insertions. These constructs were then tested in the same minireplicon assay. The H-trailer(TTS) vector was able to drive expression at levels similar to those of the RSV plasmid. In contrast, the H-trailer plasmid elicited roughly a third of the luciferase expression of the RSV plasmid under the same conditions. The homotypic MPV plasmid also exhibited greater luciferase activity when its trailer had been modified relative to the unmodified construct. In contrast, the addition made no significant difference when the plasmids were co-transfected with PIV5 RNP plasmids (N, P and L) (Figure 3.11). Overall, these results suggest that the RSV TTS sequence is sufficient to increase luciferase expression to equivalent levels between HMPV and hRSV.

Summary

The work within the minireplicon has provided unique insights on the poorly understood mechanism underlying viral gene transcription. Given these data, it is likely that RNA folding, predicted for several different viruses in this study, is playing a large role in the regulation of viral gene transcription. Further, there appears to be a difference in the

level of selectivity of viral polymerases though all paramyxoviruses may be able to drive a minimal level of transcription given an HMPV or hRSV promoter. There also appears to be some level of complementation possible between different paramyxoviruses, which is suggestive of conservation within areas of the different large proteins. However, no report examining such conservation has yet been conducted. Finally, both the role of RNA folding in viral gene transcription and the greater potential selectivity of the hRSV RdRp are supported by the data showing that the HMPV trailer becomes a better inducer of RNA synthesis with the addition of the hRSV-specific TTS. Altogether, this work represents a solid beginning to research in an area that is not well characterized in NNS biology.

Subsection III: HMPV Assembly Project

Having observed the underlying complexities that regulated the pH-dependent fusion activity of HMPV and gained insight into the dynamics of promoter activity for the virus, this work had successfully provided insights into early events governing the HMPV infection process. In order to attain a more complete understanding of this pathogen, however, one must explore the temporal and spatial relationship between these early events and the cellular processes governing later ones in the infected cell, namely viral particle assembly and egress.

These studies specifically focus on the dynamic association between two viral proteins that are indispensible in bridging the gap from RNA synthesis to progeny virus dissemination. As the nucleocapsid protein performs its chief role as a viral RNA chaperone, it must be able to associate with the phosphoprotein in its role as a polymerase cofactor; however, this association must also be less transient as these two proteins are intimately linked along with the viral polymerase and genomic RNA in the packaged virus particle. As such, the best investigative tool available was a timecourse study to demonstrate how these two factors differentially distribute throughout the course of infection. From there, one can begin to piece together function from localization and the aid of additional assays.

HMPV nucleocapsid and phosphoprotein interact variably in the presence and absence of infection

It has been previously reported that HMPV N and P co-localize to cytoplasmic inclusion bodies, which can be detected both during infection and transient expression [30]. However, that same report found that a detectable interaction was observed biochemically only in the case of infection. We sought to further examine the interaction among proteins required for HMPV RNA synthesis using co-immunoprecipitation assays. These experiments included the HMPV nucleocapsid, large polymerase, and phosphoprotein as well as a recombinant form of HMPV P harboring a DYKDDDDK epitope tag at its carboxyl terminus immediately following the final amino acid of the polypeptide (P-FLAG).

After transfection of A549 cells with various DNA constructs, the cells were then either infected or mock infected for 24 hours prior to metabolic labeling. Immunoprecipitations were then performed using an antibody to HMPV P. The results showed that HMPV P can pull down HMPV L in the presence or absence of infection, though additional forms of the polymerase appear to be detected in infected cells (Figure 3.12A and B). It should be noted that HMPV L can only be detected when transfected, likely due to low copy number within infected cells. The polymerase was also found to co-immunoprecipitate with HMPV P-FLAG, suggesting that the additional of the epitope tag did not affect the ability of the protein to bind a major interacting partner (Figure 3.12C). Due to the presence of an apparent background band of similar size to WT P when lysates were probed with the FLAG antibody, any potential co-immunoprecipitation between P-FLAG

and HMPV cannot be assessed. Further, the necessity of 10% polyacrylamide gels for proper migration of HMPV L meant that HMPV P and any HMPV N that may have co-immunoprecipitated could not be resolved.

To address this we employed a different approach to clarify the potential N-P interaction within cells. Cells were infected for either 6 or 24 hours, and immunoprecipitations with antibodies to HMPV P or the FLAG tag were performed. HMPV N that had co-immunoprecipitated was then assayed by western blotting. An interaction between HMPV N and P was not detected in uninfected cells, but interactions were observed at 6 hours post infection (hpi) with and with a greater amount of N observed at 24hpi (Figure 3.13A). This finding is consistent with a previous study [30]. In contrast, HMPV P-FLAG was found to be associated with HMPV N in the presence or absence of infection.

While it had appeared that P-FLAG and WT P were equivalent in the overexpression and radiolabeling studies, we wished to exclude the possibility of large variation in the amount of protein present between those cells transiently expressing N, P or P-FLAG and those that had been infected. As such, we performed western blotting analysis of each of these three proteins from cells that had been transfected overnight or infected for 24 hours (Figure 3.13B). There was virtually no difference between HMPV N levels when transfected or from infected cells with a difference of only 0.2% (Figure 3.13C). When transiently expressed, HMPV P levels were increased by 74% over infection. This level of expression was slightly higher than that co-expression of HMPV N and P. Interestingly, the level P-FLAG was also lower than that of WT P. Given these results, it

is likely that any observed variation in the interactions between these proteins is not due to drastic changes to expression levels under different conditions.

Overexpression of HMPV phosphoprotein results in alterations to morphology of the infected cell

I next sought to determine the cellular effects of expression of each of these proteins. Following transfection of A549 cells, we observed that HMPV N expressed alone was distributed throughout the cytoplasm; however some local areas of concentration were observed (Figure 3.14A). Interestingly, while either HMPV P or P-FLAG was detected throughout the cytosol, there was an apparent concentration of protein at the cellular periphery (Figure 3.14B-C). Further, HMPV P and P-FLAG were readily detected in filamentous processes at the periphery of these cells. Such extensions have been described as a characteristic of infection with RSV, though the particular constituents of such structures seem to vary between viruses [71]. These results suggest that the P protein may contribute to the formation of these structures.

We next explored how co-expression of HMPV N and P affects protein distribution. It has been previously reported that the HMPV N and WT P proteins co-localize to cytoplasmic punctae similar to the inclusion bodies observed during infection [30], and we observed a similar result (data not shown). Expression of HMPV P-FLAG with HMPV N resulted in high levels of observed co-localization (Table 3.2); however, unlike with WT P, there were no observed inclusions formed by the proteins. HMPV N was now exhibited increased presence at the periphery, similar to the localization of P-FLAG

alone (Figure 3.14D-F). One additional difference between cells expressing P-FLAG alone and those co-expressing HMPV N was the induction of apparent membrane blebbing. Interestingly, these rounded structures were observed at the periphery of cells only where both HMPV N and P-FLAG were both present. This suggests that the interaction between these two viral proteins may be sufficient to curve membranes or form structures akin to those of viral particles under these conditions.

HMPV infectious particle detection coincides with shift in viral protein distribution during infection

Given the findings with P-FLAG and HMPV N localization, we sought to compare that to that of HMPV N with WT P in the context of infection. We conducted a time course study of these proteins at 6, 12, 24 and 48hpi to note how their relative localization changed over time. At the earliest point, 6hpi, discernible punctate structures were apparent, but co-localization between the two proteins was sporadic and potentially consistent with ongoing translation (Figure 3.15B). Interestingly, these nascent polypeptides were primarily perinuclear in their distribution. As infection proceeded and protein expression increases, HMPV P was observed throughout the infected cell at 12hpi. The P protein was observed within perinuclear inclusions with HMPV N and at the cellular periphery in filaments. By contrast, N remained concentrated within punctate bodies, some without HMPV P (Figure 3.15C).

As microscopy indicated a large increase in phosphoprotein between 6 and 12hpi, we conducted metabolic radiolabeling experiments at the same time points to determine the

58

amount of HMPV P (and P-associated nucleocapsid) present. Consistent with the microscopy, P and co-immunoprecipitated N proteins were only faintly observed at 6hpi while a marked increase in protein was observed by 12 hours (Figure 3.16).

By 24 hours, both N and P appeared more diffuse than earlier while the cytoplasmic inclusion bodies containing both proteins were dramatically larger than previously observed (Figure 3.15D). Notably, HMPV N was also partially present at the periphery of the cell. While HMPV N appears to be present either only at the periphery or within inclusions, HMPV P is still observed throughout the cytoplasm in addition to within inclusion bodies. At 48hpi, cytoplasmic bodies persisted but were morphologically distinct from those seen earlier as less HMPV N was observed at their centers (Figure 3.15E). Further, HMPV P appears to be all but excluded from these bodies with relatively smaller amounts detected only at their edges. More globally, HMPV P appeared much more diffuse than the more condensed distribution of HMPV N.

HMPV N and P move about the infected cell independently of one another

Our results suggested that the localization of HMPV N and P changed throughout the course of infection. To assess the role of the cellular microtubule network in HMPV N and P motility, infected A549 cells were treated at 9hpi with 7µg/ml nocodazole or vehicle control (DMSO). Infection continued in the presence of the drug for a total of 12 or 24 hours. While both HMPV P and HMPV N were observed within punctate and filamentous distributions at 24hpi without nocodazole treatment (Figures 3.17C-D), disruption of microtubules completely ablated the peripheral localization for HMPV N

specifically (Figures 3.17F and 3.17H). Additionally, propagation of HMPV in the presence of nocodazole resulted in titer reduction of greater than one order of magnitude (Table 3.3). This result suggests that HMPV N is translocating from inclusions in a microtubule-dependent manner. Further, as HMPV P localization was not drastically affected by the drug (Figure 3.17E and 3.17G), it also suggests that HMPV N and P move to the periphery of the cell via different mechanisms.

To shed light on the correlation between HMPV N and P translocation and virus assembly, we conducted an egress assay to assess viral particle budding from infected cells at the same time points as our microscopy studies. Supernatants of infected cells were assayed for HMPV P content following purification by centrifugation on a 20% sucrose cushion. HMPV particles were barely detected at 24hpi but readily observed at 48hpi, suggesting that viral assembly and budding occur at these times (Figure 3.18). These data show that detectable egress is temporally consistent with the peripheral localization of HMPV N and P at the cellular periphery, suggesting this translocation may have a role in HMPV assembly.

Localization of newly synthesized HMPV RNA is consistent with that of the nonstructural proteins throughout infection

i next wished to determine if synthesized RNA followed a similar distribution to HMPV N and P throughout infection. To do so, I utilized 5-bromouridine labeling, which has been employed only in non-paramyxoviral systems, such as vesicular stomatitis virus [47]. Again, the labeling periods were consistent with the time points previously

established at 6, 12, 24 and 48hpi. At the earliest point, we observed RNA in perinuclear, punctate structures of similar scale to those containing HMPV N and P at the same period (Figure 3.19B). By 12hpi, a more diffuse, yet still tightly perinuclear, pattern of RNA distribution was observed (Figure 3.19C). This perinuclear location is consistent with that of inclusion bodies containing HMPV N and P at 12hpi (Figure 3.15C). Interestingly, the RNA was still detected within somewhat punctate areas at this point as well. At 24hpi, a more diffuse pattern was observed (Figure 3.19D). This apparent spreading of RNA was similar to what was seen in viral proteins, particularly HMPV N, at this point during infection. By 48hpi RNA was still observed in punctate bodies though they appeared small and diffuse throughout the infected cell. This is also consistent with the viral protein time course in that some morphological distinction was observed relative to earlier times. Also RNA was present within filamentous extensions that were morphologically similar to those that had been observed to be concentrated with HMPV P (Figure 3.19E). This result suggests a potential role for these filaments in viral budding as this was the same period when egress was robust. Overall, these data suggest that the RNA-rich punctate bodies observed at early time points in the time course may be the same as the cytoplasmic inclusions containing HMPV N and P. By extension, the results would be consistent with such inclusion bodies as sites of RNA synthesis during HMPV infection.

Summary

The data presented in this subsection serves to underscore the spatial link between viral RNA synthesis and particle assembly. It was found that proteins necessary for genomic

replication and gene transcription displayed similar localization to newly synthesized viral RNA to a large degree, particularly HMPV N. This finding, along with the fact that expression of HMPV P, either alone with HMPV N, can imitate much of the cellular morphology of an infected cell at the later stages of infection with the concentration of proteins within filamentous extensions, suggests that there is a high level of coordination between the two processes. Further, there are indications of the underlying mechanism orchestrating this process, as HMPV N, at least, seems to be affected by the disruption of microtubules. However, the fact that such disruption only decreases, but does not ablate, viral growth is consistent with a much more complex system linking the RNA synthesis to packaging and egress both spatially and temporally during HMPV infection.

Table 3.1 Estimated distances between β-carbons of selected amino acid residues in F_2 in the HMPV F homology model

Starting residue	Ending residue	Distance (Å)
E51	R163	4
D54	R163	5
E56	R163	10
E51	K166	8
D54	K166	5
E56	K166	10

Table 3.1. Estimated distances between β-carbons of selected amino acid residues in

F2 in the HMPV F homology model

The table lists the approximated values between the β-carbons of amino acids within the

CBF2 and HRA regions of HMPV F. All values are based upon the homology modeling

done based on the crystal structure of PIV5 F in the prefusion form. The distances, listed

in angstroms, allow for an estimation of the likelihood of salt bridge formation between

these adjacent residues. This table was prepared with Dr. Andres Chang.

Sample	Pearson	M1	M2
NPF(1)	0.77	0.901	0.548
NPF(3)	0.85	0.771	0.834
NPF(4)	0.858	0.919	0.723
NPF(5)	0.813	0.789	0.765
NPF(6)	0.751	0.761	0.611
NPF(7)	0.869	0.949	0.662
Mean	0.8185	0.848333	0.6905

Table 3.2. Analysis of co-localization between transiently expressed HMPV N and P-FLAG.

The table shows the calculated co-localization coefficients for immunofluorescence assays following transfection of HMPV N and P-FLAG into A549 cells. The samples selected are from three different experiments (1 and 3, 4 and 5 or 6 and 7). The Pearson coefficient measures co-localization after adjustment for intensity between two channels and is the slope of the line of a plot of relative fluorescent intensities of the channels examined. The range for this value ranges from 0 (exclusion) to 1 (full co-localization). The Manders coefficients (M1 and M2) are taken as fractions of overlap between given channels. In this instance, M1represents the portion of all N that overlaps with P-FLAG. M2 stands for the fraction of P-FLAG overlapping with N in each field. These data were generated with aid of the JACOP plugin within the ImageJ software application.

Treatment	Avg. Titer (pfu/mL)
Vehicle (DMSO)	2.8×107
Nocodazole	1.01×10^6

Table 3.3. Results of HMPV propagation in the presence or absence of nocodazole.

Recombinant HMPV expressing GFP was initially propagated as described with incubation of the virus on A549 cells for 2 hours prior to washing. Prior to the addition of propagation medium, the volumes of OptiMEM + L-glutamine were treated with either 7μg/mL nocodazole in DMSO or an equal volume of vehicle. Cells were treated daily with TPCK trypsin until cytopathic effects were evident. Virus was harvested from cells and tittered by serial dilution followed by fluorescent counting. The nocodazole-treated cultures exhibited a reduction in titer greater than one order of magnitude or approximately 27-fold.
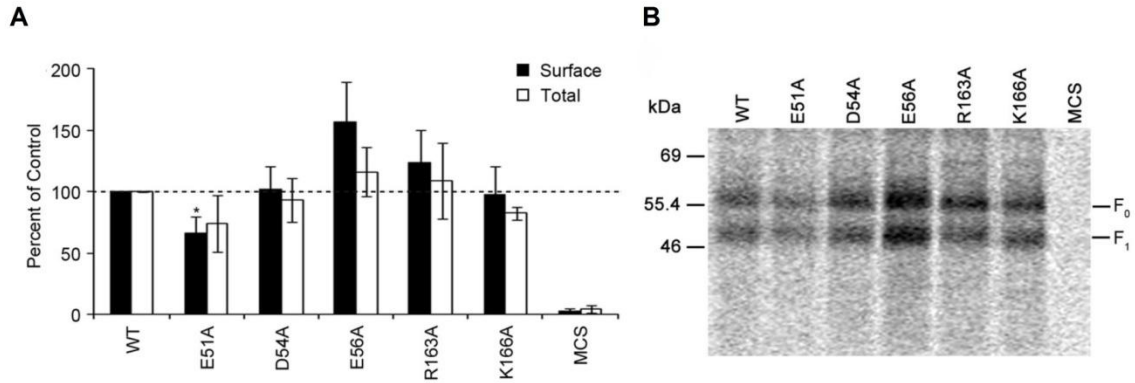
Figure 3.1. HMPV F CBF2-HRA alanine mutants all express near or above WT levels.

Following alanine scanning site-directed mutagenesis of HMPV F, the constructs were transfected into Vero cells and assayed for protein presence at the cell surface 24 hours post transfection via surface biotinylation. (A) Results of experiments normalized to WT expression for both total and surface expression show that only E51A is reduced in its expression while all other mutants are at or above WT. (B) A representative gel showing the relative expression of the synthesized CBF2-HRA mutants. Dr. Andres Chang and I contributed evenly to the work in this figure, each doing the assays multiple times and combining the results.
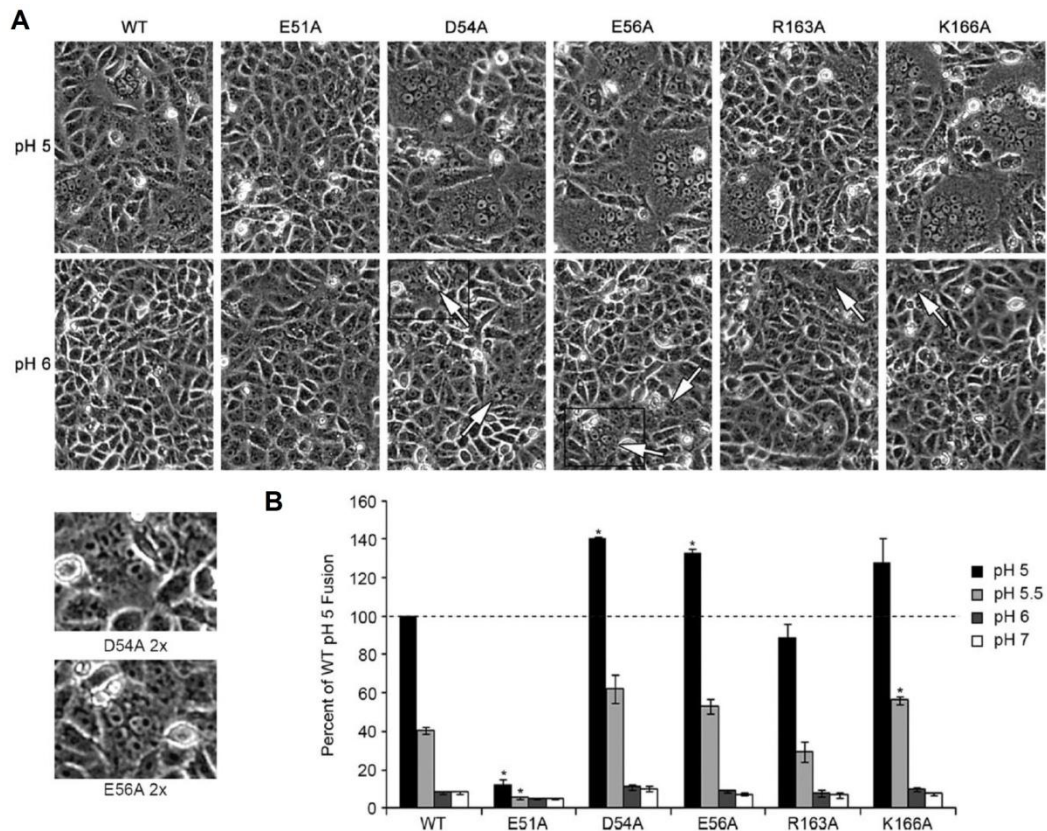
Figure 3.2. HMPV F CBF2-HRA mutants exhibit varied levels of fusogenic activity.

 (A) Fusion activity was assessed by syncytia assay where all mutants save E51A were shown to be fusogenic at pH5 with D54A and E56A displaying larger syncytia than WT. At pH 6 these more fusogenic mutants were also able to mediate membrane fusion. Images are representative of greater than three separate experiments. (B) A luciferase reporter gene assay was used to measure the fusogenicity of each mutant and agreed with the syncytia results, showing D54A and E56A to be hyperfusogenic and E51A to be incompetent to mediate cell-cell fusion. Dr. Andres Chang and I contributed evenly to the work in this figure, each doing the assays multiple times and combining the results.
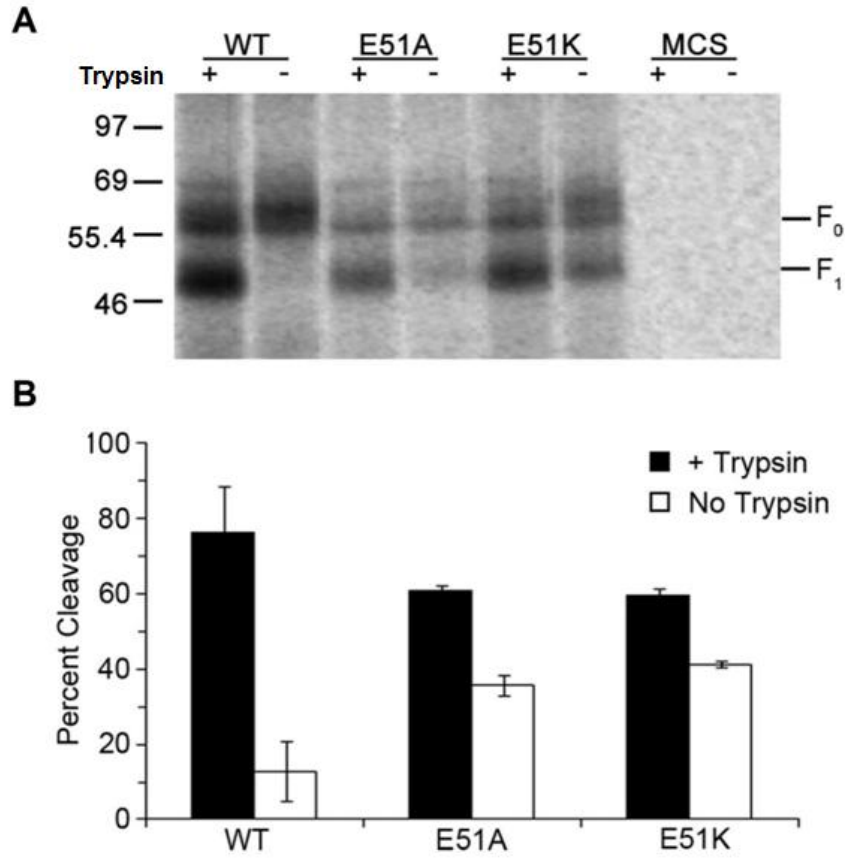
Figure 3.3. Substitution of E51 leads to alterations in HMPV F proteolytic processing.

(A) Representative gel showing the surface expression of HMPV F mutants and (B) quantification of the amount of cleaved protein in the presence and absence of trypsin. Both E51A and E51K mutants were shown to be cleaved at roughly twice the levels of WT without trypsin cleavage, suggesting a greater sensitivity to aberrant proteolysis. Dr. Andres Chang and I contributed evenly to the work in this figure, each doing the assays and combining the results.
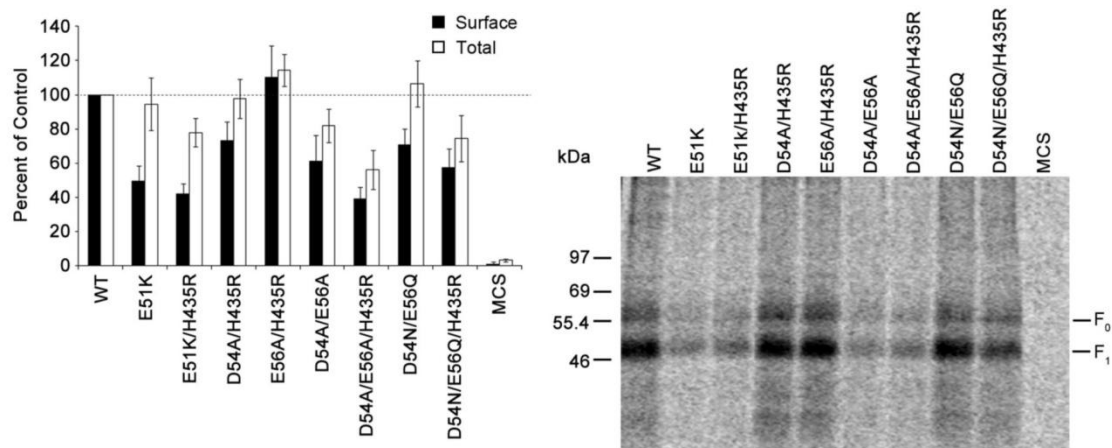
Figure 3.4. Combined mutagenesis of H435 and F2 residues affect protein stability.

Total and surface expression of HMPV F mutants was performed and showed that while combination of the hyperfusogenic mutations H435R and either D54A or E56A did not affect protein expression, combining the two F2 mutations or all three mutations did result in lower detection of protein levels. However, substitution with the isosteric residues served to stabilize the protein relative to the alanine mutants in all cases. An E51K mutation with or without H435R also exhibited a marked reduction in expression. Dr. Andres Chang and I contributed evenly to the work in this figure, each doing the assays multiple times and combining the results.
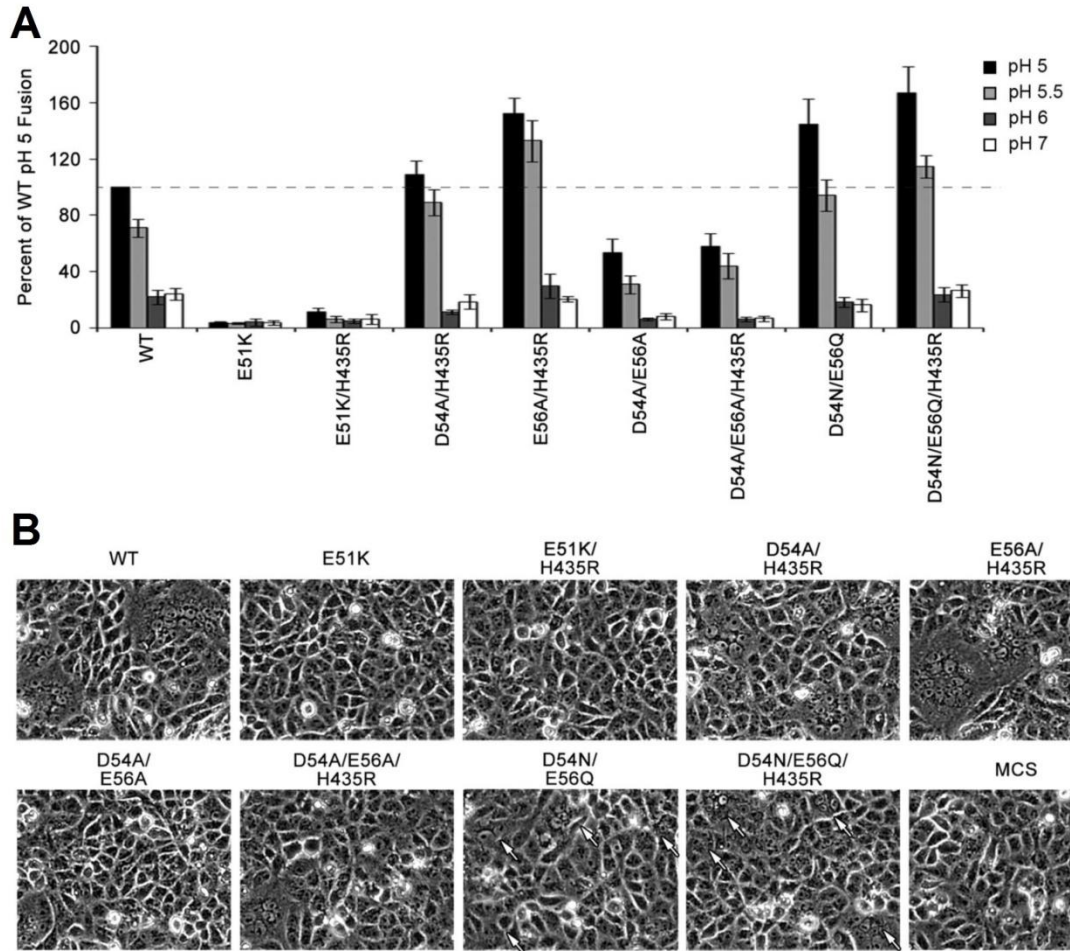
Figure 3.5. Combinatorial mutagenesis of different regions of HMPV F result in alterations to fusion activity.

(A) Reporter gene fusion assay and (B) syncytia assay results at pH 5 show that combination of hyperfusogenic (D54A/H435R, E56A/H435R) or stabilizing mutations (D54N/E56Q, D54N/E56Q/H435R) promoted fusion at higher levels than WT while those that destabilized surface expression (D54A/E56A and D54A/E56A/H435R) all were sub-WT in their fusion activity at all pH levels also. Smaller syncytia form for the stabilizing mutants. Dr. Andres Chang and I contributed evenly to the work in this figure, each doing the assays multiple times and combining the results.

A Trailer Fold Predictions

B Leader Fold Predictions

HMPV   RSV   HMPV   RSV
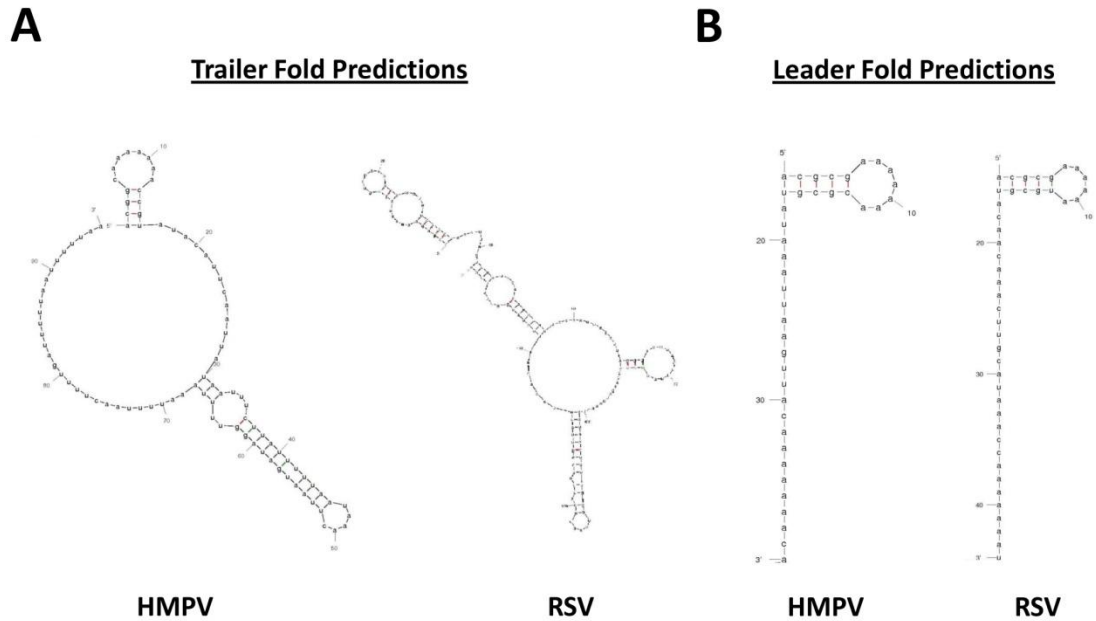
Figure 3.6. Comparison of HMPV and RSV RNA promoter fold predictions.

RNA sequences for HMPV and RSV were imported into the SplicePort RNA folding predicton software. The folds that were predicted to be the most thermodynamically favorable were assessed relative to each other. (A) The trailer promoters exhibit some similarities in their general fold though the RSV trailer is significantly longer than that of HMPV. This extra length appears to result in a self-folding terminal region. (B) The leader promoters are much more similar, featuring a mostly linear RNA with a single terminal stem loop.

A Trailer Fold Predictions
B Leader Fold Predictions

PIV5   VSV   PIV5   VSV
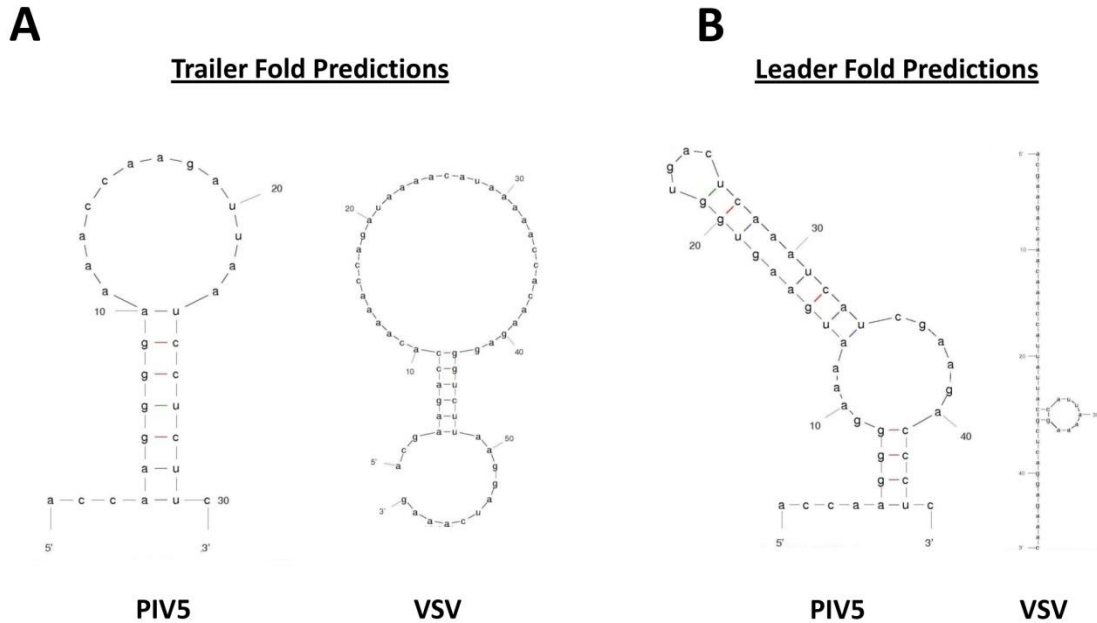
Figure 3.7. Other NNS viral promoters are predicted to differ from HMPV and RSV.

Sequences corresponding to the promoter sequences for both PIV5, a paramyxovirus, and VSV, a rhabdovirus, were entered into SplicePort to determine the similarity of the predicted folds to HMPV and RSV. (A) The trailer for PIV5 is more reminiscent of the pneumovirus leaders with its terminal stem loop and short linear sequence while the VSV trailer has a unique relative to either of the predicted trailer promoters from the members of *Pneumovirinae*. (B) The VSV leader features a predominantly linear arrangement with a single loop, which may be more similar to HMPV and RSV than the PIV5 leader, which features a stem loop stem structure and very little linear character.
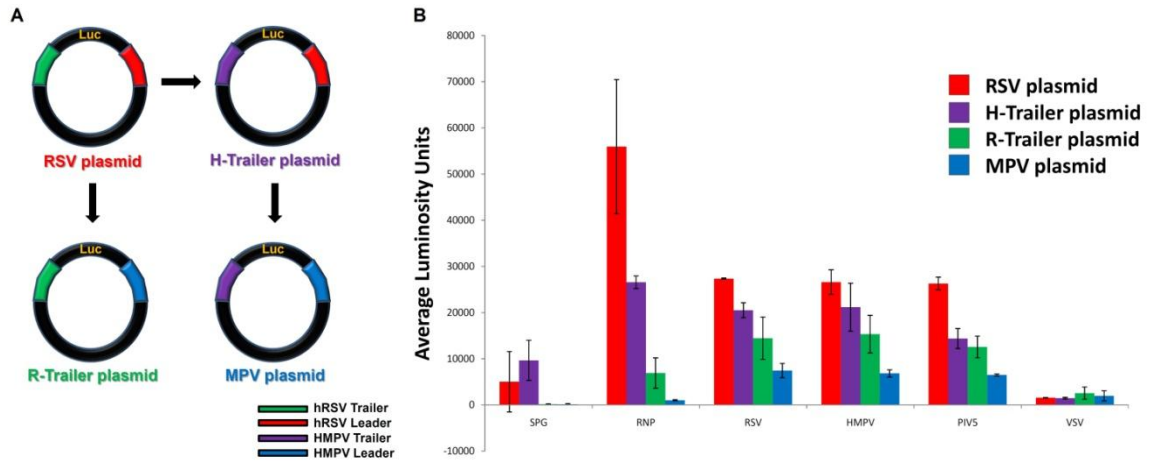
Figure 3. 8. Different promoter combinations vary in their ability to drive viral transcription.

(A) Catalog of the synthesized minireplicon vectors. The arrows show the order in which each plasmid was created from the RSV plasmid by the replacement of hRSV promoter sequences with those of HMPV. (B) In the minireplicon assay, the most expression of the reporter product was consistently observed with those constructs with an RSV promoter at 24 hours post transfection/infection. The loss of the RSV leader, however, seemed to be less deleterious than that of the trailer, suggesting a large role for that promoter in the assay. Interestingly, any paramyxovirus was capable of driving roughly equal amounts of gene expression while VSV was not able to promote expression for any construct.
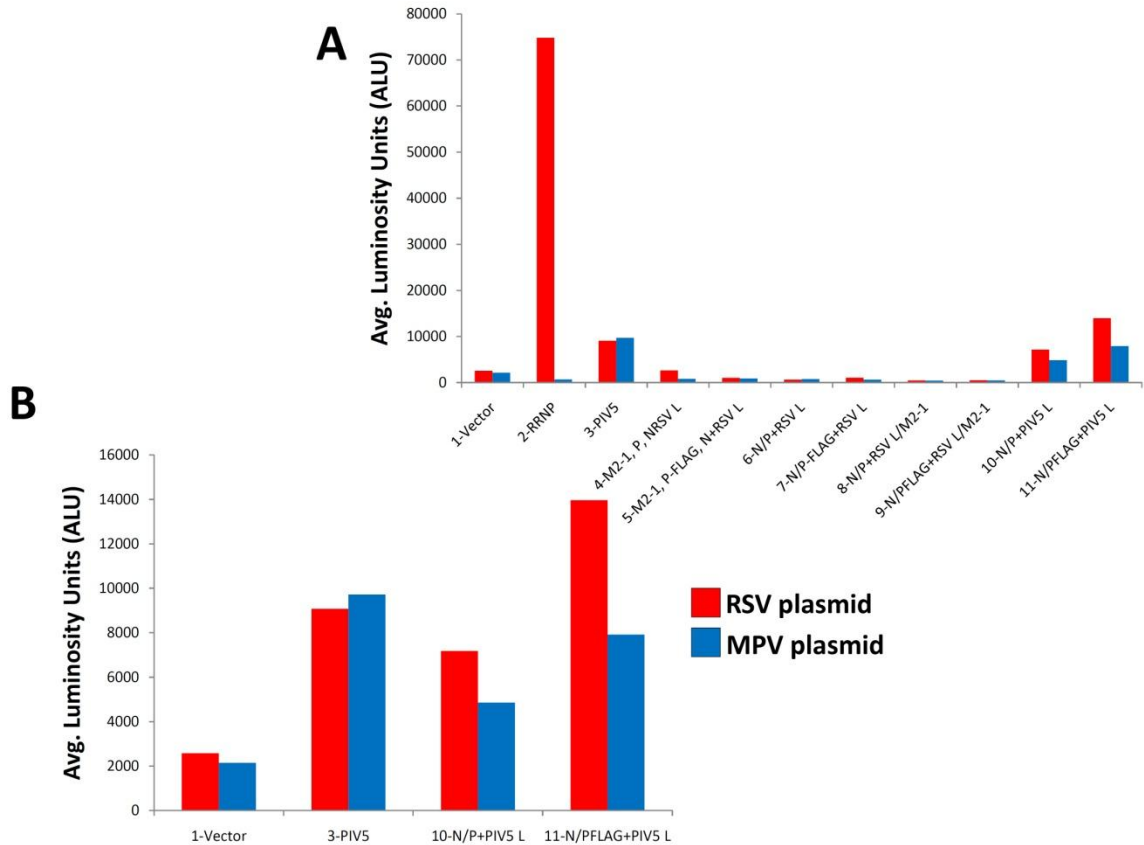
Figure 3.9. PIV5 L is able to complement other HMPV RNP components.

(A) The minireplicon assay was used to establish what viral polymerase, if any, could complement for the loss of HMPV L. While RSV L did not exhibit any expression above background levels, PIV5 L was able to promote luciferase activity in concert with HMPV N and P or P-FLAG at levels comparable to that of PIV5 N, P and L. (B) An inset of the same data as in A to better illustrate the effects of the complementation.

A   **B**   **C**

hRSV trailer terminal sequence (TTS)   Modified HMPV trailer (TTS+linker)   hRSV trailer
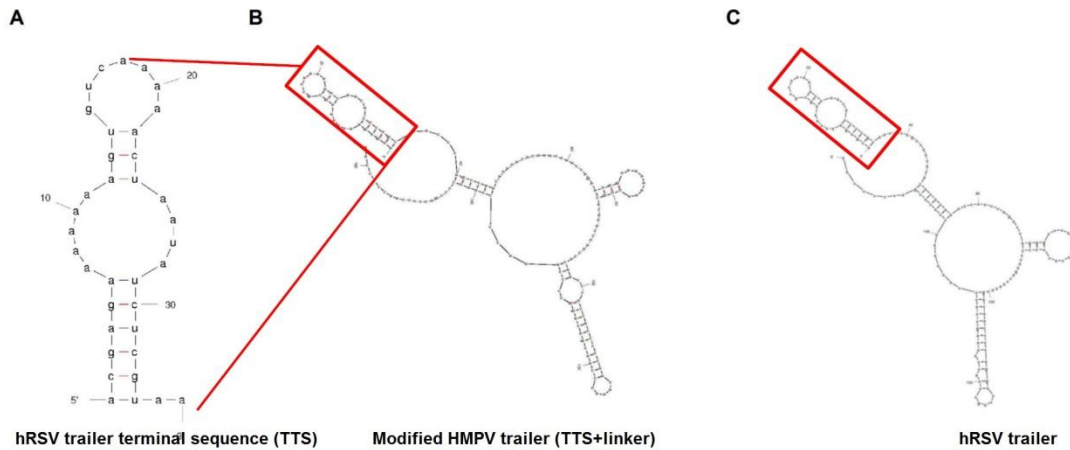
Figure 3.10. Predicted RNA folding of the HMPV trailer mimics that of the hRSV trailer with the addition of the TTS.

SplicePort renderings of RNA folding predictions for (A) the hRSV trailer terminal sequence (TTS), (B) HMPV trailer with the TTS and its linker and (C) hRSV trailer are shown. These demonstrate the similarity between the predicted fold of the two promoters when the HMPV trailer is modified. The addition of the TTS did not appear to dramatically alter the folding of the rest of the HMPV trailer relative to the previous predictions without this modification.
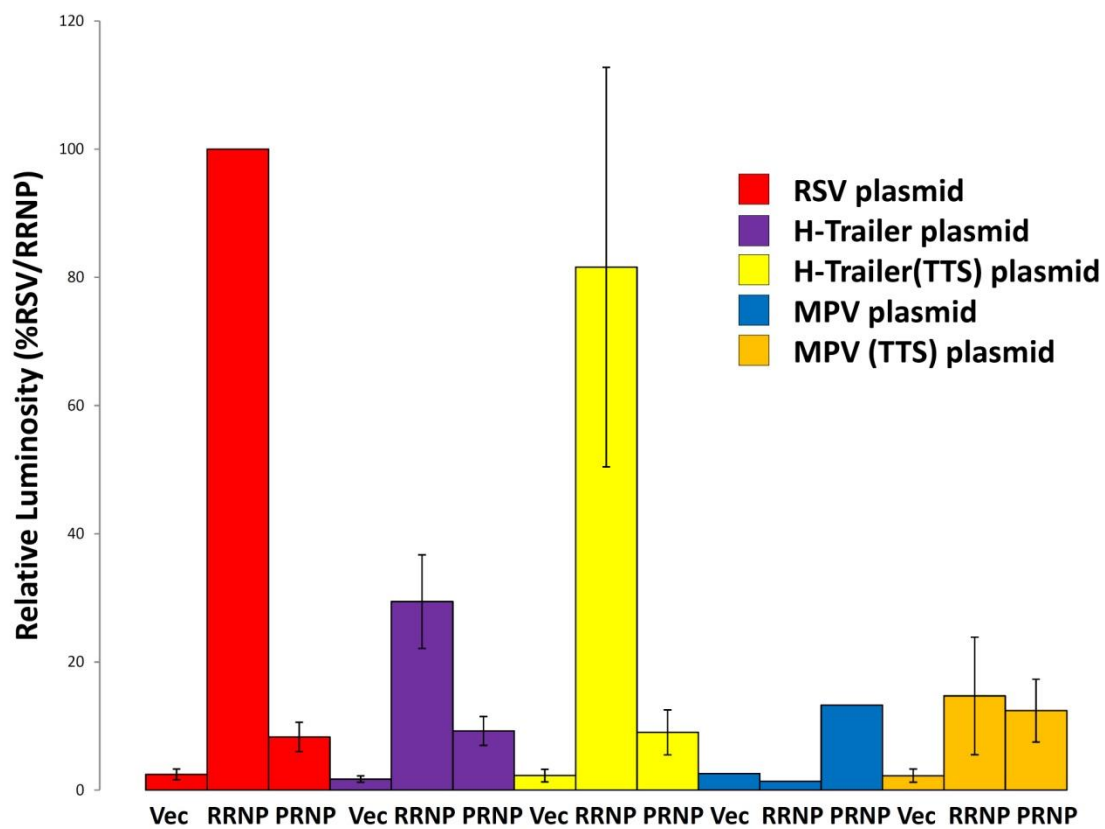
Figure 3.11. Addition of TTS to HMPV minireplicon promoters significantly increases luciferase activity.

When the 36nt TTS from the RSV trailer (along with its requisite linker region) is added to the HMPV trailer in either the homotypic or heterotypic plasmid, viral transcription activity as assessed by luciferase activity markedly increases. In the case of the H-trailer plasmid, such an addition makes no significant difference between the construct and the RSV homotypic plasmid.
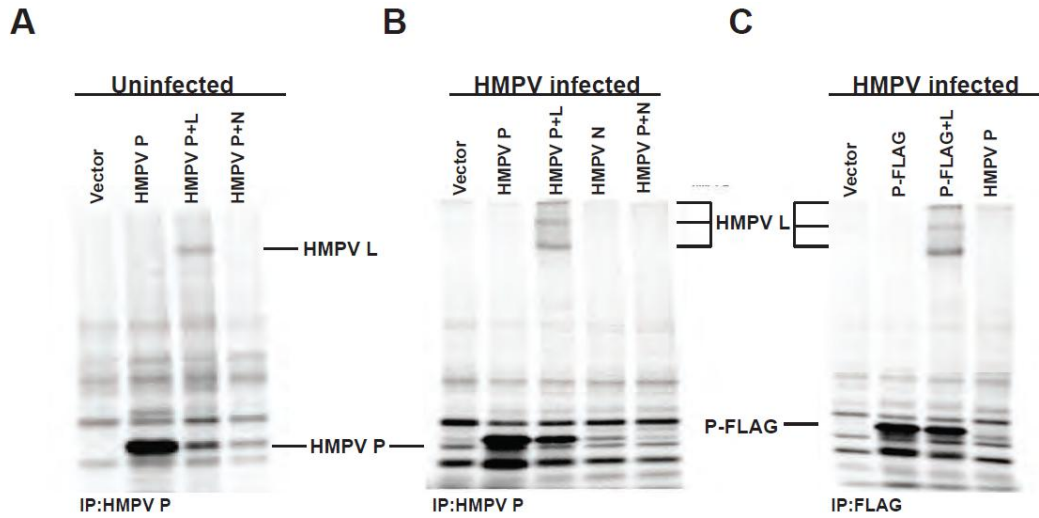
Figure 3.12. Different interactions are observed for HMPV P constructs in the presence and absence of infection.

(A) A549 cells were transfected with plasmids encoding the HMPV construct denoted above each lane before proteins and metabolically labeled with 35S before immunoprecipitation with either HMPV P or FLAG antibody. (B-C) Cells were transfected as before then infected at 24hpt prior to radiolabeling. Samples were assayed with either HMPV P or FLAG antibody.

A

Mock infected

	MCS	HMPV N	HMPV P	HMPV N/P	P-FLAG	P-FLAG/N	
HMPV N —							6HPT
HMPV N —							24HPT

IP: HMPV P/FLAG
WB: HMPV N

HMPV infected

	Viral input	MCS	HMPV N	HMPV P	HMPV N/P	P-FLAG	P-FLAG/N	
HMPV N —								6HPI
HMPV N —								24HPI

B

α-HMPV N

	Virus input	HMPV inf. (24HPI)	HMPV N
α-Tubulin —			
N —			

α-HMPV P

	Virus input	HMPV inf. (24HPI)	HMPV P	HMPV N+P
P —				

α-FLAG

	P-FLAG	
PFLAG —		50
		37

C

78
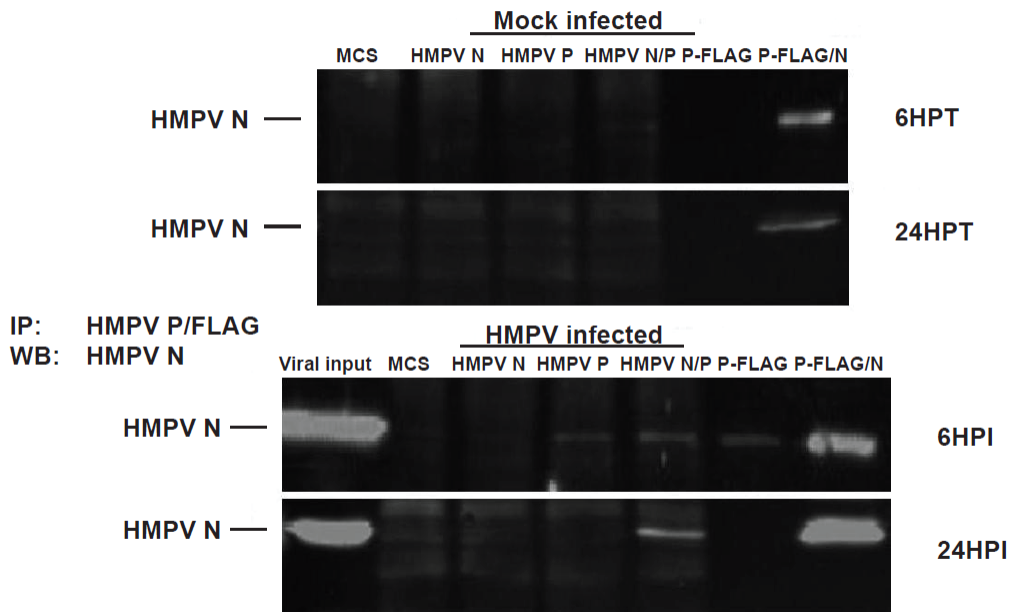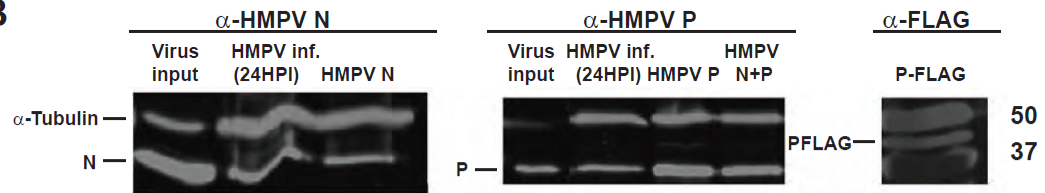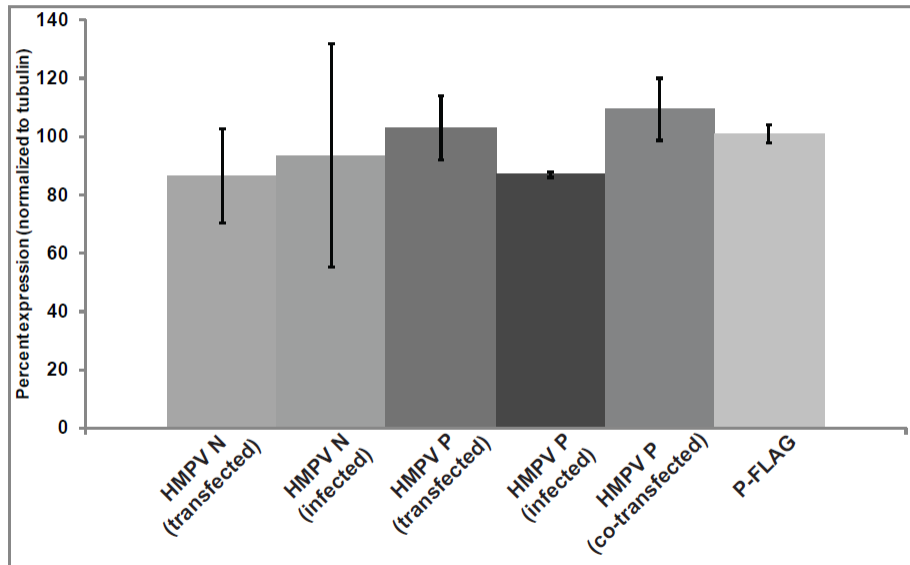
Figure 3.13. HMPV N and P-FLAG interact irrespective of cellular infection state.

(A) A549 cells were transfected plasmids encoding the HMPV construct denoted above each lane. At 24hpt, cells were either infected with HMPV (MOI=5) or mock infected for the amount of time indicated. Samples were then immunoprecipitated with an HMPV P antibody, and the bound fraction was blotted with an HMPV N antibody. (B) A549 cells were either infected with HMPV (MOI=5) or transfected with HMPV plasmid constructs. At 24hpt, samples were blotted for HMPV N or P. Gels are representative of three independent experiments. (C) Quantification HMPV protein levels normalized to alpha-tubulin expression from same lysates.
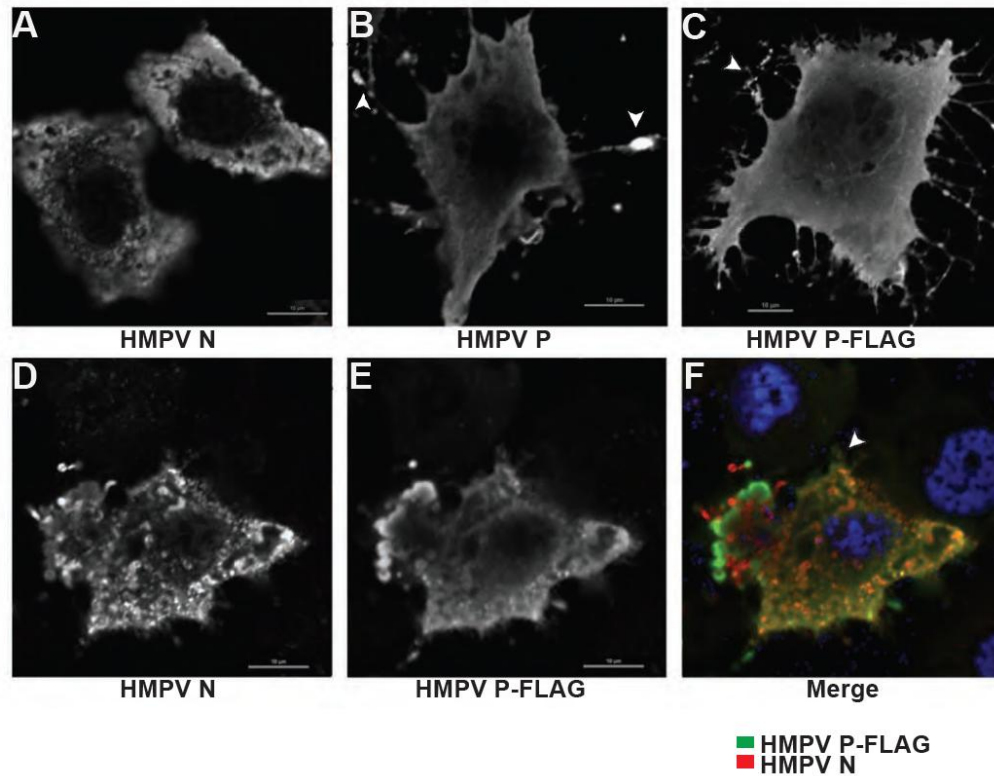
Figure 3.14. HMPV phosphoprotein concentrates at cellular periphery and in filamentous extensions.

A549 cells were transfected with 2.5ug pCAGGS plasmid DNA encoding the HMPV (strain CAN97-83) construct denoted below each panel (A-C). (D-F) A549 cells transfected with equal amounts HMPV N and HMPV P-FLAG pCAGGS constructs. Cells were imaged at 30 hours post transfection. Images are representative cells from no less than three separate experiments. Arrows point to concentrations of protein within filamentous extensions of each cell.

| A | B | C | D | E |

Mock   6HPI   12HPI   24HPI   48HPI

HMPV P
HMPV N

HMPV N

HMPV P

81
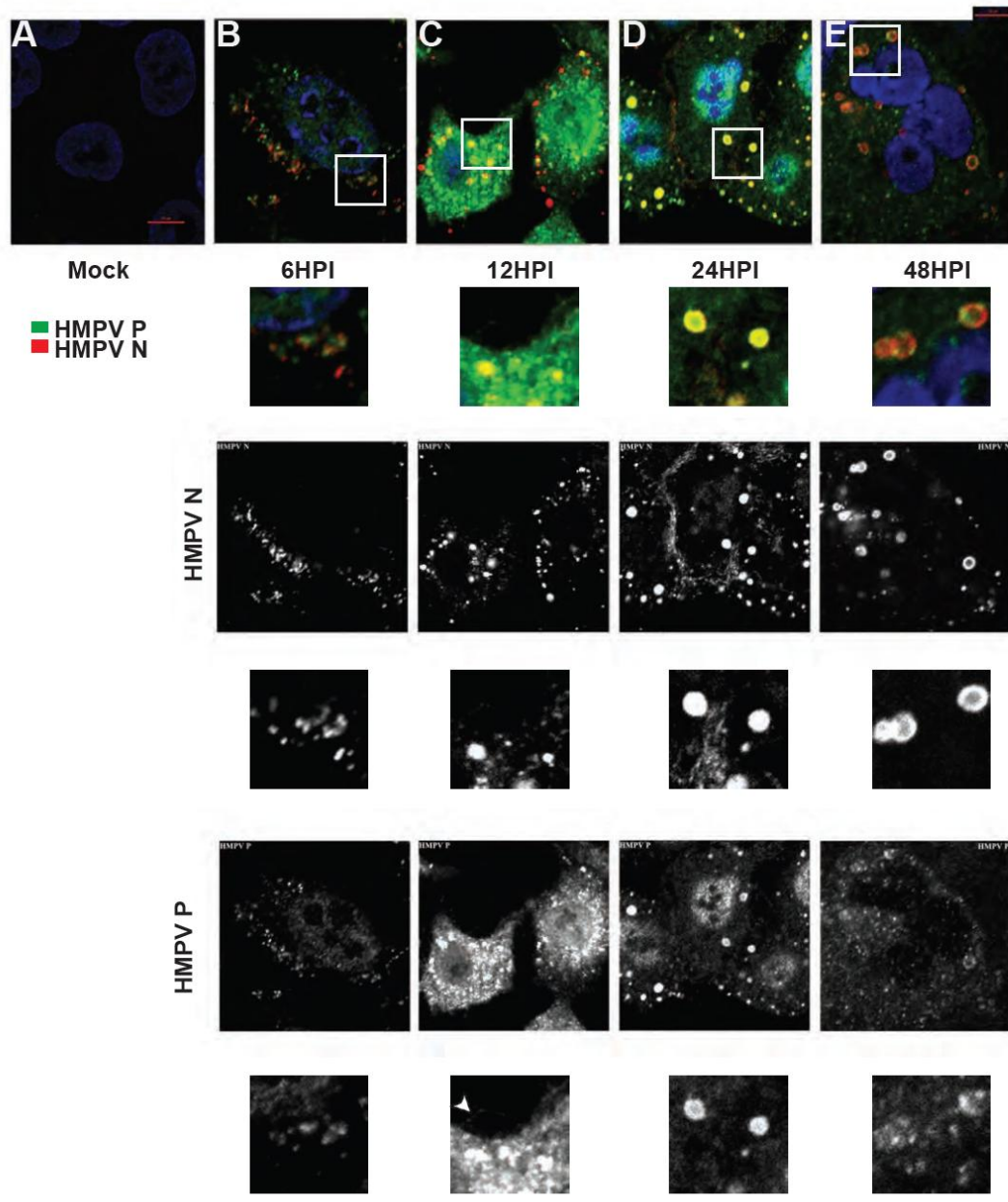
Figure 3.15. The distribution and co-localization of HMPV N and P varies within infected cells over time.

(A-E) A549 cells were infected with HMPV (strain CAN97-83) at an MOI of 5 for variable lengths of time (6-48h) prior to being fixed with 4% formaldehyde and processed for confocal microscopy. Images displayed are representative of at least three independent experiments. Arrows indicate protein with filamentous extension.
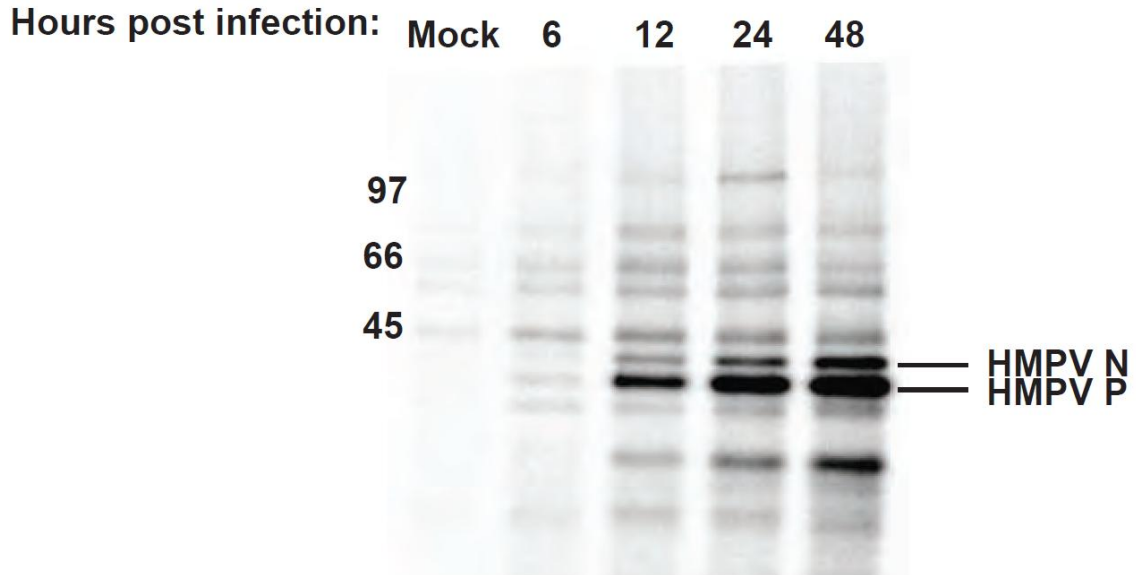
Figure 3.16. HMPV P levels markedly increase between 6 and 12 hours post infection.

A549 cells were infected with HMPV (MOI=5) for various lengths of time with 35S radiolabeling occurring at 1hpi through the end. Cells were then lysed to detect the amount of HMPV P and N that had been synthesized over the specific period.
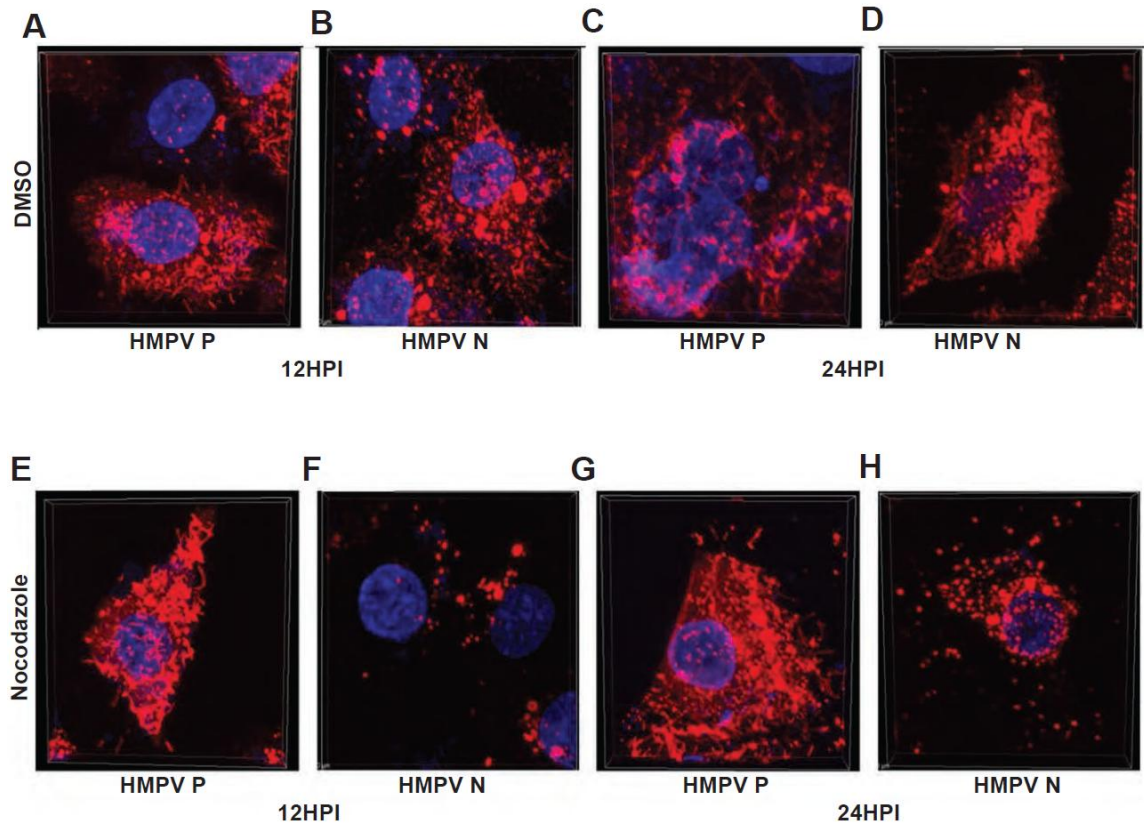
Figure 3.17. HMPV HMPV N and P translocate to the cellular periphery independently by 24 hours post infection.

(A-H) Confocal microscope Z-stack renderings of A549 cells infected with HMPV for the indicated length of time. In all cases, either DMSO or 7µg/ml nocodazole was added at 9hpi before allowing infection to proceed to end of time point.
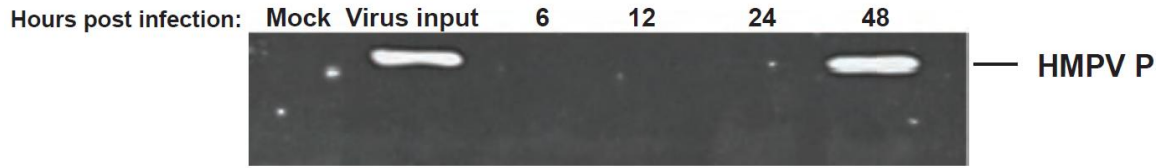
Figure 3.18. HMPV N and P peripheral transition temporally corresponds to viral egress.

A549 cells infected with HMPV (MOI=5) or mock infected for the amounts of time indicated. Cellular supernatants were then collected and centrifuged on a 20% sucrose cushion before being reconstituted and blotted with an HMPV P antibody. Work in this figure was done by Farah El-Najjar.
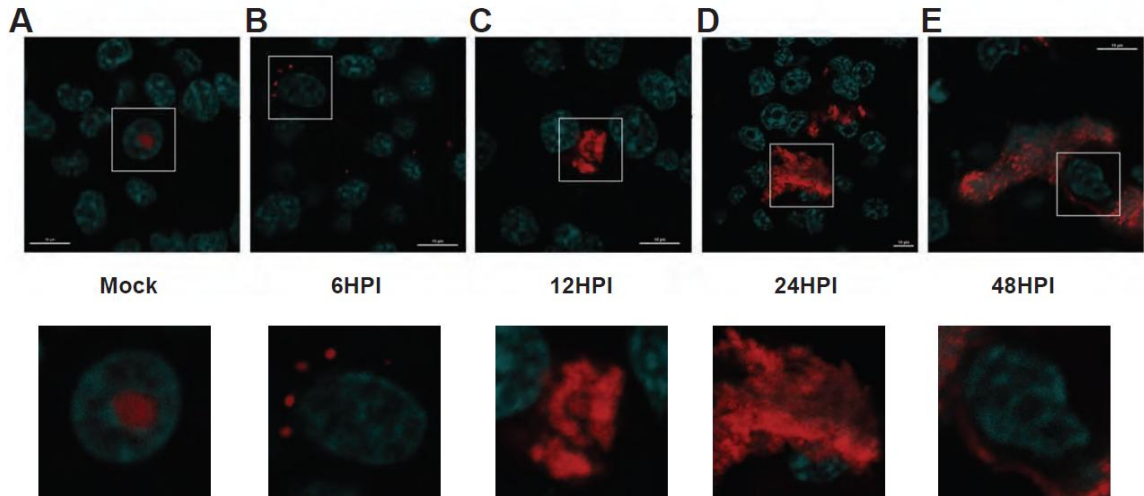
Figure 3.19. Labeled nascent RNA within HMPV-infected cells undergoes changes to its distribution similar to those of the non-structural proteins.

BSR cells were infected with HMPV (strain CAN97-83) at an MOI of 5 for variable lengths of time (6-48h), with the latter portion of that period being used to starve cells of uridine (2h) and label newly-synthesized RNA over a 3h interval with 5-bromouridine. Infection was ended with fixation before samples were processed for confocal microscopy. Nascent RNA is colored in red while nuclei, stained with DAPI, are colored cyan.

Chapter IV: Discussion

Subsection I: HMPV Fusion

The experimental results of these studies have demonstrated that processes governing the triggering of the HMPV fusion protein are even more complex than had been originally hypothesized. Specifically, the results showed that at least two regions within the metastable prefusion form influence this event. However, not even relaxing the constraints of both of these regions were sufficient to alleviate the necessity of low pH to induce the conformational change associated with HMPV fusion activity.

Studies of paramyxoviral fusion were buoyed significantly with the crystallization of PIV5 F in its prefusion form. The protein was stabilized with use of GCN4 tags replacing the transmembrane domains, and this allowed for some of the first structure-function studies of fusion proteins within this viral family [35]. Consequently, a block of residues within the F_2 region with conservation between PIV5 and Hendra virus F proteins was identified that demonstrated effects on the stability of the fusion protein when mutated. These effects were attributed to the modulation of the triggering of fusion [45]. However, it was not until a pH-dependent triggering mechanism for a paramyxovirus was found that this region's contribution to triggering fusion as opposed to other processes during the event could be tested [23].

These results show that HMPV F (CAN97-83) exhibits an enrichment in charged residues within this very region. As such, the ensuing mutagenesis studies that implicated CBF_2

as a regulator of HMPV F triggering are very much in agreement with previous work in the field. In fact, the results of the two studies mirror each other on the face of issue with both studies identifying mutations that exhibit either hypo- or hyperfusogenic phenotypes. Further, they both support the overall view of the field in that metastability is by and large controlled by the trigger of fusion. Delving even more deeply into the data, some of the findings in this work are entirely consistent with the other study. The idea that HMPV F isosteric mutations could, at least, attenuate the effects of a hyperfusogenic mutant with a presumed promiscuous trigger (e.g. D54N/E56Q/H435R) being a prime example. In that report, the authors concluded that side chain density played a role in the maintenance of optimal metastability in that an alanine substitution at I49 in PIV5 F resulted in an increase in fusion. The results reported here only go to underscore that this conservation observed between PIV5 and Hendra likely applies to a wider portion of *Paramyxoviridae*, at least as far as HMPV.

It is important to note that while I have implemented studies using the CAN97-83 strain of HMPV, which has been demonstrated to fuse in a pH-dependent manner, some argue that this is merely an anomaly among paramyxoviruses. In fact, it has been published that only a small number of known HMPV strains with Clade A exhibit greater fusion activity at reduced pH [24]. However, this argument is based, in part, upon the fallacy that all isolated strains of the virus currently available for research purposes mimic the population of virus strains at large. This is simply not the case. In fact, it is far more likely that a large number of clinically relevant strains are not available as such, given the observed differences between lab strains and newer clinical isolates for many viruses. To

that end, any suggestions as to the abundance of strains that present a particular activity are hasty, at best. Further, the authors of this work tested only five strains (one from each known clade and two from A2), showing that both their selected A1 strain and one of the two A2 strains tested (CAN97-83) exhibited the very activity that they go on to categorize as rare. In any event, the true value of a strain like the one used in these studies is that questions regarding the steps regulating the fusion process can be more carefully examined as there are both permissive and restrictive conditions under which we can test these hypotheses.

Among the discoveries facilitated within this system was the role of H435 in HMPV F-mediated fusion [25]. It was found that when H435 is mutated to alanine, fusion is drastically reduced. Interestingly, this particular histidine was only one of several that were examined for a role in HMPV F fusion. The underlying hypothesis was that this histidine was working in concert with surrounding positively charged residues to modulate triggering. This work also established H368 as an effector of HMPV F activity. This latter point was then expanded upon by another group, which in addition to implicating these histidine, examined the contribution of some of the adjacent positively charged residues [26]. Alanine scanning showed these residues to have an effect on triggering and to be fully consistent with the results reported here.

In fact, the results of these studies, while consistent with these reports in the field, allow for a much more complete picture of the complexities that are associated with HMPV F triggering. The findings show that while charge-charge interactions certainly play a role

in area around H435, the overall data suggest that both electrostatic and steric interactions are involved. Specifically, results showed that H435E or H435D mutations, a mimic for a protonated histidine, could ablate the ability of triggering, likely through the stabilization of interactions between H435 and some combination of K295, R396, and K438 [27]. However, the data also shows that isosteric mutations in F_2, namely at D54 and E56, can stabilize the protein as measured by cell surface expression. Taken together, this suggests a system in which triggering has no one on/off switch but rather a series of lynchpins that must be released in order to allow triggering to occur. To that end, it would appear that the necessity of low pH would likely only impact the electrostatic interactions but not others regulating this event.

To add yet another layer of complexity to HMPV fusion and entry, this virus has been reported to be equally infectious without its attachment protein [28]. This stands in stark contrast to the vast majority of paramyxoviruses, which are thought to need contacts between the fusion and attachment proteins to trigger fusion [86-88]. One can infer that such an obligate interaction between these proteins would minimize the amount of premature activation of fusion in these systems, essentially ensuring that attachment precedes triggering. In the absence of such a requirement, such as for HMPV, the need for some regulation of triggering within the protein itself becomes all the more crucial. As such, the pH dependency and multiple regions contributing to the control of this event for HMPV F would be a logical, expected outcome given the data presently accepted by the field.

Subsection II: HMPV Minireplicon

As many interesting questions that have arisen from the results of the work on the fusion protein, there may be even more conjecture surrounding the minireplicon project and HMPV promoter activity particularly. The results showed that there was a significant difference in the amount of transcription being driven by either hRSV promoter relative to that of HMPV; however, there may be some bias in the system given the subcloning techniques used to create the constructs. Further, I observed that any tested paramyxovirus was capable of driving roughly equivalent expression from any given set of promoters, suggesting that all within the family may have a degree of conservation with regard to polymerase-promoter interactions. On a similar note, the HMPV N and P plasmids were shown to be able to drive some RNA synthesis in concert with PIV5 L but not hRSV L, which again may be demonstrating conservation in particular domains of the RdRp. The results of this work certainly demonstrate that this interaction between the viral promoters and the proteins responsible for HMPV RNA synthesis warrant further study. These experiments would serve to further explain the ability of paramyovirus replication components to be interchanged.

With regard to paramyxovirus promoter activity as a director of RNA synthesis, hRSV stands out as an exemplar due to the inordinate amount of work performed over more than a decade with this particular virus. For instance, it has been shown that there is little difference between the leader and trailer promoters' abilities to drive RNA synthesis and that different nucleotides are required specifically for normal levels of either transcription or replication [68, 89]. Some of these moieties included 1U, 2G, 6U, and 7U for

replication (trailer promoter) or 3C, 5C, 8U, 9U, 10U, and 11U for transcription (leader). It is likely that similar results would be observed in HMPV as all these nucleotides in both the trailer and leader promoters are conserved. In fact, the one similar study examining the promoter activity of HMPV specifically did find that 2G was critical for maintaining viral replication but not transcription [90].

Bolstered by the similarities between the viral promoters observed in these studies, it seemed that the best way to approach questions about HMPV promoter activity would be in the context of the much more well-characterized hRSV system. As such, the minireplicon system established for these studies was meant to give comparative results. Given that premise of the experiment, the novel finding of hRSV promoters being capable of driving significantly greater gene expression relative to HMPV is difficult to place in the context of what has been reported in the field. However, given the myriad of similarities between the two pathogens, the discovery of such a difference is quite interesting. What remains unclear is the effect, if any, this difference may have on the overall infectious cycle of either virus.

Similarly, the fact that each paramyxovirus was able to equivalently induce transcription from a given set of promoters is also quite surprising. This result was further corroborated by the ability of PIV5 L to compensate for the loss HMPV L in the minireplicon assay. This concept of polymerase complementation and minireplicon degeneracy has been examined before with different constituents. In one instance, an HMPV minireplicon system was shown to be functional with any member of the

subfamily *Pneumovirinae*, including avian metapneumovirus (AMPV) or hRSV. However, bovine parainfluenza virus (PIV3) exhibited no such activity in the system [29]. Such a result suggested that there is some level of phylogenetic conservation required for RNA synthesis even within the *Paramyxoviridae* viral family. Further, replacement of the HMPV L gene with that of AMPV L resulted in attenuation of viral growth *in vivo* despite the minireplicon results.

However, a more recent study offers another methodology. In that work, the large polymerase proteins of three different viruses (measles, Nipah and hRSV) were truncated at points that had been shown to be tolerant of epitope tag insertions without detriment to functionality. After these protein fragments were synthesized, they were used in different combinations to determine the extent of trans-complementation possible between different viruses [91]. The authors found that no significant activity when different viral polymerase fragments were combined but that most RNA synthetic activity could be restored with the combination of homotypic fragments. Both of these studies seem to agree that even relatively phylogenetically similar agents may not be able to combine to drive RNA synthesis.

These results make sense insofar as different viruses are considered molecularly distinct agents for a reason and, therefore, trans-complementation is not likely. To that end, it would also seem that these studies are in disagreement with the findings reported here. However, this is simply not the case. Firstly, neither of the other reports compared the interactions between viral proteins as was done with these studies. For example, it was

shown that PIV5 L, in concert with HMPV P and N, was able to drive some RNA synthesis from either the RSV or MPV plasmid at levels roughly equivalent to that of PIV5 L, N and P. Conversely, hRSV L was not able to do so. This result suggests that PIV5 L is more able to interact with HMPV N and P than hRSV L. Further, it should be noted that the authors of the first report mentioned did not directly compare HMPV and hRSV, so there is not direct conflict with these results. There is even a region of PIV5 L with greater homology to HMPV L than hRSV L within the polymerase active site (692-7[HMPV]/720-5[PIV5]). The significance of this region with respect to template recognition, however, is not immediately clear.

The results reported here are also not at odds with those of the more recent study either. The overall premise of the authors' work was that separate domains of the polymerase do not function well when derived from different viruses. While the implications of domains within the polymerase polypeptide folding independently are very interesting, it does not rule out trans-complementation altogether. Rather, within the context of my work, it is extremely plausible that there are particular intramolecular interactions that are specific to each viral RdRp that affect overall functionality. In that case, substitution of the entire protein would be the only way to observe any sort of trans-complementation.

Finally, it is important to not overstate the phylogenetic relationship with regard to complementation as other factors, such as varying degrees of selectivity regarding template recognition are likely playing a role. The addition of the hRSV trailer terminal sequence (TTS) made the HMPV promoter a much better template for the hRSV

polymerase. This resulted in greater reporter gene expression. This suggests a certain level of specificity for this sequence in the case of this particular viral RdRp. Such an assertion is supported by a recent study of hRSV promoter-driven intiation of RNA synthesis. In that study, initiation was found to vary between two different start positions with different, non-templated extensions at the end of the collected antigenomes [92]. Analysis of this 3' terminal extension on promoter activity indicated that it can inhibit RNA synthesis initiation, indicating that hRSV polymerase-promoter interactions are more complex than previously thought and suggesting potentially sophisticated mechanisms for regulating promoter activity during infection.

To that end, the other results, in which hRSV L did not exhibit trans-complementation with HMPV N and P, are not surprising. If there is a greater stringency to the template recognition for hRSV, then it would follow that this condition is being contributed to by not only L but P and N as well. As such, HMPV P and N, despite sequence homology to their hRSV counterparts, may not be sufficient to confer the same level of selectivity. This could potenitally lead to aberrant template binding and abortive RNA synthesis.

Subsection III: HMPV Assembly

Overall, the findings presented focus on the temporal and spatial elements that underlie a productive HMPV infection from RNA synthesis to egress. One of the major results is that both HMPV N and P appear to move toward the plasma membrane prior to budding. While our work demonstrates that transient expression of HMPV P results in an observable concentration of the protein within filamentous processes, it is unknown whether these extensions are present in the cell prior to expression of the phosphoprotein. The data do not exclude the possibility that HMPV P could induce the formation of these extensions or, at least, that they form due to cellular signaling as a consequence of the presence of HMPV P in the cell. However, the mechanism for such events is unclear. One possibility is the modulation of cytoskeletal elements, particularly those that interact with actin filaments.

In one of these studies, association of hRSV P and F-actin was observed throughout infection beyond 8 hours post infection [93]. Further, the filaments could be prevented by either inhibition of phosphatidyl-3-kinase (PI3K) or the small GTPase Rac. These results suggested that hRSV proteins were forming these filaments via signal transduction pathway involving PI3K and Rac. Another report showed a role for RhoA, another small GTPase associated with the actin cytoskeleton, in hRSV budding [94]. In that case, it was formation of filamentous virions, specifically, that was affected. Interestingly, a more recent study shows that an interaction between the hRSV F glycoprotein and a complex of N, P and M is necessary to form the viral filaments. However, while residues in the cytoplasmic tail of F affected this process, it was apparent that these filaments

lacked F-actin, tubulin or ezrin [71]. These studies show that actin may be interacting with viral factors but that it is likely not the main component of the formation of hRSV filaments.

In agreement with the work on hRSV, no detectable interaction between HMPV P and a selection of various focal adhesion-specific proteins, including vinculin and α-actinin, was found (data not shown). This would suggest that filamentous actin is not responsible for the extensions observed in cells either expressing HMPV P or infected. In the absence of involvement with actin or microtubules (Figures 3.17E and 3.17G), it is plausible that the protein itself may be able to deform membranes in such a manner as to cause this morphology. If this were the case, one may also expect that HMPV P would be a minimal component for the formation virus-like particles; however, further study will be required to expand upon this finding and determine the underlying mechanism of this process as well as the role, if any, of filament formation in HMPV assembly.

Similarly, it has yet to be determined whether or not the potential membrane blebbing that was observed with the co-expression of HMPV P-FLAG and the nucleocapsid protein was actually perturbation of the membrane in a manner consistent with formation of virus particles. It has been reported that various paramyxoviral matrix proteins, alone or in concert with other viral factors, such as glycoproteins or the nucleocapsid, can alter cellular morphology and induce the formation of virus-like particles [95-101]. A finding that HMPV N and P can promote similar budding would be interesting as it would demonstrate that a combination of viral proteins can do so without the need of the matrix protein.

It is possible that, while HMPV N and P are always capable of particle formation, coalescence within inclusion bodies effectively secludes them from trafficking to the periphery. This is supported by the observations that P-FLAG and N, while not forming inclusions, do interact even in instances where WT P and N do not, such as in uninfected cells. Such a finding would also represent a novel association between HMPV N and P that is distinct from the inclusion body and the transient interaction during RNA synthesis.

The assertion that important N-P interactions can occur outside of inclusion bodies is further bolstered by other data surrounding HMPV P-FLAG. For example, the C-terminus of the phosphoprotein has been implicated as the domain responsible for binding the nucleocapsid in many viruses [102-104]. In these experiments the epitope tag was placed at this terminus, yet the proteins are still capable of interaction (Figure 3.13A). Additionally, the tag did not affect the protein's ability to concentrate within filamentous extensions (Figure 3.14C) or interact with the polymerase (Figure 3.12C). Consequently, we were unable to draw any conclusions regarding interaction between WT P and P-FLAG, due, in part, to differences between antibodies used in the immunoprecipitation. Evidence for or against such an interaction would be significant as the phosphoproteins of most members in *Mononegavirales* are thought to take on a higher order structure for at least some of its function [51-52]. This, however, has not yet been demonstrated for HMPV. As such, it is unclear if such an self-association would be necessary to retain optimal functionality.

The data regarding the HMPV N-P interaction, by contrast, allows for several conclusions to be drawn, particularly with respect to the role of inclusion bodies. These structures became a central focus of these experiments, and there is mounting evidence to suggest that inclusions are sites of RNA synthesis for NNS viruses. In fact, there is quite a bit of support for this assertion in the case of rhabdoviruses [105-106]. The issue is that there is no such support for this claim for paramyxoviruses. The results of these studies, in which newly-synthesized RNA mimic the observed distribution of viral proteins from punctate bodies to a more diffuse localization, are wholly consistent with the premise that inclusions are sites of viral RNA synthesis. However, it cannot be stated definitively if these bodies are the sole sites of this activity, particularly beyond 12 hours post infection as a more diffuse distribution is then observed. By contrast, HMPV N and P inclusions are still readily detected at 24hpi.

One caveat of the labeling assay is that it is impossible to distinguish RNA that was synthesized at the beginning of the labeling period from that assembled 2 or more hours later. Technically, it would be very difficult to label only during those brief periods as a substantial period of time is necessary to effectively starve the cells of uridine. Ultimately, this could mean that inclusions are strictly for the synthesis of RNA and that mRNA or viral genomes are moved away from these sites and nearer to the periphery of the cell. Additionally, the inability to use a second probe to observe where the HMPV proteins associated with RNA synthesis were localized relative to the RNA was a limitation that does not allow for a more definitive result. As both the RNA probe (anti-

BrdU) and anti-HMPV antibodies were from mouse hosts, there was no way to be able to observe both within one experiment.

Observations made in different systems may also shed light upon conserved modes of actions by different viruses. In the case of HMPV, the detection of viral protein within filamentous extensions at later points during infection fits well with what has been reported for hRSV [107]. These data are consistent with the premise that HMPV utilizes these extensions as mode of transmission for more efficient spread of progeny viruses to adjacent cells. Similar evidence has been previously reported for RSV with regard to filament formation likely occurring ahead of budding [108]. Though the cellular events involved in the formation or utilization of these structures may vary, this similarity is consistent with a potential overarching mechanism of viral transmission among the *Pneumovirinae* subfamily. In such a mechanism, these processes would make cell-cell contacts between adjacent cells. Therefore, the virus can utilize them as budding platforms, which then allows for direct orientation of progeny virus to uninfected cells. This would provide an efficient manner to establish productive infection within a host while minimizing exposure to the extracellular environment, which can lead to greater immune responses. If established and characterized, this process could provide a potential target against which to design therapies and antiviral compounds specifically targeted to halting filament budding, thus inhibiting transmission.

The time course studies conducted in this report demonstrate the progression of infection and highlight the temporal nature of specific functionalities as well. These results are also consistent with a similar study on Ebola, another NNS virus [109]. It was reported

that Ebola inclusion bodies, containing nucleocapsid, phosphoprotein and matrix equivalents, move to the perinuclear space upon entry. RNA synthesis, which began in these small punctate structures, expands to one side of the cell. Viral nucleocapsids are then assembled and shuttle to the plasma membrane. While there are certainly differences between these viruses, including the minimal constituents of the inclusion body, the similarities to our observations suggest that many, if not all, NNS viruses generally approach the tasks necessary for establishing a productive infection in a similar manner. There will have to be more studies within different viral systems before more concrete conclusions regarding conservation of the infectious cycle of these viruses can be made, however.

Chapter V: Implications and Significance

Subsection I: HMPV Fusion

One of the more interesting findings from the initial mutagenesis studies was that there were residues in both the CBF2 region and within HRA that showed a phenotype when alanine was substituted for the charged side chain. Ultimately, work with the HRA mutants had to be abandoned given the fact that there was no way to assess whether the effects of the mutation were due to modulation of triggering or an effect adoption of the post-fusion conformation. These residues, particularly K166, are almost certainly influencing HMPV F. In the absence of conformation-specific antibodies to HMPV F, one could combine the HRA mutations with those of the CBF2 region and/or H435R. What is most likely, however, for this theoretical K166A/D54A/E56A/H435R mutant is what was observed for the mutant without K166A—increased instability. In fact, it is entirely possible that such a mutation would result in such a degree of instability that the protein would never be able to get through the secretory pathway without triggering.

Thusly, there is a conundrum of studying the pH dependency of HMPV F. One cannot definitively state that all regions regulating the low pH trigger of the protein have been identified unless a mutant is produced that is relieved of this constraint on its fusion activity. However, dynamics of the metastable state of HMPV F are likely such that relaxing these constraints to such a degree would almost certainly result in a protein that would not be able to be presented on the cell surface. Combining hyperfusogenic mutants from the two regions in this work led to a protein that was substantially less

stable. Given that there is likely at least one other region also modulating the low pH dependency of the triggering of fusion, the protein with a similar mutation in this region would likely become all the more unstable. From a pathogenic standpoint, metastability requires that a protein be able to maintain a pre-fusion form not only through the secretory pathway but also for some period of time on the surface of a viral particle. For this reason, it is unlikely that combinatorial mutagenesis studies alone will be able to identify all regions responsible for regulation of HMPV F triggering.

Similar to the issue of identifying further areas governing low pH triggering, identification of the protease that is responsible for the cleavage of HMPV F *in vivo* is a tough proposition. The results show that a single point mutation at position 51 was sufficient to halt fusion activity. Upon further study, it was found that this mutation altered the proteolytic processing of the protein. What was fascinating about these results is that neither of the two mutations tested were at all conservative, so there is little evidence that can be gleaned from that aspect of the studies.

Ideally, additional mutations at E51 would be synthesized, representing much less radical changes; these would include E51D and E51Q. The former mutation retains the charge at the position but with an amino acid side chain that is one carbon shorter. Similarly, the latter retains the size of the side chain without the charge. Since, the hypothesis is that the less conservative mutations were sufficient to locally alter protein conformation such that aberrant cleavage could occur, these mutants would shed light on just what type of forces are responsible for the maintenance of that proper fold. If E51D alone exhibited

alterations to cleavage, it would be suggestive that amino acid packing is playing a role in the maintenance of the structure. Conversely, if only E51Q were aberrantly processed, it would suggest that charge-charge interactions are playing a role in the process. Given the results of similar isosteric mutagenesis at D54 and E56, the first scenario is more plausible as these mutations appeared to have somewhat of a stabilizing effect. It is also possible that both additional mutants would exhibit the same phenotype as the others. In this case, one may need to investigate the possible role of the coordination of metal ions about the site, which could have a profound impact on protease activity.

Another area within these studies that merits closer investigation is the potential crosstalk between (and/or hierarchy of) the two identified areas of HMPV F that regulate triggering. The combinatorial mutagenesis study was specifically looking for a mixture of mutations that would allow for triggering at higher pH. As previously discussed, this may not be feasible within these methods. However, more can certainly be learned about the interplay between the region about H435 and the CBF2. For example, one would test whether an extremely hyperfusogenic F2 mutant such as E56A would be sufficient rescue the phenotype of H435D/E, which had been shown to lock the prefusion form into place. In theory, the converse of this could also be tested, but a mutation in F2 that does not allow conformational change to the post-fusion has yet to be identified. In fact, the lack of such a phenotype for any mutant in the F2 region suggests that H435 is dominant with respect to electrostatic interactions that modulate triggering.

The results of this work on the pH dependent triggering of HMPV F illustrate the complexities of regulation of HMPV fusion. By having a single protein that can independently mediate fusion, the virus is dependent upon the activity of this protein more than others as a high error rate in replication or assembly can still theoretically lead to a viable pathogen. However, if metastability is altered even slightly it can result in a premature triggering event or one that does not occur at all. In either case the result is no infection. Given the importance of this protein to the viral infectious cycle, it is little wonder that there would be multiple layers of regulation of the fusion trigger. What is the most remarkable is that all of this is encoded within the primary sequence of the protein and how it folds. If nothing else, these studies demonstrate the efficiency of HMPV and similar viruses to be able to so elegantly orchestrate the cascade of event necessary to enter a cell through a single protein.

Subsection II: HMPV Minireplicon

It must be remembered that the minireplicon system created for this work was heavily derived from the system established by the lab of Dr. Richard Plemper with the gracious gift of the RSV minireplicon plasmid. This fact must be taken into account when analyzing these data objectively as one may argue that these results are artifacts of the subcloning process and that HMPV does not truly have such a relatively low level of transcription. However, the data do not support this assertion. After every construct was synthesized and independently sequenced to ensure proper cloning, they were all tested under the same conditions with plasmids encoding the hRSV transcription machinery. These conditions are what likely make levels of HMPV gene expression seem comparatively meager. This baseline was intentionally set up to allow for maximal signal from the RSV internal control in addition to the fact that the HMPV L construct had questionable functionality when used in the minireplicon assay, even after codon optimization.

Further, it is plausible that the RSV RdRp has either lower binding affinity for the HMPV promoters. Other data provides evidence to this end, including the fact that PIV5 L but not hRSV L was able to complement the loss of HMPV L. Additionally, the HMPV trailer became much more active with RSV L once the TTS was added, suggesting that optimal promoter interaction with RSV L only occurs with that sequence at the trailer's terminus. Taken together, it is much more likely that part of the lower transcription rate observed in HMPV can be attributed to the enhanced selectivity of hRSV L for the TTS.

Another interesting finding is the ability of all tested paramyxoviruses to drive equal levels of transcription from a given minireplicon system and with a lower signal is lower than that of co-transfection of plasmids encoding the N, P and L. The second point can be explained by the fact that a live virus has its own genome with which the RNA synthesis machinery can interact, so dampening of the signal under such conditions is inevitable. The initial point, however, may be best explained by a relatively recent concept in the field of virology known as the quasispecies theory. The basic idea of the quasispecies theory is that RNA viruses exist as hypermutable individuals within a cellular population, and as genetic diversity is crucial to the survival of any population in a given system, these individuals are not monolithic in their genomic sequences as many often like to think. In addition to the consensus or base sequence that has been selected for over generations, genetic polymorphisms are maintained at relatively steady levels within a given population to allow for rapid adaptation to a changing cellular environment (reviewed in [33]).

This theory relates to the minireplicon assay through the findings that live virus infection of all paramyxoviruses drove similar levels of expression. I have already discussed the plausibility of the different paramyxoviral polymerases having variable selectivity for particular sequences at the viral promoter. However, it is similarly plausible under quasispecies theory that a segment of the virus population possesses polymorphisms that allow for broader recognition and this minireplicon assay has actually selected for these individuals in the viral population. Given the length of incubation (24 hours) during the

assay, this would be more than sufficient time for these individuals to induce transcription of the minireplicon reporter gene. However, the more likely explanation is that there is simply some level of conservation with regard to paramyxoviral promoter binding, despite differences in the predicted RNA structures, especially given that VSV could not induce gene transcription at any time during these assays.

This idea of paramyxoviral conservation is further bolstered by the complementation of HMPV N and P with PIV5 L. Beyond the complementation itself, the fact that PIV5 L, either with its nucleocapsid and phosphoprotein or that of HMPV, could drive relatively equal rates of transcription for either the RSV or MPV promoter provides further evidence that the issues from the initial assays, in which the MPV plasmid seemed to be nearly non-functional, were likely due to the use of hRSV proteins to induce the signal. Under the assumption that the L protein governs the specificity of the protein-RNA interaction at the viral promoter during the initiation of RNA synthesis, it is likely that PIV5 L has a less stringent recognition motif than that hRSV L. Further, there is only one region by ClustalW alignment where PIV5 L has greater sequence identity to HMPV L than does hRSV L (692-7[HMPV]/720-5[PIV5]), which putatively maps to conserved Domain III, which also contains the polymerase active site. However, there are no studies that definitively demonstrate which domains of the polymerase interact with the viral promoter.

Such a study of interactions between the RdRp and the viral promoters is just one of a host of future directions that this work shows as needing to be addressed. In the case of

such a study, one could crosslink viral polymerases (or individually folded domains of each) to the RNA. After using RNase to digest unbound RNA, sequencing of the cDNA would give the bound portion of the nucleic acid. Similarly, the HMPV-PIV5 L complementation could be further explored through site-directed mutagenesis studies of the region of high conservation in Domain III followed by either the aforementioned binding assay or the minireplicon assay.

As one can look in more detail at the contribution of the large protein to the results of these studies, so too can the contribution of the promoters themselves be further evaluated. Given that an alteration to the trailer promoter yielded a significant change in measured gene transcription, one must first evaluate the contribution of both promoters to transcription. In fact, it is still unclear whether the modification of the HMPV trailer made the construct more suited to the minireplicon assay because the trailer promoter itself is contributing directly to transcription of gene products or, more consistent with the body of work in the field, that the greater activity at the trailer promoter facilitated more genomic replication [89]. Increased replicase activity would, in turn, lead to more available genomes for transcription (Figure 1.6).

There are several ways to address this question. One of the most direct would be to disable the ability of the minigenome to replicate itself, while not affecting the ability to produce mRNA. For HMPV, it has been reported that a transversion at the second position of the trailer (C2G) selectively ablates genomic replication but not gene transcription in a minigenome system [90]. Introduction of this mutation into the TTS

modified trailers could show that the enhancement observed was due to greater replication if this particular mutant returns to levels of expression consistent with the non-modified promoter. Similarly, this contribution from the trailer can be measured by selectively quantifying the amount of antigenomic RNA present by either Northern blotting or quantitative RT-PCR.

The results of these experiments have shown that there appear to be differences between viruses with regard to the promoter's ability to induce gene transcription. Additionally, they have shown that combinations of various viral proteins within the *Paramyxoviridae* family can functionally compensate for one another to varying degrees. They have also identified a region that seems to confer specificity to the trailer promoter for the hRSV polymerase. Despite these findings, major questions remain to be addressed in the characterization of viral promoter dynamics and their interactions with the polymerase.

Subsection III: HMPV Assembly

To this point I have discussed both HMPV fusion and transcription. However, the final portion of the presented work may present some of the most intriguing questions with respect to what these very initial experiments could lead to with further study. Among these exploratory findings were that HMPV P concentrates within filamentous extensions during the latter stages of infection but prior to detectable egress of viral particles. There was also evidence to show that HMPV N coalesces in a lattice-like distribution at similar points post infection and that this is likely microtubule-dependent. In addition, it was shown that viral RNA retains a punctate structure within the cell throughout infection prior to being visualized in the filamentous extension by 48 hours post infection.

Moving forward from these results with the ultimate goal of identifying and targeting unique interactions among viral factors during HMPV infection, several experimental directions can be explored at the level of RNA synthesis and particle assembly. Chief among such experiments should be a focus on definitive characterization of HMPV N and P from entry to egress. Using the P-FLAG protein in a comparative analysis with the WT protein, one can conduct a controlled proteolytic digest such that the interacting regions of N and P or P-FLAG, P and itself or P-FLAG and P-FLAG and itself can all be done. Following gel electrophoresis and mass spectrometry, regions of interaction can be characterized for HMPV. The technical difficulty of this experiment would be quite high, but there is an alternative. Structural analysis has been used to show such contacts for other viruses and can be a way forward with HMPV as well [102-103].

From there, it would be most logical to next attempt to establish a cellular mechanism for the alteration in localization of both HMPV N and P over the course of infection. One cellular factor that may be playing a role in this is Rab11, a small GTPase that typically localizes to recycling endosomes. However, it is known that Rab11 can move about the cell on microtubules, which would explain the effect of nocodazole on HMPV N (Figure 3.15) [110]. Checking for a direct interaction of Rab11 with HMPV N, P or P-FLAG would be the best manner in which to initiate these studies. Additionally, the use of a dominant-negative (GDP-locked) Rab11 has been shown to mimic cytoskeletal disruption for elements carried by these vesicles [111]. Expression of this dominant negative protein in an HMPV-infected cell could be directly compared to the effects of nocodazole. If HMPV N translocation is similarly affected in both cases, this would be evidence of a microtubule-dependent role for Rab11 in the process.

While elucidation of the mechanism behind the observed translocation of HMPV N is interesting on its own, one would be remiss to not also attempt to link RNA synthesis to this process as well. One straightforward experiment to this end would entail following newly synthesized RNA in cells that had been treated with nocodazole. This would yield a definitive answer as to whether the HMPV nucleocapsid that is observed in a lattice-like distribution at 12 or 24 hours post infection is primarily associated with RNA or free protein. If the RNA is similarly restricted to punctate bodies following drug treatment, it would implicate this viral lattice as an intermediary in the transition from RNA synthesis to virion assembly. Further, Rab11-postive compartments have been demonstrated to move influenza A viral RNA from the nucleus [112]. While HMPV RNA does not enter

the nucleus, its concentration at the perinuclear space early in infection suggests potential conservation of this mechanism.

Closer examination of the interaction between HMPV N and P, would be similarly interesting as study N alone. Specifically, one could assess the ability of these proteins to form VLPs in the absence of infection. This is particularly interesting given the microscopy for co-expression of HMPV N and P-FLAG in which membrane blebs were visualized (Figure 3.14D-F). If any combination of N, P and P-FLAG were sufficient for VLP formation, then it would also raise questions as to the function of the matrix protein, which is typically thought to be integral to the process for most NNS viruses [95-101]. Even in that scenario, however, the matrix protein could still have a large role in organization of complete virus particle. Moreover, one could then attempt to understand the underlying mechanism of this phenomenon. For example, it may be possible to link the concentration of HMPV P to the filamentous extensions and VLP formation.

In order to do this, however, a greater understanding of how and when the extensions are used by the virus must be had. A simple interaction screen with proteins known to associate with focal adhesions, such as talin or RhoA, would be a start. If any interactions are found, knockdowns of the interacting proteins followed by infection may shed light on how the virus is using the extensions. Such a result could even spatially link viral assembly with particle egress.

As there have been technical issues visualizing HMPV RNA and HMPV proteins simultaneously due to antibody host limitations, one way around this would be to create chimeric proteins that are auto-fluorescent. Using an mCherry fusion, for example, with HMPV N or P would easily allow for visualization of both protein and RNA within one experiment. Such a study would be extremely informative as to where the viral proteins and RNA localize with respect to one another throughout HMPV infection. Such a method may even allow for visualization of the large polymerase, to which there is currently no antibody for HMPV.

The study of HMPV assembly has lagged behind other viral processes in the first decade since its characterization. As more facets of this agent's pathogenicity come to light with regard to fusion and entry, it will be even more crucial to be able to have an understanding of the subsequent steps in infection as well through continued studies like those proposed here. This comprehensive characterization of HMPV biology is the only way to intelligently design further potential antiviral therapies.

Subsection IV: Overall Implications and Significance

The studies presented herein allow for a working model of the HMPV infectious cycle from beginning to end with new insights at several critical junctures in the process. An infectious particle is likely internalized by the host cell following attachment, mediated by the fusion protein. Once within the rapidly acidifying compartment, the fusion protein is able to sense the pH drop via a protonation event at H435. Simultaneously, the hypercharged region in CBF_2, containing numerous acidic amino acids, potentially have salt bridges disrupted. These events, and others that we do not yet fully understand, all slightly alter the conformation of the metastable trimer such that it is triggered to adopt the postfusion form.

Once the viral RNP core enters the cytosol RNA synthesis occurs, likely within inclusion bodies. This transcriptive activity, which occurs largely in the perinuclear space, is bolstered over time by full genomic replication, allowing for greater concurrent synthesis of viral gene products. Over time these viral proteins either translocate from the inclusion body or traffic directly to either the plasma membrane (P) or the viral lattice (N and P). Gradually, HMPV P concentrates in the peripheral filamentous extensions. HMPV N and viral RNA are also concentrated in these areas at slightly later times. As these processes extend to adjacent cells, viral budding occurs at or around 24 hours from initial infection, becoming more pronounced as infection progresses.

The combination of the results from these studies has significantly contributed to the understanding of the overall pathogenesis of human metapneumovirus. Like most other

emerging pathogens, HMPV has often been viewed through the prism of its similarities to more well-studied viruses since its characterization in 2001. In contrast, this work sought to shed light on novel processes at the cellular and macromolecular level that govern seminal events at critical points during an infection. To that end, this goal was successfully met as novel characteristics of HMPV function were found within the fusion protein, a necessary component of viral entry. Further, activity of the HMPV promoters was assessed, and the dynamics of the major protein-protein interaction linking RNA synthesis to viral assembly was elucidated. Overall, the conclusion is that while HMPV is similar to many viruses in many respects, it is first and foremost a uniquely interesting intracellular parasite that considerably deviates from the dogma of similar viruses in some respects while following the trend of similar viruses in others.

The chief implications of these studies are that several new questions arise surrounding each of the areas of HMPV functionality addressed herein. These include concerns as to how interrelated each of these processes truly are; for example, while the more direct query of what requirements are necessary to alleviate the necessity of low pH to trigger the fusion protein is intriguing, one must consider what effects this may have downstream in the process of HMPV infection. In this instance, viral entry through an endocytic compartment may be favored as a means of orienting the RNP core of the particle toward a specific locale within the cytoplasm, such as the perinuclear space. Further, if one allows that specialized carriers, such as Rab11, are involved in the trafficking of viral components either to the perinuclear space or away from the nucleus at later points in

infection, then it would logically follow that entry to the cell through such a compartment may spatially link this interaction with that carrier at the earliest moment possible.

The best way to test this hypothesis would be via the creation of recombinant viruses. First one must create a virus (or VLP) presenting a different glycoprotein on its surface, such as PIV5 F with its attachment protein HN, that has been demonstrated to obligately enter at the plasma membrane. However, all internal components should be HMPV-specific. One can then follow the assembly of this virus in a similar manner as described in these works. Significant deviation from the observed pattern would suggest one of two underlying and equally interesting conclusions. The first is that entry via endocytosis is necessary for proper assembly due to spatially orienting the proteins to a specific subcellular location. The second, and far less likely, conclusion would be that the glycoprotein in its post-fusion conformation is somehow orienting the RNP to its proper location within the cell for optimal assembly.

Just as viral entry can be theoretically linked to assembly, even greater crosstalk can be expected between the replication and assembly processes. The results showed that HMPV P goes from a virtually exclusive localization within inclusion bodies at 6 hours post infection to the filamentous extensions by 12 and 24 hours. This change in localization seems to occur prior to that of HMPV N or the viral RNA being visualized in these peripheral areas. Given the possibility that these extensions are integral to the egress process for HMPV, therein is a rationale for a relatively slow transcription rate for HMPV. This phenomenon may allow more time for greater viral protein accumulation

and, therefore, establishment of cellular egress structures (concentrated with HMPV P) prior to ramping up particle assembly. This is also consistent with the observation of RNA throughout the infected cell only at timepoints in which some viral budding could be detected (24 and 48hpi). An alternative explanation for a slow rate of transcription is enhanced evasion of the innate immune response. It is also plausible that mRNA half-life of HMPV transcripts is much greater than that of cellular genes or even other viruses, such as hRSV.

Finally, the unique reagents assembled throughout the course of this work lend themselves to studies that address interesting complex aspects of HMPV biology and pathogenesis. For example, one can readily measure the ability of HMPV P-FLAG to drive transcription within the minireplicon system in the absence of WT P. This would be informative on numerous fronts. Primarily, it would provide evidence as to the necessity of inclusion bodies as replication sites since these do not form with P-FLAG and N, though the fact that they still interact does not rule out the possibility of RNA synthesis functionality remaining intact. One can also co-express the viral proteins on separate plasmids and attempt to create a P-FLAG recombinant virus, which could then be tested in all assays from RNA synthesis to egress.

Perhaps the most striking aspect of this work as a whole is not any particular result but rather how much is simply not known about HMPV specifically. This virus, clinically relevant as it is, remains something of an enigma with the picture becoming more complex as each novel characteristic of its pathogenicity is revealed To that end, these findings do not represent a conclusion but rather a beginning. This work, along with that

of many others, is the initiation of a greater understanding of a pathogen that ultimately infects virtually every human on the planet and has been responsible for countless hospitalizations and fatalities for more than half a century.

REFERENCES

1. Steffen DL, X.K., Nikolov DB, Broder CC, *Henipavirus mediated membrane fusion, virus entry and targeted therapeutics.* Viruses, 2012. **4**(2): p. 280-308.
2. Lamb, R.A., Kolakofsky D., *Paramyxoviridae: The Viruses and Their Replication*, in *Fields Virology*, D.M. Knipe, Howley, P.M., Editor. 2007, Lippincott William & Wilkins. p. 1305-1333.
3. Dereeper A., A.S., Claverie J.M., Blanc G., *BLAST-EXPLORER helps you building datasets for phylogenetic analysis.* BMC Evol Biol., 2010. **10**(8).
4. Dereeper A., G.V., Blanc G., Audic S., Buffet S., Chevenet F., Dufayard J.F., Guindon S., Lefort V., Lescot M., Claverie J.M., Gascuel O., *Phylogeny.fr: robust phylogenetic analysis for the non-specialist.* Nucleic Acids Res., 2008. **2008 July 1**(36 (Web Server Issue)): p. W465-9.
5. RC, E., *MUSCLE: multiple sequence alignment with high accuracy and high throughput.* Nucleic Acids Res., 2004. **32**(5): p. 1792-7.
6. Guindon S., G.O., *A simple, fast, and accurate algorithm to estimate large phylogenies by maximum likelihood.* Syst Biol., 2003. **52**(5): p. 696-704.
7. Anisimova M., G.O., *Approximate likelihood ratio test for branchs: A fast, accurate and powerful alternative.* Syst Biol., 2006. **55**(4): p. 539-52.
8. Chevenet F., B.C., Banuls AL, Jacq B, Chisten R., *TreeDyn: towards dynamic graphics and annotations for analyses of trees.* BMC Bioinformatics, 2006. **2006, Oct 10**(7): p. 439.
9. van den Hoogen, B.G., et al., *A newly discovered human pneumovirus isolated from young children with respiratory tract disease.* Nat Med, 2001. **7**(6): p. 719-724.
10. Hamelin ME, B.G., *Human metapneumovirus: a ubiquitous and long-standing respiratory pathogen.* Pediatr Infect Dis J., 2005. **24**(11 suppl): p. S203-7.
11. Caracciolo, et al., *Human Metapneumovirus Infection in Young Children Hospitalized With Acute Respiratory Tract Disease: Virologic and Clinical Features. [Article].* Pediatric Infectious Disease Journal May, 2008. **27**(5): p. 406-412.
12. Feuillet F, L.B., Rosa-Calatrava M, Boivin G, *Ten years of human metapneumovirus research.* J Clin Virol., 2012. **53**(2): p. 97-105.
13. Heikkinen T, O.R., Peltola V, Jartti T, Vainionpää R., *Human metapneumovirus infections in children.* Emerg Infect Dis. , 2008. **14**(1): p. 101-6.
14. Dokos C, M.K., Rellensmann G, Werner C, Schuler-Lüttmann S, Müller KM, Schiborr M, Ehlert K, Groll AH, *Fatal human metapneumovirus infection following allogeneic hematopoietic stem cell transplantation.* Transpl Infect Dis, 2013(2013 Apr 1).
15. Falsey, A.R., et al., *Humoral immunity to human metapneumovirus infection in adults.* Vaccine, 2010. **28**(6): p. 1477-1480.
16. Ryder, A.B., et al., *Soluble recombinant human metapneumovirus G protein is immunogenic but not protective.* Vaccine, 2010. **28**(25): p. 4145-4152.
17. Hamelin ME, C.C., Sackett M, Kiener P, Suzich J, Ulbrandt N, Boivin G., *The prophylactic administration of a monoclonal antibody against human metapneumovirus attenuates viral disease and airways hyperresponsiveness in mice.* Antivir Ther., 2008. **13**(1): p. 39-46.
18. Kitanovski L, K.S., Pokorn M, Dolničar MB, Rajić V, Stefanović M, Jazbec J, *Treatment of Severe Human Metapneumovirus (hMPV) Pneumonia in an Immunocompromised Child With Oral Ribavirin and IVIG.* J Pediatr Hematol Oncol, 2013(2013 May 9).

19. Park SY, B.S., Lee SO, Choi SH, Kim YS, Woo JH, Sung H, Kim MN, Kim DY, Lee JH, Lee JH, Lee KH, Kim SH, *Efficacy of oral ribavirin in hematologic disease patients with paramyxovirus infection: analytic strategy using propensity scores.* Antimicrob Agents Chemother, 2012. **57**(2): p. 983-9.

20. Mendes G, S.A., Sigiliano L, Machado F, Kaiser C, Romeiro N, Gestinari L, Santos N, Romanos MT, *In vitro anti-HMPV activity of meroditerpenoids from marine alga Stypopodium zonale (Dictyotales).* Molecules, 2011. **16**(10): p. 8437-50.

21. van den Hoogen BG, B.T., Osterhaus AD, Fouchier RA, *Analysis of the genomic sequence of a human metapneumovirus.* Virology, 2002. **295**(1): p. 119-32.

22. de Graaf, M., et al., *Specificity and functional interaction of the polymerase complex proteins of human and avian metapneumoviruses.* J Gen Virol, 2008. **89**(4): p. 975-983.

23. Schowalter RM, S.S., Dutch RE, *Characterization of human metapneumovirus F protein-promoted membrane fusion: critical roles for proteolytic processing and low pH.* J Virol., 2006. **80**(22): p. 10931-41.

24. Herfst S, M.V., Ver LS, Wierda RJ, Osterhaus AD, Fouchier RA, Melero JA., *Low-pH-induced membrane fusion mediated by human metapneumovirus F protein is a rare, strain-dependent phenomenon.* J Virol., 2008. **82**(17): p. 8891-5.

25. Schowalter RM, C.A., Robach JG, Buchholz UJ, Dutch RE, *Low-pH triggering of human metapneumovirus fusion: essential residues and importance in entry.* J Virol., 2009. **83**(3): p. 1511-22.

26. Mas V, H.S., Osterhaus AD, Fouchier RA, Melero JA., *Residues of the human metapneumovirus fusion (F) protein critical for its strain-related fusion phenotype: implications for the virus replication cycle.* J Virol., 2011. **85**(23): p. 12650-61.

27. Chang A, H.B., Winter CC, Buchholz UJ, Dutch RE, *Potential electrostatic interactions in multiple regions affect human metapneumovirus F-mediated membrane fusion.* J Virol., 2012. **86**(18): p. 9843-53.

28. Chang A, M.C., Buchholz UJ, Dutch RE., *Human metapneumovirus (HMPV) binding and infection are mediated by interactions between the HMPV fusion protein and heparan sulfate.* J Virol., 2012. **86**(6): p. 3230-43.

29. de Graaf M, H.S., Schrauwen EJ, Choi Y, van den Hoogen BG, Osterhaus AD, Fouchier RA., *Specificity and functional interaction of the polymerase complex proteins of human and avian metapneumoviruses.* J Gen Virol., 2008. **89**(Pt 4): p. 975-83.

30. Derdowski A, P.T., Glover N, Qian R, Utley TJ, Burnett A, Williams JV, Spearman P, Crowe JE Jr, *Human metapneumovirus nucleoprotein and phosphoprotein interact and provide the minimal requirements for inclusion body formation.* J Gen Virol., 2008. **89**(Pt 11): p. 2698-708.

31. Chang A, D.R., *Paramyxovirus Fusion and Entry: Multiple Paths to a Common End.* Viruses, 2012. **4**(4): p. 613-36.

32. Bowden TA, C.M., Jones EY, Stuart DI, *Shared paramyxoviral glycoprotein architecture is adapted for diverse attachment strategies.* Biochem Soc Trans, 2010. **38**(5): p. 1349-55.

33. Krzyzaniak MA, Z.M., Gerez JA, Picotti P, Helenius A., *Host cell entry of respiratory syncytial virus involves macropinocytosis followed by proteolytic activation of the F protein.* PLoS Pathog, 2013. **9**(4): p. e1003309.

34. Wen X, K.J., Leser GP, Cox RG, Lamb RA, Williams JV, Crowe JE Jr, Jardetzky TS., *Structure of the human metapneumovirus fusion protein with neutralizing antibody identifies a pneumovirus antigenic site.* Nat Struct Mol Biol., 2012. **19**(4): p. 461-3.

35. Yin H-, W.X., Paterson RG, Lamb RA, Jardetzky TS, *Structure of the parainfluenza virus 5 f protein in its metastable, prefusion conformation.* Nature, 2006. **439**: p. 38.

36.   Joshi SB, D.R., Lamb RA., *A core trimer of the paramyxovirus fusion protein: parallels to influenza virus hemagglutinin and HIV-1 gp41.* Virology, 1998. **248**(1): p. 20-34.

37.   Shirogane Y, T.M., Iwasaki M, Ishiguro N, Takeuchi H, Nakatsu Y, Tahara M, Kikuta H, Yanagi Y, *Efficient multiplication of human metapneumovirus in Vero cells expressing the transmembrane serine protease TMPRSS2.* J Virol., 2008. **82**(17): p. 8942-6.

38.   Welch BD, L.Y., Kors CA, Leser GP, Jardetzky TS, Lamb RA, *Structure of the cleavage-activated prefusion form of the parainfluenza virus 5 fusion protein.* Proc Natl Acad Sci USA., 2012. **109**(41): p. 16672-7.

39.   Smith EC, G.S., Tamm LK, Creamer TP, Dutch RE, *Role of sequence and structure of the Hendra fusion protein fusion peptide in membrane fusion.* J Biol Chem, 2012. **287**(35): p. 30035-48.

40.   Smith EC, P.A., Chang A, Masante C, Dutch RE, *Viral entry mechanisms: the increasing diversity of paramyxovirus entry.* FEBS J., 2009. **276**(24): p. 7217-27.

41.   Roymans D, D.B.H., Arnoult E, Geluykens P, Gevers T, Van Ginderen M, Verheyen N, Kim H, Willebrords R, Bonfanti JF, Bruinzeel W, Cummings MD, van Vlijmen H, Andries K, *Binding of a potent small-molecule inhibitor of six-helix bundle formation requires interactions with both heptad-repeats of the RSV fusion protein.* Proc Natl Acad Sci USA., 2010. **107**(1): p. 308-13.

42.   Rachakonda PS, V.M., Korte T, Ludwig K, Böttcher C, Huang Q, Schmidt MF, Herrmann A, *The relevance of salt bridges for the stability of the influenza virus hemagglutinin.* FASEB J., 2007. **21**(4): p. 995-1002.

43.   Harrison, S., *Viral membrane fusion.* Nat Struct Mol Biol., 2008. **15**(7): p. 690-8.

44.   Huang Q, S.R., Ludwig K, Korte T, Böttcher C, Herrmann A, *Early steps of the conformational change of influenza virus hemagglutinin to a fusion active state: stability and energetics of the hemagglutinin.* Biochim Biophys Acta., 2003. **1614**(1): p. 3-13.

45.   Gardner AE, D.R., *A conserved region in the F(2) subunit of paramyxovirus fusion proteins is involved in fusion regulation.* J. Virol., 2007. **81**(15): p. 8303-14.

46.   Lahaye, X., et al., *Functional Characterization of Negri Bodies (NBs) in Rabies Virus-Infected Cells: Evidence that NBs Are Sites of Viral Transcription and Replication.* J Virol., 2009. **83**(16): p. 7948-58.

47.   Heinrich BS, C.D., Rahmeh AA, Whelan SP, *Protein expression redirects vesicular stomatitis virus RNA synthesis to cytoplasmic inclusions.* PLoS Pathog, 2010. **6**(6): p. e1000958.

48.   Gerlier D, L.D., *Interplay between innate immunity and negative-strand RNA viruses: towards a rational model.* Microbiol Mol Biol Rev., 2011. **75**(3): p. 468-90.

49.   Smallwood S, H.T., Neubert WJ, Moyer SA., *Different substitutions at conserved amino acids in domains II and III in the Sendai L RNA polymerase protein inactivate viral RNA synthesis.* Virology, 2002. **304**(1): p. 135-45.

50.   Rahmeh AA, S.A., Danek, EI, Kranzusch PJ, Liang, B, Walz T, Whelan SP, *Molecular architecture of the vesicular stomatitis virus RNA polymerase.* Proc Natl Acad Sci USA., 2010. **107**(16): p. 20075-80.

51.   Asenjo, A., et al., *Residues in human respiratory syncytial virus P protein that are essential for its activity on RNA viral synthesis.* Virus Research, 2008. **132**(1-2): p. 160-173.

52.   Çevik, B., S. Smallwood, and S.A. Moyer, *Two N-terminal regions of the Sendai virus L RNA polymerase protein participate in oligomerization.* Virology, 2007. **363**(1): p. 189-197.

53.   Chattopadhyay, S. and A.K. Banerjee, *Phosphoprotein, P of human parainfluenza virus type 3 prevents self-association of RNA-dependent RNA polymerase, L.* Virology, 2009. **383**(2): p. 226-236.

54.   Smallwood, S., et al., *Mutations in Conserved Domain II of the Large (L) Subunit of the Sendai Virus RNA Polymerase Abolish RNA Synthesis.* Virology, 1999. **262**(2): p. 375-383.

55.   Chattopadhyay, A., T. Raha, and M.S. Shaila, *Effect of single amino acid mutations in the conserved GDNQ motif of L protein of Rinderpest virus on RNA synthesis in vitro and in vivo.* Virus Research, 2004. **99**(2): p. 139-145.

56.   Grdzelishvili, V.Z., et al., *A Single Amino Acid Change in the L-Polymerase Protein of Vesicular Stomatitis Virus Completely Abolishes Viral mRNA Cap Methylation.* J. Virol., 2005. **79**(12): p. 7327-7337.

57.   Galloway, S.E., P.E. Richardson, and G.W. Wertz, *Analysis of a structural homology model of the 2'-O-ribose methyltransferase domain within the vesicular stomatitis virus L protein.* Virology, 2008. **382**(1): p. 69-82.

58.   Li, J., J.T. Wang, and S.P.J. Whelan, *A unique strategy for mRNA cap methylation used by vesicular stomatitis virus.* Proceedings of the National Academy of Sciences, 2006. **103**(22): p. 8493-8498.

59.   Murphy, A.M. and V.Z. Grdzelishvili, *Identification of Sendai Virus L Protein Amino Acid Residues Affecting Viral mRNA Cap Methylation.* J. Virol., 2009. **83**(4): p. 1669-1681.

60.   Wiegand, M.A., et al., *De Novo Synthesis of N and P Proteins as a Key Step in Sendai Virus Gene Expression.* J. Virol., 2007. **81**(24): p. 13835-13844.

61.   Chiu YH, M.J., Chen ZJ, *RNA Polymerase III Detects Cytosolic DNA and Induces Type I Interferons through the RIG-I Pathway.* Cell., 2009. **138**(3): p. 576-91.

62.   García, J., et al., *Cytoplasmic Inclusions of Respiratory Syncytial Virus-Infected Cells: Formation of Inclusion Bodies in Transfected Cells That Coexpress the Nucleoprotein, the Phosphoprotein, and the 22K Protein.* Virology, 1993. **195**(1): p. 243-247.

63.   McDonald, T.P., et al., *Evidence that the respiratory syncytial virus polymerase complex associates with lipid rafts in virus-infected cells: a proteomic analysis.* Virology, 2004. **330**(1): p. 147-157.

64.   Brown, G., et al., *Evidence for an association between heat shock protein 70 and the respiratory syncytial virus polymerase complex within lipid-raft membranes during virus infection.* Virology, 2005. **338**(1): p. 69-80.

65.   Carromeu C, S.F., Tamura RE, Farinha Arcieri LE, Ventura AM, *Intracellular localization of human respiratory syncytial virus L protein*, in *Archives of Virology*. 2007. p. 2259-2263.

66.   Fearns, R., M.E. Peeples, and P.L. Collins, *Mapping the Transcription and Replication Promoters of Respiratory Syncytial Virus.* J. Virol., 2002. **76**(4): p. 1663-1672.

67.   Keller, M.A. and G.D. Parks, *Positive- and negative-acting signals combine to determine differential RNA replication from the paramyxovirus simian virus 5 genomic and antigenomic promoters.* Virology, 2003. **306**(2): p. 347-358.

68.   Fearns R, C.P., Peeples ME, *Functional analysis of the genomic and antigenomic promoters of human respiratory syncytial virus.* J Virol., 2000. **74**(13): p. 6006-14.

69.   Noton SL, D.L., Tremaglio CZ, Fearns R, *The respiratory syncytial virus polymerase has multiple RNA synthesis activities at the promoter.* PLoS Pathog, 2012. **8**(10): p. e1002980.

70.   Longhi S, O.M., *Structural disorder within the measles virus nucleoprotein and phosphoprotein.* Protein Pept Lett, 2010. **17**(8): p. 961-78.

71. Shaikh FY, C.R., Lifland AW, Hotard AL, Williams JV, Moore ML,Santangelo PJ, Crowe JE, Jr., *A critical phenylalanine residue in the respiratory syncytial virus fusion.* MBio. , 2012. **3**(1): p. e00270-11.

72. Russell RJ, G.S., Haire LF, Stevens DJ, Xiao B, Ha Y, Skehel JJ., *H1 and H7 influenza haemagglutinin structures extend a structural classification of haemagglutinin subtypes.* Virology, 2004. **325**(2): p. 287-296.

73. Gardner, A.E. and R.E. Dutch, *A conserved region in the F(2) subunit of paramyxovirus fusion proteins is involved in fusion regulation.* J Virol, 2007. **81**(15): p. 8303-14.

74. Yin, H.S., et al., *Structure of the parainfluenza virus 5 F protein in its metastable, prefusion conformation.* Nature, 2006. **439**(7072): p. 38-44.

75. Barlow, D.J. and J.M. Thornton, *Ion-pairs in proteins.* Journal of Molecular Biology, 1983. **168**(4): p. 867-885.

76. Kumar, S. and R. Nussinov, *Close-Range Electrostatic Interactions in Proteins.* ChemBioChem, 2002. **3**(7): p. 604-617.

77. Dutch, R.E. and R.A. Lamb, *Deletion of the cytoplasmic tail of the fusion (F) protein of the paramyxovirus simian virus 5 (SV5) affects fusion pore enlargement.* J. Virol., 2001. **75**: p. 5363-5369.

78. Biacchesi, S., et al., *Modification of the trypsin-dependent cleavage activation site of the human metapneumovirus fusion protein to be trypsin independent does not increase replication or spread in rodents or nonhuman primates.* J Virol, 2006. **80**(12): p. 5798-806.

79. Schickli, J.H., et al., *An S101P Substitution in the Putative Cleavage Motif of the Human Metapneumovirus Fusion Protein Is a Major Determinant for Trypsin-Independent Growth in Vero Cells and Does Not Alter Tissue Tropism in Hamsters.* J. Virol., 2005. **79**(16): p. 10678-10689.

80. Biacchesi, S., et al., *Genetic diversity between human metapneumovirus subgroups.* Virology, 2003. **315**(1): p. 1-9.

81. Schowalter, R.M., S.E. Smith, and R.E. Dutch, *Characterization of human metapneumovirus F protein-promoted membrane fusion: critical roles for proteolytic processing and low pH.* J. Virol., 2006. **80**(22): p. 10931-10941.

82. van den Hoogen, B.G., et al., *A newly discovered human pneumovirus isolated from young children with respiratory tract disease.* Nat Med, 2001. **7**(6): p. 719-24.

83. Daniels, R.S., et al., *Fusion mutants of the influenza virus hemagglutinin glycoprotein.* Cell, 1985. **40**: p. 431-439.

84. Rachakonda, P.S., et al., *The relevance of salt bridges for the stability of the influenza virus hemagglutinin.* The FASEB Journal, 2007. **21**(4): p. 995-1002.

85. Hanley LL, M.D., Teng MN, Djang R, Collins PL, Fearns R., *Roles of the respiratory syncytial virus trailer region: effects of mutations on genome production and stress granule formation.* Virology, 2010. **406**(2): p. 241-52.

86. Whitman SD, D.R., *Surface density of the Hendra G protein modulates Hendra F protein-promoted membrane fusion: role for Hendra G protein trafficking and degradation.* Virology, 2007. **363**(2): p. 419-29.

87. Mahon PJ, M.A., Iorio RM., *Role of the two sialic acid binding sites on the newcastle disease virus HN protein in triggering the interaction with the F protein required for the promotion of fusion.* J Virol., 2011. **85**(22): p. 12079-82.

88. Kim YH, D.J., Grigoryan G, Leser GP, Fadeev AY, Lamb RA, DeGrado WF., *Capture and imaging of a prehairpin fusion intermediate of the paramyxovirus PIV5.* Proc Natl Acad Sci USA., 2011. **108**(52): p. 20992-7.

89. Fearns R, P.M., Collins PL., *Mapping the transcription and replication promoters of respiratory syncytial virus.* J Virol., 2002. **76**(4): p. 1663-72.

90. Kitagawa, Y., et al., *Human metapneumovirus M2-2 protein inhibits viral transcription and replication.* Microbes and Infection, 2010. **12**(2): p. 135-145.

91. Dochow M, K.S., Crowe JE Jr, Moore ML, Plemper RK., *Independent structural domains in paramyxovirus polymerase protein.* J Biol Chem, 2012. **287**(9): p. 6878-91.

92. Noton SL, D.L., Tremaglio CZ, Fearns R, *The respiratory syncytial virus polymerase has multiple RNA synthesis activities at the promoter.* PLoS Pathog, 2012. **8**(10): p. e1002980.

93. Jeffree CE, B.G., Aitken J, Su-Yin DY, Tan BH, Sugrue RJ, *Ultrastructural analysis of the interaction between F-actin and respiratory syncytial virus during virus assembly.* Virology, 2007. **369**(2): p. 309-23.

94. Gower TL, P.M., Peeples ME, Collins PL, McCurdy LH, Hart TK, Guth A, Johnson TR, Graham BS, *RhoA signaling is required for respiratory syncytial virus-induced syncytium formation and filamentous virion morphology.* J Virol., 2005. **79**(9): p. 5326-36.

95. Portner A, M.K., *Localization of P, NP, and M proteins on Sendai virus nucleocapsid using immunogold labeling.* Virology, 1986. **150**(2): p. 469-78.

96. Coronel EC, M.K., Takimoto T, Portner A, *Human Parainfluenza Virus Type 1 Matrix and Nucleoprotein Genes Transiently Expressed in Mammalian Cells Induce the Release of Virus-Like Particles Containing Nucleocapsid-Like Structures.* J Virol., 1999. **73**(8): p. 7035-8.

97. Ghildyal R, M.J., Murray M, Vardaxis N, Meanger J, *Respiratory syncytial virus matrix protein associates with nucleocapsids in infected cells.* J Gen Virol., 2002. **83**(Pt 4): p. 753-7.

98. Patch JR, C.G., Wang LF, Eaton BT, Broder CC, *Quantitative analysis of Nipah virus proteins released as virus-like particles reveals central role for the matrix protein.* J Virol., 2007. **4**(1).

99. Rozenblatt S, K.T., Pinhasi O, Bratosin S, *Infective substructures of measles virus from acutely and persistently infected cells.* J Virol., 1979. **32**(1): p. 329-33.

100. Runkler N, P.C., Schneider-Schaulies S, Klenk HD, Maisner A, *Measles virus nucleocapsid transport to the plasma membrane requires stable expression and surface accumulation of the viral matrix protein.* Cell Microbiol, 2007. **9**(5): p. 1203-14.

101. Sugahara F, U.T., Watanabe H, Shimazu Y, Kuwayama M, Fujii Y, Kiyotani K, Adachi A, Kohno N, Yoshida T, Sakaguchi T, *Paramyxovirus Sendai virus-like particle formation by expression of multiple viral proteins and acceleration of its release by C protein.* Virology, 2004. **325**(1): p. 1-10.

102. Assenberg R, D.O., Ren J, Vidalain PO, Verma A, Larrous F, Graham SC, Tangy F, Grimes JM, Bourhy H., *Structure of the nucleoprotein binding domain of Mokola virus phosphoprotein.* J Virol., 2010. **84**(2): p. 1089-96.

103. Delmas O, A.R., Grimes JM, Bourhy H., *The structure of the nucleoprotein binding domain of lyssavirus phosphoprotein reveals a structural relationship between the N-RNA binding domains of Rhabdoviridae and Paramyxoviridae.* RNA Biol., 2010. **7**(3): p. 322-7.

104. Cox R, G.T., Purushotham S, Deivanayagam C, Bedwell GJ, Prevelige PE, Luo M., *Structural and Functional Characterization of the Mumps Virus Phosphoprotein.* J Virol., 2013.

105.   Heinrich BS, C.D., Rahmeh AA, Whelan SP, *Protein expression redirects vesicular stomatitis virus RNA synthesis to cytoplasmic inclusions.* PLoS Pathog., 2010. **6**(6): p. e1000958.

106.   Lahaye, X., et al., *Functional Characterization of Negri Bodies (NBs) in Rabies Virus-Infected Cells: Evidence that NBs Are Sites of Viral Transcription and Replication.* Journal of Virology, 2009. **83**(16): p. 7948-7958.

107.   Shaikh FY, U.T., Craven RE, Rogers MC, Lapierre LA, Goldenring JR, Crowe JE Jr., *Respiratory syncytial virus assembles into structured filamentous virion particles independently of host cytoskeleton and related proteins.* PloS One., 2012. **7**(7): p. e40826.

108.   Brown G, A.J., Rixon HW, Sugrue RJ, *Caveolin-1 is incorporated into mature respiratory syncytial virus particles during virus assembly on the surface of virus-infected cells.* J Gen Virol, 2002. **83**(Pt 3): p. 611-21.

109.   Nanbo A, W.S., Halfmann P, Kawaoka Y, *The spatio-temporal distribution dynamics of Ebola virus proteins and RNA in infected cells.* Sci Rep., 2013. **2013**(3): p. 1206.

110.   Vossenkämper A, N.P., Wiesner B, Furkert J, Rosenthal W, Klussmann E., *Microtubules are needed for the perinuclear positioning of aquaporin-2 after its endocytic retrieval in renal principal cells.* Am J Physiol Cell Physiol., 2007. **293**(3): p. C1129-38.

111.   Charest-Morin X, F.S., Lodge R, Roy C, Gera L, Gaudreault RC, Marceau F., *Inhibitory effects of cytoskeleton disrupting drugs and GDP-locked Rab mutants on bradykinin B_2 receptor cycling.* Pharmacol Res., 2013. **71**: p. 44-52.

112.   Chou YY, H.N., Gao Q, Palese P, Singer R, Lionnet T., *Colocalization of Different Influenza Viral RNA Segments in the Cytoplasm before Viral Budding as Shown by Single-molecule Sensitivity FISH Analysis.* PLoS Pathog, 2013. **9**(5): p. e1003358.

VITA

Brent A. Hackett

Date and Place of birth: July 26, 1985, Louisville, KY, USA

EDUCATION:

University of Kentucky, 2008-2013
    Advisor: Dr. Rebecca E. Dutch

University of Kentucky, 2004-2008
    Degree: Bachelor of Science, Biology

POSITIONS AND EMPLOYMENT:

Graduate student, Molecular and Cellular Biochemistry Department, University of
Kentucky College of Medicine, 2008-2013

Undergraduate research assistant, University of Kentucky College of Dentistry, 2007-
2008

PROFESSIONAL ASSOCIATIONS:

American Society for Virology, 2010-Present

AWARDS/HONORS:

Awarded NIH Underrepresented Minority Supplemental Grant (with Rebecca Dutch),
2011-2013
FASEB Virus Entry and Assembly Meeting Best Presentation Award, 2012

American Society of Virology Student Travel Awardee (to attend ASV Annual Meeting), 2011

University of Kentucky Max Steckler Intramural Fellowship, 2010

FASEB MARC Travel Award (to attend Experimental Biology Meeting), 2010

University of Kentucky Lyman T. Johnson Fellowship, 2008-2011

University of Kentucky William C. Parker Scholarship recipient, 2004-2008

PUBLICATIONS:

Chang A., **Hackett, B.A.**, Winter C.C., Buchholz U.J., Dutch R.E. "Potential electrostatic interactions in multiple regions affect HMPV F-mediated membrane fusion." J Virol. 2012 Sep;86(18):9843-53. doi: 10.1128/JVI.00639-12. Epub 2012 Jul 3.

Hackett, B.A., El-Najjar F.J., Dutch R.E. "Alteration of HMPV phosphoprotein and nucleocapsid localization coincide with critical events during infection." (manuscript submitted to *Virology*)

TALKS:

Hackett, B.A., et al. "Insights into the Life Cycle of Human Metapneumovirus," UK MCB Departmental Retreat, June 2012—Carrolton, KY

Hackett, B. A., et al. "Potential electrostatic interactions in multiple regions affect HMPV F-mediated membrane fusion," Southeastern Regional Virology Conference, March 10, 2012—Atlanta, GA

Hackett, B. A., et al. "Role of electrostatic interactions in the fusion activity of the HMPV F protein," American Society of Virology Annual Meeting, July 20, 2011—Minneapolis, MN

POSTER PRESENTATIONS:

Hackett, B.A., et al. "Potential electrostatic interactions in multiple regions affect HMPV F-mediated membrane fusion," FASEB Virus Structure and Assembly Meeting, June 2012—Saxtons River, VT

Hackett, B. A., Chang, A. "Modulation of the fusion activity of HMPV F through disruption of novel electrostatic interactions," UK MCB Departmental Retreat, May 2011—Corbin, KY

Hackett, B.A. "Modification of the pH-dependent function of the HMPV F protein," UK MCB Departmental Retreat, May 2010—Corbin, KY

Hackett, B.A. "Modification of the pH-dependent function of the HMPV F protein," Experimental Biology 2010, ASBMB, April 23, 2010—Anaheim, CA

INVITED SEMINARS:

Critical Events in Human Metapnuemovirus Infection: From Entry to Egress, University of Arizona, Tucson, AZ, June 2013

Critical Events in Human Metapnuemovirus Infection: From Entry to Egress, University of Pennsylvania, Philadelphia, PA, June 2013